UNIVERSIDADE FEDERAL DO CEARÁ
CENTRO DE TECNOLOGIA
DEPARTAMENTO DE ENGENHARIA DE TELEINFORMÁTICA
PROGRAMA DE PÓS-GRADUAÇÃO EM ENGENHARIA DE TELEINFORMÁTICA

FRANCISCO RAFAEL VASCONCELOS GUIMARÃES

INTERFERENCE MANAGEMENT FOR 4G CELLULAR NETWORKS AND BEYOND

FORTALEZA
2018

FRANCISCO RAFAEL VASCONCELOS GUIMARÃES

INTERFERENCE MANAGEMENT FOR 4G CELLULAR NETWORKS AND BEYOND

Tese apresentada ao Curso de Doutorado em Engenharia de Teleinformática da Universidade Federal do Ceará, como parte dos requisitos para obtenção do Título de Doutor em Engenharia de Teleinformática. Área de concentração: Sinais e Sistemas

Orientador: Prof. Dr. Walter da Cruz Freitas Júnior

FORTALEZA
2018

Dados Internacionais de Catalogação na Publicação
Universidade Federal do Ceará
Biblioteca Universitária
Gerada automaticamente pelo módulo Catalog, mediante os dados fornecidos pelo(a) autor(a)

G978i Guimarães, Francisco Rafael Vasconcelos.
Interference management for 4G cellular networks and beyond / Francisco Rafael Vasconcelos Guimarães. – 2018.
114 f. : il. color.

Tese (doutorado) – Universidade Federal do Ceará, Centro de Tecnologia, Programa de Pós-Graduação em Engenharia de Teleinformática, Fortaleza, 2018.
Orientação: Prof. Dr. Walter da Cruz Freitas Júnior.

1. Redes celulares. 2. Gerência de interferência. 3. 5G. 4. TDD Dinâmico. I. Título.

CDD 621.38

FRANCISCO RAFAEL VASCONCELOS GUIMARÃES

INTERFERENCE MANAGEMENT FOR 4G CELLULAR NETWORKS AND BEYOND

Presented Thesis for the Post-graduate Program in Teleinformatics Engineering of Federal University of Ceará as a partial requisite to obtain the Ph.D. degree in Teleinformatics Engineering.

Approved at: 05/25/2018.

EXAMINATION BOARD

_____
Prof. Dr. Walter da Cruz Freitas Júnior (Supervisor)
Universidade Federal do Ceará, Fortaleza, Brazil

_____
Prof. Dr. Yuri Carvalho Barbosa Silva
Universidade Federal do Ceará, Fortaleza, Brazil

_____
Prof. Dr. Charles Casimiro Cavalcante
Universidade Federal do Ceará, Fortaleza, Brazil

_____
Prof. Dr. Cristiano Magalhães Panazio
Universidade de São Paulo, São Paulo, Brazil

_____
Prof. Dr. Gustavo Fraidenraich
Universidade Estadual de Campinas, Campinas, Brazil

_____
Prof. Dr. Gábor Fodor
Royal Institute of Technology, Stockholm, Sweden

...to my beloved fiancée Aline Memória.

ACKNOWLEDGEMENTS

First of all, I would like to thank my fiancée, Aline Memória, for all the emotional support, even if she did not have a clue on what I was doing during my Ph.D study. Thank you for the comprehension and encouragement for the 5 months of internship in Sweden and for all those 5 years of PhD. Without you, this work could not be finished.

I would like to thank my family: my parents (Mazé and Assis), brother (Danilo), mother in law (Fátima), sister in law (Amanda) and father in law (Ricardo), each of them has contributed somehow for this success. A special thank to my mother who always believed on me and has invested on my studies. Thank you mom, I love you. Also I would like to give a special thank to my sister in law for the good times we had together, for the moments we laughed together and make me think about the simple things in life.

I would like to express my gratitude to my advisor Prof. Dr. Walter Freitas for the continuous support of my Ph.D study and related research, for his patience and knowledge. I also want to thank Prof. Yuri Carvalho for the discussions, even if he was not my advisor, he has contributed a lot for this thesis with valuables comments and discussions.

I want to thank Prof. Dr. Gábor Fodor from KTH and Ericsson Research in Sweden for the acceptance of being my advisor during the 5 months internship on Ericsson in 2016. I would like to thank him for his immense knowledge and motivation. His guidance helped me in the research and to write of this thesis.

My sincere thanks also goes to Prof. Dr. Rodrigo Cavalcanti who provided me an opportunity to join Gtel team as intern, and who gave access to the laboratory and research facilities and also made it possible the internship on Ericsson which was valuable for me as a person and as a researcher. Also I would like to thank Funcap for the financial supporting.

I would like to thank the rest of my thesis committee: Prof. Dr. Charles Casimiro Cavalcante, Prof. Dr. Cristiano Magalhães Panazio, and Prof. Dr. Gustavo Fraidenraich, for their insightful comments and encouragement, but also for the hard question which incented me to widen my research from various perspectives.

At last but not least, I thank my fellow labmates in for the stimulating discussions, mainly my Project team (Khaled, Eduardo, Darlan and Lászlon) for the weekly meetings and discussions which helped me a lot to develop my thesis. I also would like to thank my work mate Hugo who shares a workstation with me and my friend Diego who helped with insightful discussions and developed the thesis template for to me.

RESUMO

Um dos requisitos para os sistemas de quinta geração (5G) é o aumento da capacidade de transmissão em até 1000 vezes ao longo da próxima década. Para atingir esse objetivo, as redes celulares devem se tornar mais densas (*relays*,*picocells*, *femtocells*) e menores (diminuição da área de cobertura), o que pode provocar um aumento da interferência entre células, diminuindo o ganho de taxa esperado. Outra característica presente em redes da próxima geração é o aumento da largura de banda das sub-portadoras, o que abre espaço para o uso da duplexação por divisão temporal (TDD) devido à sua flexibilidade no uso do espectro. Desta forma, o TDD dinâmico é a escolha mais natural, pois cada base pode escolher sua configuração baseada em seu próprio tráfego, adaptando-se às necessidades de seus usuários em cada célula. Entretanto, caso duas células transmitam em direções distintas, além das interferências intra e intercelular, dois outros tipos de interferência ocorrem: *downlink* (DL)-*uplink*, entre bases, e UL-DL, entre usuários. Desta forma, deve existir algum tipo de gerência de interferência para que a performance do sistema não seja degradada. Neste contexto, esta tese aborda as técnicas de *beamforming* (BF), controle de potência (CP) e alocação de *streams* para gerenciamento de interferência em redes celulares na busca de responder aos seguintes questionamentos: "*Como gerenciar a interferência em redes com TDD dinâmico de forma distribuída?*", "*Para sistemas com múltiplas antenas, como determinar a melhor alocação de streams para cada usuário?*". Para que estas perguntas sejam respondidas, este trabalho é dividido em três partes. A primeira parte se refere a um estudo do estado da arte em que algoritmos clássicos de BF e CP são comparados a algoritmos existentes na literatura através de simulações computacionais a fim de motivar o uso de soluções distribuídas e mais efetivas para gerência de interferência. Já a segunda parte deste trabalho aborda redes que operam com TDD dinâmico, em que são propostos dois novos algoritmos de BF distribuídos baseados na abordagem de *preço* (*pricing*). Os algoritmos são comparados com as abordagens clássicas descritas na primeira parte da tese para usuários com uma antena (MISO) ou múltiplas antenas (MIMO). Também é apresentada uma análise de sinalização, convergência e complexidade para os algoritmos propostos. Por fim, a última parte aborda redes MIMO em que um novo algoritmo baseado na abordagem gananciosa (*greedy*) para resolver o problema de alocação de *streams* é proposto. É mostrado através de simulações que o algoritmo proposto é melhor do que qualquer esquema fixo de seleção e apresenta um desempenho muito próximo da solução ótima, possuindo menor complexidade.

Palavras-chave: Beamforming, Gerência de Interferência, TDD dinâmico

ABSTRACT

The next fifth generation (5G) systems expect a traffic volume around 1,000 times greater than fourth generation (4G) systems. In order to reach this requirement, the cellular networks need to be denser and smaller which can lead to a high intercell interference, reducing the expected performance gains. Another feature for next generation networks is the increasing of sub-carriers bandwidth , which motivates the use of time division duplexing (TDD) approach due the flexibility in the use of the available spectrum. Therefore, the dynamic TDD is a natural choice for such networks due the capability of each base station (BS) to choose its own transmission direction adapting to users' traffic fluctuations. However, if two BSs transmit in opposite directions in addition of intra and intercell interference there will be downlink (DL)-uplink(UL) interference, between BSs, and UL-DL interference between users. Thus, it must exist some kind of interference management to prevent the system performance loss due the presence of interference. In this context, this thesis considers the beamforming (BF), power control (PC) and stream allocation techniques for interference management in order to answer the following questions "How to manage with the interference in dynamic TDD networks?", "How to determine the best stream allocation for multiple-input multiple-output (MIMO) systems?". To answer these questions we divided this works in three parts. The first part studies the BF state of art where we compare the classical BF and PC algorithms with some approaches existing in literature in order to motivate the usage of distributed solutions for interference management. The second part addresses the interference problem for dynamic TDD networks, where we propose two novel distributed algorithms based on pricing approach. We compare our proposed algorithms with the classical BF approaches for multiple-input single-output (MISO) and MIMO systems. We also present an analysis regarding to signalization, convergence and complexity aspects. The last part addresses the stream allocation problem for MIMO networks where we present a novel greedy based algorithm which finds the best stream allocation that outperforms any fixed scheme and has a small performance gap when compared to the optimum solution, with less complexity.

Keywords: Beamforming, Interference Management, Dynamic TDD

LIST OF FIGURES

LIST OF TABLES

LIST OF ABBREVIATIONS AND ACRONYMS

3GPP	3rd generation partnership project
4G	4th Generation
5G	5th generation
AWGN	additive white Gaussian noise
BD	block diagonalization
BF	beamforming
BS	base station
CBF	coordinated beamforming
CDF	cumulative distribution function
CDI	channel distribution information
CoMP	coordinated multi-point
CSI	channel state information
CSIT	channel state information at the transmitter
DL	downlink
DoF	degrees of freedom
DPC	dirty paper coding
DTDD	dynamic time division duplex
EE	energy efficiency
eIMTA	enhanced interference mitigation and traffic adaptation
FDD	frequency division duplex
GEE	global energy efficiency
GSSA	greedy stream selection algorithm
IA	interference aligment
IC	interference channel
IPNP	interference plus noise power
KKT	Karush-Kuhn-Tucker
LoS	line-of-sight
LTE	long-term evolution
MIMO	multiple-input multiple-output
MIMO-IC	MIMO-interference channel
MISO	multiple-input single-output
MISO-IC	MISO-interference channel
MMSE	minimum mean square error
MRT	maximum ratio transmission
MSE	mean square error
NLoS	non-line-of-sight

PB	pricing-based
PBA	pricing-based algorithm
PC	power control
QCQP	quadratically constrained quadratic program
QoS	quality of service
SINR	signal-to-interference-plus-noise ratio
SISO	single-input single-output
SNR	signal-to-noise ratio
SPBA	sub-optimal pricing-based algorithm
TDD	time division duplexing
TTI	transmission time interval
UE	user equipment
UL	uplink
ZF	zero-forcing

SUMMARY

1 INTRODUCTION

This is an introductory chapter where we present the context on this thesis in Section 1.1. After that, we present the overview and our main contributions in Section 1.2, followed by the thesis products on Section 1.3. Finally, on Section 1.4, we present the notation that we will use through this thesis.

1.1 Thesis Context

Mobile wireless networks will experience in the next years a large growth in numbers of devices and data rate. For 5^{th} generation (5G) networks, it is estimated that the number of devices will be around 50 billion [1] and the expected traffic volume will be 1,000 times greater than nowadays [2].

With these requirements, the networks become smaller (decreasing its coverage) and denser in space (relays, picocells, femtocells) or frequency (full channel reuse for e.g.). This leads to a traffic load imbalance between users, as the signal transmitted to a specific user is received by the others within the transmission range, due to the broadcast nature of the channel.

To this end, dynamic time division duplexing (TDD) cellular systems are used to adapt the number of uplink and downlink time slots in each cell to dynamically change cell-specific traffic demands [3]. The long-term evolution (LTE) systems standardized by the 3^{rd} generation partnership project (3GPP), for example, support the so-called enhanced interference mitigation and traffic adaptation (eIMTA) schemes to enable the dynamic allocation of subframes to uplink (UL) and downlink (DL) transmissions [4]. Such dynamic TDD systems better support asymmetric and fluctuating traffic demands than systems with fixed subframe allocations in both homogeneous and heterogeneous environments [5]. This gain increases as the traffic asymmetry increases, and can reach up to 200 percent packet throughput gains in a 10 MHz LTE system under realistic assumptions [6].

The use of dynamic TDD has influence in the network dynamics giving rise to common types of interference including base station (BS)-to-BS and UE-to-UE interference mainly due to conflicting TDD configurations in neighbor cells, synchronization errors, and also due to the lack of synchronicity among neighbor cells [6, 7], which limit the network throughput [8]. Recognizing the inherent tradeoff between adapting the dynamic time division duplex (DTDD) configuration to the prevailing traffic demands and causing new types of interference in neighbor cells, the 3GPP has specified measurement reporting and signaling support for eIMTA schemes in urban, rural and indoor environments [3, 4].

In this context, some key aspects on interference management arise, among them we can cite *power control (PC)*, *beam design* and interference aligment (IA). Optimize the power consumption of BSs and UEs is one of the main keys to enhance the network performance [9].

For a downlink transmission perspective, the great benefit is to mitigate the interference, since the received power for the unintended users is reduced. For the uplink point of view, besides reducing the interference, PC saves the user's battery which is a strong constraint for high data applications.

The beam design, also referred as beamforming [10], is a powerful tool for interference management using multiple antennas features. It seeks to increase the signal force into a desired direction while suppressing signal power for the other directions which increases the data rate and reduces or even eliminates interferences.

The IA [11, 12] is another technique that aims to eliminate the interference which takes advantage of MIMO systems. It seeks to divide the transmission space into two subspaces: in one subspace it tries to confine the most part of the interference where the other is (almost) interference free for user transmission.

Therefore, the interference management plays a crucial role for guaranteeing the quality of service (QoS) for different users and applications, given that the cellular networks are expected to be strongly interference-limited.

1.2 Thesis Overview and Contributions

Developing algorithms and strategies to deal with interference is a topic of interest for 5G networks, since it limits the amount of data that can be transmitted over a channel. In this thesis, we aim to present and develop solutions and algorithms for interference mitigation in such systems, in special by exploring beamforming techniques for IA and dynamic TDD systems. The outline of each chapter is presented as follows.

In **Chapter 2**, we address the beamforming problem. We present a background about beamforming, including the state-of-art and its strategies, which is divided into two parts. The first one takes into account the classical beamforming strategies: maximum ratio transmission (MRT), zero-forcing (ZF) and minimum mean square error (MMSE). The second part presents three centralized beamforming optimization problems: power minimization, sum-rate maximization and an energy efficiency (EE) beamforming. Evaluations comparing some of these techniques are provided and a discussion is presented where we conclude that distributed beamforming techniques are the best option for interference management.

In **Chapter 3**, we address the dynamic TDD problem. We start with a description about the dynamic TDD networks by presenting the motivation behind it and comparing with the classical TDD networks. We also introduce the interference problem related to such kind of networks, where we come up with a state-of-the-art in interference management area. We present the dynamic TDD multi-user multi-cell multiple-input single-output (MISO) system model and we describe the downlink beamforming (BF) problem related to this scenario. We show that the UL users are strongly affected by DL transmission, then, to cope with that, we make the use of interference pricing where we penalize the DL users by the amount of interference they cause in all network users, including the downlink ones. To this end, we developed two algorithms,

a nearly optimal approach where we relax the rank constraint that can run either in parallel or sequential way solved with the help of the CXV routine and a sub-optimal heuristic which still achieves a better performance than the zero-forcing (ZF) BF, converging in less iterations than the first considered approach. We present results showing the benefits of the proposed approaches and we include a section where we discuss about the convergence, complexity and signaling overhead issues.

In **Chapter 4**, we address the dynamic TDD MIMO problem. We extend the problem in Chapter 3 by considering multiple antennas at the UE side. We rewrite all the system model, equations and the optimization problem for the MIMO scenario. We present simulations results where we vary the number of antennas at the UE and we show the benefits of a multiple antenna UE for the dynamic TDD scenario.

In **Chapter 5**, we address the IA problem. We present the classical strategies to perform the beamforming for K-user MIMO systems: closed-form solution, MMSE and max-signal-to-interference-plus-noise ratio (SINR). We also address the degrees of freedom (DoF) and feasibility issues which still are an open problem. Based on that information, we come up with a greedy stream selection algorithm (GSSA), where it is a less complex alternative to the exhaustive search to determine the best stream allocation, and, consequently, the number of DoF for the IA problem. The developed algorithm is a suboptimal approach, but we show by simulations that it approximates the best solution with less complexity.

In **Chapter 6**, we summarize the main conclusions obtained along the thesis. Furthermore, we point out the main research directions that can be considered as an extension of the study performed in this thesis.

1.3 Thesis Products

The first part of this thesis which is related to Chapters 2 and 5 was developed under the context of Ericsson/UFC technical cooperation projects

- UFC.35: *Interference Alignment Techniques for Wireless Networks*, August/2012 - July/2014;
- UFC.42: *Interference Management for Super Dense Scenarios*, October/2014 - September/2016,

in which a number of three technical reports, one in UFC.35 and two in UFC.42 have been delivered and the following conference paper was produced:

- F. R. V. Guimarães, D. C. Moreira, W. C. Freitas Jr., Y. C. B. Silva, and F. R. P. Cavalcanti, "Greedy algorithm for stream selection in a MIMO interference channel, *in Proc. Simpósio Brasileiro de Telecomunicações*, Sep. 2015.

The second part of this thesis is related to Chapters 3 and 4 which includes a five-months Ph.D. internship at KTH/Ericsson Research, Stockholm/Kista where we developed under the context of the following Ericsson/UFC technical cooperation projects

- UFC.42: *Interference Management for Super Dense Scenarios*, October/2014 - September/2016,
- Internship Report, *Pricing-based Algorithm for dynamic TDD Networks* - August/2016.
- TIDE5G: *Dynamic Time Division Duplexing Evolution for 5G Systems* November/2016 - October/2018,

in which a number of three technical reports, one in UFC.42 and two in TIDE5G have been delivered and the following journal paper was produced:

- F. R. V. Guimarães, G. Fodor, W. C. Freitas Jr., and Y. C. B. Silva, "Pricing-based distributed beamforming for dynamic time division duplexing systems, *IEEE Transactions on Vehicular Technology*, vol. 67, no. 4, pp. 3145-3157, April 2018. **doi: 10.1109/TVT.2017.27 77477**

1.4 Notation

Throughout this thesis, bold lowercase letters ($\mathbf{a}$) represent a vector and bold uppercase letters ($\mathbf{A} \in \mathbb{C}^{i \times j}$) are used to denote a matrix drawn from the $i \times j$ matrix space defined on the complex field. $\mathbf{A}^H$ represents the Hermitan of a matrix $\mathbf{A}$, $\mathbf{A}^{[\star k]}$ is used to denote the k-th column of a matrix $\mathbf{A}$, $\mathbb{R}\{\cdot\}$ corresponds to the real part of a number. $|\mathcal{A}|$ is the cardinality of a set $\mathcal{A}$. $\mathbb{E}[\cdot]$ and $\mathrm{Tr}[\cdot]$ are the expectation and trace operators, respectively, while $\mathrm{dom}(a)$ represents the domain of a function a and $\mathrm{diag}(\cdot)$ creates a block-diagonal matrix. Finally, $\mathcal{N}(0, N_0)$ represents a Gaussian distribution with zero mean and variance N_0.

2 COORDINATED BEAMFORMING OVERVIEW

In this chapter our focus is to present an overview of some coordinated beamforming (CBF) strategies, from which we gain some insights for developing novel algorithms or strategies for interference management in the next chapters. First, we present a general system model for the MISO-interference channel (IC) in Section 2.2. After that, in Section 2.3.1 we describe the classical BF approaches (MRT, ZF and MMSE), which we will make user in next chapters. Then, three different beamforming approaches are discussed where, for each one, we present their corresponding problem formulation, algorithm description and some illustrative results. The strategies are mainly characterized by their optimization objectives, which are based on power minimization, in Section 2.3.2, sum-rate maximization, in Section 2.3.3, and energy efficiency, in Section 2.3.4. Finally, some conclusions and perspectives are presented in Section 2.4.

2.1 Introduction

As mentioned in Chapter 1 that the interference management plays a crucial role for 5G systems, given that the cellular networks are expected to be strongly interference-limited. In order to achieve performance gains, in this kind of scenario, some techniques were studied in the literature to increase the transmit data rates, save power consumption or maintain a certain QoS level for the network users.

Among these techniques we can cite the dirty paper coding (DPC) [13, 14, 15] and beamforming [16, 17, 18, 19, 20, 21, 22, 23, 24, 25, 26, 27, 28]. The DPC technique performs a pre-cancellation of the known interference to achieve system capacity. However, DPC is a complex approach and several strategies have been studied to overcome this issue. Multi-user beamforming, then, has been widely studied because it can provide a good system performance but with lower complexity than DPC.

Beamforming refers to a spatial filtering applied on transmitter and/or receiver in order to favor some directions over others [10]. Hence, the interference in a MIMO-IC can be mitigated and system performance can be increased. The beamforming techniques can be classified into two main groups, namely coordinated and uncoordinated [29]. In the *uncoordinated beamforming* techniques, the beams are calculated in each transmitter without any cooperation among them. This approach leads to a low complexity algorithm but it does not yield the best solution.

With *coordinated beamforming (CBF)* there are multiple cells containing multiple antennas, which jointly optimize their respective beamformers to improve the overall system performance. In particular, the data stream for each user only needs to be (pre-)processed at its own BS (and not across all BSs as it would be the case with joint processing). Furthermore, the BSs do not need to be symbol-synchronized, as required with signal-level coordination. For 5G

scenarios, where the cells have smaller radius and become denser, the cooperation among BSs is the best choice to fulfill the system specifications.

Figure 2.1 shows how the transmit beamforming process occurs. The user's data is multiplied by a pre-determined weight, w_n, in each antenna, also referred as precoders, before it is sent over the channel. This multiplication creates a constructive interference in the user's desired direction and a destructive interference to the unintended directions.

Figure 2.1 – Beamforming process.

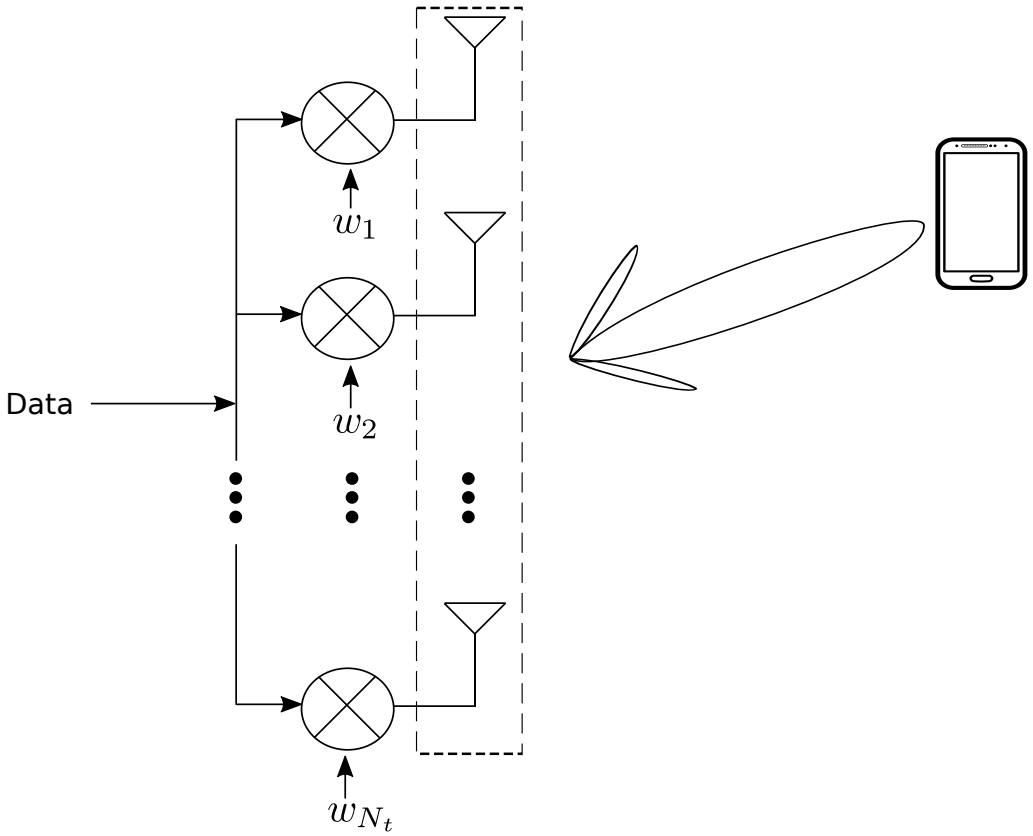

Source: Created by the author.

In the literature there have been some misconceptions regarding the definitions of the different approaches of CBF. In order to make it clear throughout the present thesis, we shall define each approach as follows

Definition 1 *A **centralized** CBF approach refers to a central node*[1] *that collects all channel information from the coordinated nodes (via back-haul link, for example) and then performs all precoder calculations for all transmitters in the network. Afterwards, it sends to all transmitter nodes their respective beamforming vectors, which will be used for transmission.*

Definition 2 *A **decentralized** CBF approach refers to the idea that each BS calculates its own precoders taking into account the global channel gains, i.e., the channel gains from the UEs to their own BSs, also known as global channel state information (CSI) [30].*

[1] This node can be a cloud radio access network architecture [22].

Definition 3 *In a **distributed** CBF approach, each BS calculates its own precoders but it only uses local information, i.e., information concerning interfering links are not shared among BSs.*

Distributed algorithms are the practical solution for next generation networks, since they only require local CSI and can be performed in a distributed way by each BS. Many works have designed beamforming algorithms for co-channel interference mitigation. The works differs from each other in terms of optimization problem and algorithm design. The beamforming schemes for the interference channel can be categorized as follows:

- Power Minimization [16, 17];
- Rate Maximization [18, 19, 20];
- Energy Efficiency (EE) [21, 22];
- Interference Alignment (IA) [23, 24, 25, 26, 27];
- Other optimization problems [28].

In power minimization beamforming schemes, the main objective is to design the precoders which will minimize the network consumed power subject to some constraints. The work in [16] shows the relationship between downlink and uplink to design a beamforming based on power constraints per antenna for a minimum SINR threshold. The authors in [17] have extended this work by developing an efficient algorithm that finds the global optimal through a jointly optimization which can also be implemented in a distributed way if TDD is considered.

The rate-maximization algorithms aim to design the beamforming in order to maximize the network throughput. The authors in [18] have proposed a coordinated linear beamforming for the multi-cell downlink interference channel. By having a set of coordinated BSs, the authors have found the optimum beamforming vectors that maximize the instantaneous weighted sum-rate. Even though they have not considered a distributed algorithm on their work, they have shown that the proposed algorithm could be implemented in a distributed way. The works in [19, 20] maximize the network throughput based on the pricing idea where the users are penalized by the amount of interference they cause on each other. The authors in [19] developed a sub-optimal approach that outperforms both MRT and ZF in terms of sum-rate while the authors in [20] proposed a decentralized beamforming that reduces the amount of exchanged information among the network nodes.

Works in [21, 22] aim to maximize the energy efficiency for MISO networks. In [21] the authors have investigated an EE coordinated beamforming in a decentralized way per BS while the work in [22] designed a suboptimal procedure based on the Karush-Kuhn-Tucker (KKT) conditions to optimize the global EE.

IA algorithms have the objective to separate the user signal and the interference into two different subspaces. The authors in [23] were the first to propose a beamforming approach for the IA problem by designing a closed-form solution for the 3-user pair interference

channel. Motivated by the work in [23], Shen *et al.* have investigated the application of ZF and MMSE precoders for a 2-user pair MIMO system in [24]. The K-user MIMO networks were also widely studied by [25, 26, 27], where each of these works have proposed different beamforming approaches for this kind of scenario. The SINR maximization algorithm was studied in [25] and [26] while [27] proposed a beamforming design via alternating minimization algorithm.

As for [28], the authors have designed a distributed beamforming in order to maximize the utility function and solve the rate outage constrained problem for a MISO channel assuming only channel distribution information (CDI) known to the transmitters.

The main objective of this chapter is to present an overview about the beamforming strategy by describing the most known approaches in literature MRT, ZF and MMSE and optimization problems related to beamforming design: power minimization [17], sum-rate maximization [18] and energy efficiency [22]. For the last three, we present the algorithm description for each of them and we present simulation results which we compare with the MRT approach. From these results, we can draw some insights for the next chapters where we make use of a classical beamforming approach, on Chapter 5, and develop new beamforming algorithms, on Chapters 3 and 4, to deal with interference and maximize the network capacity.

2.2 Beamforming Scenario

The considered scenario for CBF is a MISO system composed by M coordinated cells, where each BS m, with $m = 1, 2..., M$, is equipped with N_{BS} antennas to simultaneously transmit its information to the users. We also consider that each cell has K users, where (m, k) represents the k-th user in cell m. This scenario is illustrated in Figure 2.2, where we have 7 cells and 3 users as an example.

Further, we define a set containing all users $\mathcal{K} \triangleq \{(m, k), k \in \{1, \ldots, K\}, m \in \{1, \ldots, M\}\}$. By assuming that the channels are constant during a certain time interval, the received signal at user (m, k) is written as

$$y_{m,k} = \underbrace{\mathbf{h}_{(m,k),m}\mathbf{w}_{m,k}x_{m,k}}_{\text{desired signal}} + \underbrace{\sum_{j=1, j\neq k}^{K} \mathbf{h}_{(m,k),m}\mathbf{w}_{m,j}x_{m,j}}_{\text{intracell interference}} + \underbrace{\sum_{d=1, d\neq m}^{M}\sum_{j=1}^{K} \mathbf{h}_{(m,k),d}\mathbf{w}_{d,j}x_{d,j}}_{\text{intercell interference}} + \underbrace{z_{m,k}}_{\text{noise}}, \tag{2.1}$$

where $\mathbf{h}_{(m,k),m} \in \mathbb{C}^{1\times N_{\mathrm{BS}}}$ represents the channel vector from transmitter m to user (m, k), $z_{m,k} \in \mathbb{C}$ denotes circular complex white Gaussian noise with distribution $\mathcal{N}(0, \sigma^2_{m,k})$, and $x_{m,k}$ represents the complex signal data sent to user (m, k) using the transmit precoder $\mathbf{w}_{m,k} \in \mathbb{C}^{N_{\mathrm{BS}}\times 1}$.

Figure 2.2 – Multi-cell multi-user scenario. In this figure, there are 7 cells with 3 users each.

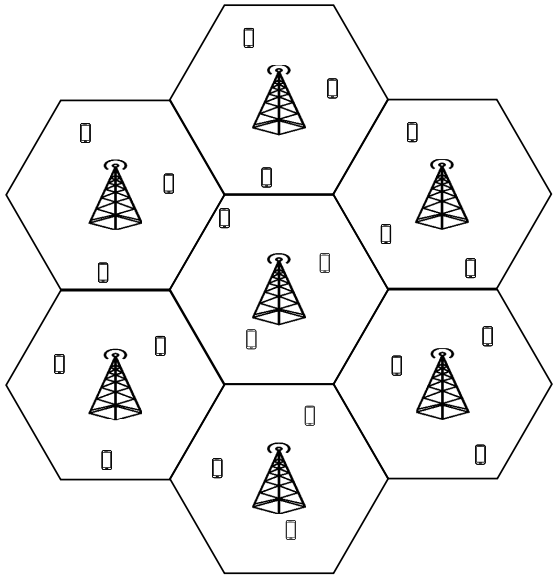

Source: Created by the author.

Then, the SINR for user k connected to a BS m can be given as

$$\gamma_{m,k} = \frac{|\mathbf{h}_{(m,k),m}\mathbf{w}_{m,k}|^2}{\sum\limits_{j,j\neq k} |\mathbf{h}_{(m,k),m}\mathbf{w}_{m,j}|^2 + \sum\limits_{d,d\neq m}\sum\limits_{j} |\mathbf{h}_{(m,k),d}\mathbf{w}_{d,j}|^2 + \sigma^2_{m,k}}. \tag{2.2}$$

For simplicity of notation we have omitted the lower and upper sum limits in (2.2), since we consider throughout this chapter that $k, j \in \{1, \ldots, K\}$ while $m, d \in \{1, \ldots, M\}$.

The beamforming design problem is related to optimizing a given function under certain constraints. We will next present three different problems, which are formulated and solved using centralized beamforming approaches found in the literature.

2.3 Overview of Beamforming Techniques

In this section we review and describe the most common linear beamforming approaches in literature to deal with interference in the system model described in Section 2.2.

2.3.1 Classical Beamforming Approaches

2.3.1.1 Maximum Ratio Transmission (MRT)

The MRT, also called as matched channel, maximizes the received signal-to-noise ratio (SNR) for each user, it means:

$$\max_{\mathbf{w}^{\mathrm{MRT}}_{m,k}} \quad |\mathbf{h}_{(m,k),m}\mathbf{w}^{\mathrm{MRT}}_{m,k}|^2. \tag{2.3}$$

Then, the MRT transmit precoder for user (m, k), $\mathbf{w}_{m,k}^{\text{MRT}}$, can be defined as [31]:

$$\mathbf{w}_{m,k}^{\text{MRT}} = \frac{\mathbf{h}_{(m,k),m}^{H}}{\alpha_p}, \tag{2.4}$$

where $\alpha_p = \mathbf{h}_{(m,k),m}\mathbf{h}_{(m,k),m}^{H}$.

2.3.1.2 Zero Forcing (ZF)

The main goal of the ZF beamforming is to eliminate the intra-cell interference, without taking into account the noise. For a given user, it is done by making all the other users in the null space of the precoder. This is written in a mathematically way as

$$\mathbf{h}_{(m,j),m}\mathbf{w}_{m,k}^{\text{ZF}} = 0 \quad , \forall j \neq k. \tag{2.5}$$

Using a matrix notation, this condition is equivalent to

$$\mathbf{H}_m\mathbf{W}_m^{\text{ZF}} = \text{diag}(\sqrt{\mathbf{p}_m}), \tag{2.6}$$

with

$$\mathbf{H}_m \triangleq [\mathbf{h}_{(m,1),m}^{T}, \mathbf{h}_{(m,2),m}^{T}, \cdots, \mathbf{h}_{(m,K),m}^{T}]^{T}, \tag{2.7a}$$

$$\mathbf{W}_m \triangleq [\mathbf{w}_{m,1}, \mathbf{w}_{m,2}, \cdots, \mathbf{w}_{m,K}], \tag{2.7b}$$

$$\sqrt{\mathbf{p}_m} \triangleq [\sqrt{p_{m,1}}, \sqrt{p_{m,2}}, \cdots, \sqrt{p_{m,K}}], \tag{2.7c}$$

where $p_{m,k}$ is the transmit power for user (m, k), respecting the power constraint, with $\text{Tr}[\mathbf{w}_{m,k}\mathbf{w}_{m,k}^{H}] = p_k$, $\forall k$ connected to m. Therefore, the ZF precoder for the user (m, k), $\mathbf{w}_{m,k}^{\text{ZF}}$, can be obtained as [32]:

$$\mathbf{w}_{m,k}^{\text{ZF}} = \frac{\mathbf{h}_{(m,k),m}^{H}[\mathbf{H}_m\mathbf{H}_m^{H}]^{-1}}{\alpha_p}, \tag{2.8}$$

where $alph_p = |\mathbf{h}_{(m,k),m}^{H}[\mathbf{H}_m\mathbf{H}_m^{H}]^{-1}|^2$.

2.3.1.3 Minimum Mean Square Error (MMSE)

The MMSE beamforming seeks to minimize the mean square error (MSE) which is the difference between the received and decoded symbols described as

$$\text{MSE} = \sum_k \sum_m \mathbb{E}[\|y_{m,k} - x_{m,k}\|^2]. \tag{2.9}$$

Replacing (2.1) in (2.9), we have

$$\text{MSE} = \sum_{k}\sum_{m}\mathbb{E}\left[\|\mathbf{h}_{(m,k),m}\mathbf{w}_{m,k}x_{m,k} + \sum_{j,j\neq k}\mathbf{h}_{(m,k),m}\mathbf{w}_{m,j}x_{m,j} + \sum_{d,d\neq m}\sum_{j}\mathbf{h}_{(m,k),d}\mathbf{w}_{d,j}x_{d,j} + z_{m,k} - x_{m,k}\|^2\right]. \tag{2.10}$$

Hence, the MMSE optimization problem for a user (m, k) is given by

$$\begin{aligned}\min_{\mathbf{w}_{m,k}} \quad & \sum_{j,j\neq k}|\mathbf{h}_{(m,k),m}\mathbf{w}_{m,j}|^2 + \sum_{d,d\neq m}\sum_{j}|\mathbf{h}_{(m,k),d}\mathbf{w}_{d,j}|^2 + \sigma_{m,k}^2 - |\mathbf{h}_{(m,k),m}\mathbf{w}_{m,k}|^2 \\ \text{subject to} \quad & \mathbf{w}_{m,k}^H\mathbf{w}_{m,k} \leq p_{m,k}.\end{aligned} \tag{2.11}$$

Hence, the MMSE precoder, $\mathbf{w}_{m,k}^{\text{MMSE}}$, is given by [33]:

$$\mathbf{w}_{m,k}^{\text{MMSE}} = \frac{\left(\sum_{m=1}^{M}\sum_{k=1}^{K}\mathbf{h}_{(m,k),m}^H\mathbf{h}_{(m,k),m} + \mathbf{I}\sigma_{m,k}\right)^{-1}\mathbf{h}_{(m,k),m}^H}{\alpha_p}, \tag{2.12}$$

where $\alpha_p = \left|\left(\sum_{m=1}^{M}\sum_{k=1}^{K}\mathbf{h}_{(m,k),m}^H\mathbf{h}_{(m,k),m} + \mathbf{I}\sigma_{m,k}\right)^{-1}\mathbf{h}_{(m,k),m}^H\right|^2$.

2.3.2 Power Minimization

2.3.2.1 Problem Formulation

In the power minimization problem, proposed and solved by [17], the objective is to coordinate the BSs across multiple cells in a multi-antenna beamforming system. Hence, they can jointly optimize their respective beamformers to improve the overall system performance. The used criterion is to minimize the weighted total transmit power under SINR constraints. The problem can be written mathematically as:

$$\begin{aligned}\arg\min_{\mathbf{w}_{m,k}} \quad & \sum_{m}\sum_{k}\alpha_{m,k}\mathbf{w}_{m,k}^H\mathbf{w}_{m,k} \\ \text{s.t} \quad & \gamma_{m,k} \geq \widehat{\Gamma}_{m,k}, \forall k \in \mathcal{K},\end{aligned} \tag{2.13}$$

where $\widehat{\Gamma}_{m,k}$ represents the SINR (signal-to-interference-plus-noise ratio) target for user k in cell m and $\alpha_{m,k}$ is the weight factor.

The constraints in (2.13) is non-convex. However, they can be transformed into a second-order-cone constraint, so the problem can be solved by convex optimization.

In order to solve the optimization problem the downlink-uplink duality is used. According to the duality theorem, the same amount of power used to achieve a given SINR value for the downlink is exactly the same for the uplink, considering the same set of SINRs, where the uplink channels are found by reversing the inputs and outputs.

The Lagrangian dual of the optimization problem in (2.13) can be written as:

$$\begin{aligned} \arg\min_{\lambda_{m,k}} \quad & \sum_m \sum_k \lambda_{m,k} \sigma^2_{m,k} \\ \text{s.t} \quad & \Lambda_{m,k} \geq \widehat{\Gamma}_{m,k},\ \forall k \in \mathcal{K}, \end{aligned} \tag{2.14}$$

where

$$\Lambda_{m,k} = \max_{\widehat{\mathbf{w}}_{m,k}} \frac{\lambda_{m,k} |\mathbf{h}_{(m,k),m} \widehat{\mathbf{w}}_{m,k}|^2}{\sum_d \sum_{j,j\neq k} \lambda_{d,j} |\mathbf{h}_{(d,j),m} \widehat{\mathbf{w}}_{m,k}|^2 + \alpha_{m,k} \|\widehat{\mathbf{w}}_{m,k}\|^2}. \tag{2.15}$$

The vector $\widehat{\mathbf{w}}_{m,k}$ is the receiver precoder of the dual uplink formulation, and it is a scaled version of the optimal $\mathbf{w}_{m,k}$. The variable $\lambda_{m,k}$ is the corresponding dual uplink power associated to the constraints in (2.13).

2.3.2.2 Algorithm Description

The main idea for the algorithm to find the best precoders is to solve the dual uplink problem in order to find $\lambda_{m,k}$, then the corresponding $\widehat{\mathbf{w}}_{m,k}$. First, we write the Lagrangian of (2.14) as

$$\begin{aligned} \mathcal{L}(\mathbf{w}_{m,k}, \lambda_{m,k}) = & \sum_m \sum_k \lambda_{m,k} \sigma^2_{m,k} + \sum_m \sum_k \mathbf{w}^H_{m,k} \cdot \\ & \left[\alpha_{m,k} \mathbf{I} - \left(1 + \frac{1}{\widehat{\Gamma}_{m,k}} \right) \lambda_{m,k} \mathbf{h}^H_{(m,k),m} \mathbf{h}_{(m,k),m} + \sum_d \sum_j \lambda_{d,j} \mathbf{h}^H_{(d,j),m} \mathbf{h}_{(d,j),m} \right] \mathbf{w}_{m,k}. \end{aligned} \tag{2.16}$$

The next step is to take the gradient of (2.16) with respect to $\mathbf{w}_{m,k}$ and set it to zero. Then, we have

$$\left[\alpha_{m,k} \mathbf{I} - \left(1 + \frac{1}{\widehat{\Gamma}_{m,k}} \right) \lambda_{m,k} \mathbf{h}^H_{(m,k),m} \mathbf{h}_{(m,k),m} + \sum_d \sum_j \lambda_{d,j} \mathbf{h}^H_{(d,j),m} \mathbf{h}_{(d,j),m} \right] \mathbf{w}_{m,k} = 0. \tag{2.17}$$

Thus

$$\Sigma_{m,k} \mathbf{w}_{m,k} = \left(1 + \frac{1}{\widehat{\Gamma}_{m,k}} \right) \lambda_{m,k} \mathbf{h}^H_{(m,k),m} \mathbf{h}_{(m,k),m} \mathbf{w}_{m,k}, \tag{2.18}$$

with

$$\Sigma_{m,k} \triangleq \alpha_{m,k} \mathbf{I} + \sum_d \sum_j \lambda_{d,j} \mathbf{h}^H_{(d,j),m} \mathbf{h}_{(d,j),m}. \tag{2.19}$$

Then, a necessary condition for $\lambda_{m,k}$ can be obtained

$$\lambda_{m,k} = \frac{1}{\left(1 + \frac{1}{\widehat{\Gamma}_{m,k}} \right) \mathbf{h}_{(m,k),m} \Sigma_m^{-1} \mathbf{h}^H_{(m,k),m}}. \tag{2.20}$$

Solving the problem in (2.14) will lead us to find the receiver precoder of the dual uplink. The optimal beamforming vector $\mathbf{w}_{m,k}$, then, is found by scaling $\widehat{\mathbf{w}}_{m,k}$ as follows

$$\mathbf{w}_{m,k} = \sqrt{\delta_{m,k}} \widehat{\mathbf{w}}_{m,k}. \tag{2.21}$$

The $\delta_{m,k}$ values can be found by a procedure described in [16]. The iterative algorithm has its global convergence guaranteed and it can be summarized in Algorithm 1.

Algorithm 1 Power Minimization Algorithm for Problem (2.13)

1: **repeat**
2: Find the optimal uplink power allocation $\lambda_{m,k}$ using (2.20).
3: Find the optimal uplink receive beamformers.

$$\widehat{\mathbf{w}}_{m,k} = \left(\sum_{d} \sum_{j} \lambda_{d,j} \sigma^2_{d,j} \mathbf{h}^H_{(d,j),m} \mathbf{h}_{(d,j),m} + \sigma^2_{m,k} \alpha_{m,k} \mathbf{I} \right)^{-1} \mathbf{h}^H_{(d,j),m}. \tag{2.22}$$

4: Find the optimal precoders using (2.21).
5: **until** converge

Table 2.1 – Simulation Parameters.

Parameter	Value
Number of transmission time intervals (TTIs)	200
Number of antennas at each BS	3
Number of antennas per user	1
Number of users per cell	2
Minimum allowed distance between BS-user	10 m
User position	randomly placed inside BS radius
Base Station radius	250 m
Noise Power	$N_0 = -116.4$ dBm
Transmission Power	20 dBm
Path Loss [34]	$128.1 + 37.6 \log_{10}(d)$ (dB) d in km

Source: Created by the author.

2.3.2.3 Results

In this section we present simulation results to illustrate the performance of the Power Minimization algorithm. The scenario is composed by 3 BSs, each one equipped with 3 transmit antennas. For each cell we have 2 single antenna users, forming, therefore, a multi-user MISO system. The simulation parameters are described in Table 2.1.

For comparison, we include simulation results for MRT, which only cares about the direct link. The MRT precoders are given by (2.4). For each user we set the power minimization SINR target as the SINR achieved for this user if the MRT precoder is used, then we can make a fair comparison between both approaches.

As the SINR from both strategies is the same, we only plot the total consumed power, which can be seen in Figure 2.3. The plot shows the cumulative distribution function (CDF) of the total power consumed in all BSs for both strategies. It can be seen that the power minimization algorithm utilizes less power to achieve the same SINR target when compared to the matched channel filter, which always uses all available power. This result was expected because the BSs in the considered algorithm work in a coordinated way to mitigate their interference while they keep the same level of SINR.

Figure 2.3 – CDF plot of the total consumed power in all BS for power minimization algorithm versus MRT.

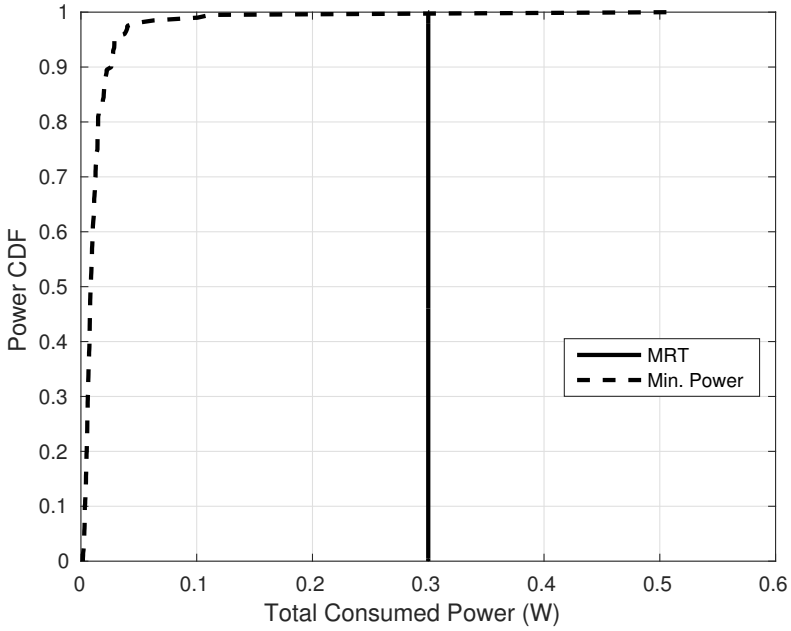

Source: Created by the author.

In Figure 2.4 we plot the total power consumed while the number of users per BS changes. From the plot, it can be seen that when the number of users per cell increases, the total power needed for achieving the same SINR also increases. This is due to the fact that the interference is proportional to the number of users, therefore, more users will result in more interference. Another reason is that now we have more users per BS to be served, therefore each BS will need to use more power to satisfy the QoS constraints.

2.3.3 Sum-Rate Maximization

2.3.3.1 Problem Formulation

The second problem of our interest is related to rate maximization. This is a classic optimization problem proposed and solved by various authors in the literature. We will use [18] as a reference to present a CBF centralized solution for the rate maximization problem. The parameters are described in Table 2.1

The system model is the same described in Section 2.2 and the optimization problem aims to maximize the weighted system sum-rate under power constraints. Then it can be formulated in the following way:

$$\begin{aligned} \arg\max_{\mathbf{w}_{m,k}} \quad & \sum_{m}\sum_{k} \alpha_{m,k}\log_2(1+\gamma_{m,k}) \\ \text{s.t} \quad & \sum_{k} \mathbf{w}_{m,k}^H \mathbf{w}_{m,k} \leq P_m, \quad \text{for } m = 1,\ldots,M, \end{aligned} \tag{2.23}$$

Figure 2.4 – Power consumed versus SINR target for Power Minimization Algorithm.

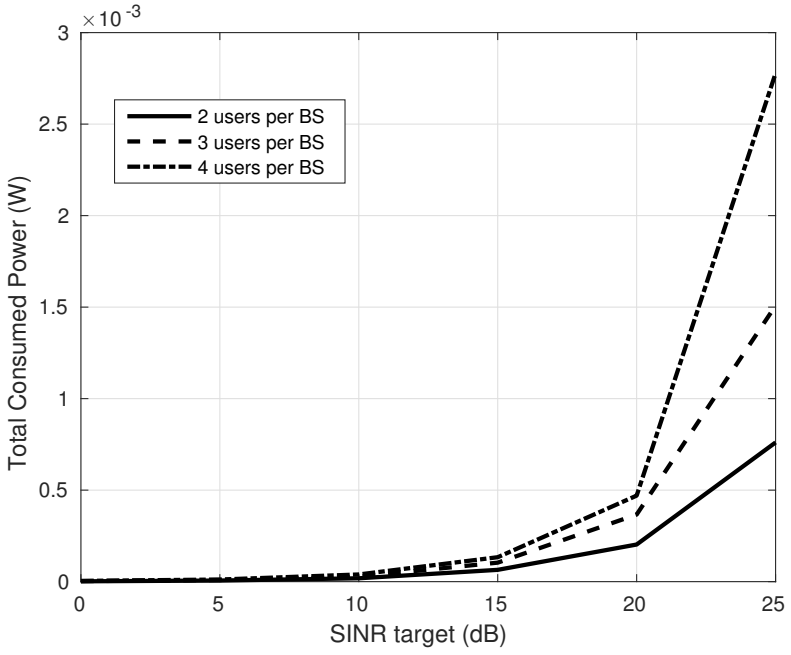

Source: Created by the author.

where P_m is the maximum power that can be consumed at BS m and $\alpha_{m,k}$ is the weight factor which reflects on the priority of the user.

The main objective of the work in [18] is to develop a low-complexity algorithm for solving (2.23). Then a centralized approach is the best choice is this case.

As done in the previous section, we can take the Lagrangian of the dual problem in (2.23) with respect to sum-power constraints. Let $\mathcal{T}$ represent the set of all precoders to be optimized and $\boldsymbol{\lambda}$ the set of all Lagrange multipliers, then we have:

$$\mathcal{L}(\mathcal{T}, \boldsymbol{\lambda}) = \sum_m \sum_k \frac{\alpha_{m,k}}{\ln 2} \ln(1+\gamma_{m,k}) + \sum_m \lambda_m \left[P_m - \sum_k \|\mathbf{w}_{m,k}\|^2 \right]. \tag{2.24}$$

By setting (2.24) to zero, we obtain:

$$(\mathbf{L}_{m,k} + \lambda_m \ln 2 \mathbf{I})\mathbf{w}_{m,k} = \frac{\alpha_{m,k}\mathbf{h}^H_{m,k}(m)\mathbf{h}_{m,k}(m)\mathbf{w}_{m,k}}{1 + \mathbf{w}^H_{m,k}\mathbf{h}^H_{(m,k),m}\mathbf{h}_{(m,k),m}\mathbf{w}_{m,k} + \mathcal{I}_{m,k}}, \tag{2.25}$$

where $\mathbf{L}_{m,k}$ is the leakage matrix for user (m, k) and it is defined by

$$\mathbf{L}_{m,k} \triangleq \sum_d \sum_j P_{d,j}\mathbf{h}^H_{(d,j),m}\mathbf{h}_{(d,j),m} - P_{m,k}\mathbf{h}^H_{(m,k),m}\mathbf{h}_{(m,k),m}, \tag{2.26}$$

with

$$P_{d,j} \triangleq \frac{\alpha_{d,j)}\gamma_{d,j}}{1 + \sum_m \sum_k \mathbf{w}^H_{m,k}\mathbf{h}^H_{(m,k),m}\mathbf{h}_{(m,k),m}\mathbf{w}_{m,k}}, \tag{2.27}$$

and $\mathcal{I}_{m,k}$ is the total co-channel interference power received at user (m, k), which is given by

$$\mathcal{I}_{m,k} = \sum_n \sum_j \mathbf{w}^H_{d,j}\mathbf{h}^H_{(m,k),d}\mathbf{h}_{(m,k),d}\mathbf{w}_{d,j} - \mathbf{w}^H_{m,k}\mathbf{h}^H_{(m,k),m}\mathbf{h}_{(m,k),m}\mathbf{w}_{m,k} \tag{2.28}$$

By adding the complementary slackness conditions

$$\lambda_m \left[P_m - \sum_k \mathbf{w}_{m,k}^H \mathbf{w}_{m,k} \right] = 0, \quad \text{for } m = 1, \ldots, M, \tag{2.29}$$

then we form a set of first-order conditions named KKT conditions.

2.3.3.2 Algorithm Description

The main idea of the algorithm proposed in [22] is to solve the KKT conditions. A central node is assumed, which has the knowledge of the CSI of all nodes.

Proposition: Let $\mathbf{B}_{m,k} = \mathbf{L}_{m,k} + (\lambda_m \ln 2)\mathbf{I}$. Then the optimal precoders for problem (2.23) have the following form[2]

$$\mathbf{w}_{m,k} = \beta_{m,k} \mathbf{B}_{m,k}^{\dagger} \mathbf{h}_{(m,k),m}, \tag{2.30}$$

where $\lambda_m \geq 0$ and $\beta_{m,k} \geq 0$ are constants to be determined. If $\lambda_m = 0$ the feasibility is only guaranteed if $\mathbf{h}_{(m,k),m} \in \text{range}\{\mathbf{L}_{m,k}\}$.

Otherwise, if $\mathbf{w}_{m,k} \neq 0$ and $\lambda_m \neq 0$, by (2.25) it is implied that $\mathbf{h}_{(m,k),m} \propto (\mathbf{L}_{m,k} + \lambda_m \ln 2\mathbf{I})\mathbf{w}_{m,k}$. Hence, the optimal precoder has the form $\mathbf{w}_{m,k} \propto (\mathbf{L}_{m,k} + \lambda_m \ln 2\mathbf{I})^{-1}\mathbf{h}_{(m,k),m}$.

If $\mathbf{w}_{m,k} \neq 0$, by plugging (2.30) in (2.24) and (2.30) in (2.23) we have the set of equations

$$\alpha_{m,k} \mathbf{h}_{(m,k),m} \mathbf{B}_{m,k}^{\dagger} \mathbf{h}_{(m,k),m}^H = 1 + \mathcal{I}_{m,k} + |\beta_{m,k}|^2 |\mathbf{h}_{m,k}(m) \mathbf{B}_{m,k}^{\dagger} \mathbf{h}_{(m,k),m}^H|^2, \tag{2.31}$$

$$\sum_k \|\beta_{m,k} \mathbf{B}_{m,k}^{\dagger} \mathbf{h}_{(m,k),m}^H\|^2 \leq P_m, \quad \text{for } m = 1, \ldots, M. \tag{2.32}$$

In order to solve the KKT conditions, we assume that we have an initial set of precoders $\tilde{\mathbf{w}}_{m,k}$, thus $\mathcal{I}_{m,k}$ and $\mathbf{L}_{m,k}$ can be easily computed. Then, we have now an updated expression for $\beta_{m,k}$, which is

$$|\beta_{m,k}|^2 = \frac{(\alpha_{m,k} \mathbf{h}_{(m,k),m} \mathbf{B}_{m,k}^{\dagger} \mathbf{h}_{(m,k),m}^H - \mathcal{I}_{m,k} - 1)^+}{|\mathbf{h}_{m,k}(m) \mathbf{B}_{m,k}^{\dagger} \mathbf{h}_{(m,k),m}^H|^2}, \tag{2.33}$$

where $x^+ = \max(x, 0)$. In [18], the authors say that λ_m can be calculated by solving (2.32) with equality via bisection method. If $\lambda_m > 0$ cannot be found, its value is set to zero. The algorithm for centralized CBF is then summarized in Algorithm 2.

2.3.3.3 Results

In this section we present simulation results to illustrate the performance of the Iterative CBF Sum-Rate Maximization algorithm. The scenario is the same described in Section 2.3.2.3 which is presented in Table 2.1.

[2] $(\cdot)^{\dagger}$ represents the pseudo-inverse operation.

Algorithm 2 Rate Maximization Algorithm for Problem (2.23)

Initialize $l_{\text{in,max}}$,$l_{\text{out,max}}$ and $\mathbf{w}_{m,k}$, $\forall k \in \mathcal{K}$
$l_{\text{out}} = 0$
repeat
    Compute $\mathbf{L}_{m,k}$ according to (2.26), $\forall k \in \mathcal{K}$
    $l_{\text{in}} = 0$
    repeat
        Compute $\mathcal{I}_{m,k}$ according to (2.28), $\forall k \in \mathcal{K}$
        for $m = 1, \ldots, M$ **do**
            Compute λ_m and $\beta_{m,k}$, for $i = 1, \ldots, K$, according to (2.32) and (2.33).
            Update $\mathbf{w}_{m,k}$, for $i = 1, \ldots, K$, according to (2.30).
        end for
        $l_{\text{in}} = l_{\text{in}} + 1$
    until not converged or $l_{\text{out}} < l_{\text{out,max}}$
    $l_{\text{out}} = l_{\text{out}} + 1$
until not converged or $l_{\text{in}} < l_{\text{in,max}}$

In Figure 2.5 we present a CDF plot comparing the sum capacity for Iterative CBF Sum-Rate Maximization and MRT. It is assumed that the precoder powers of the considered algorithm is the same as that of the MRT strategy, which means that both algorithms use all available power at the BSs. It can be seen that the studied algorithm outperforms the matched channel in terms of rate, leading to a significant improvement of the network capacity by optimizing the beam direction in order to mitigate intracell and intercell interference, as proposed by the algorithm.

Figure 2.5 – CDF plot of sum capacity for Sum-Rate Maximization algorithm versus MRT.

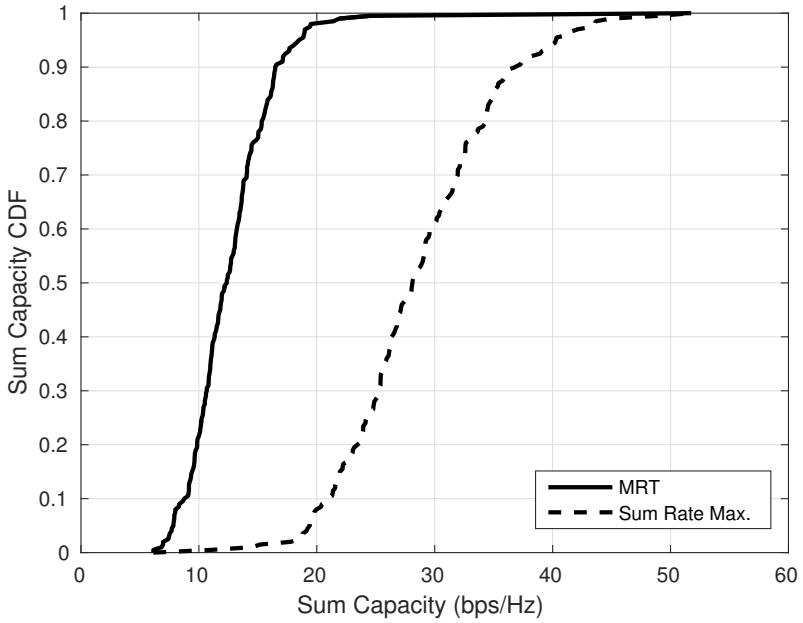

Source: Created by the author.

2.3.4 Energy Efficiency (EE)

2.3.4.1 Problem Formulation

In Sections 2.3.2 and 2.3.3 our objective was to minimize the total consumed power and maximize the total achievable rate, respectively. In this section these two problems will be combined into another problem that aims to maximize the energy efficiency of the system.

By using the work in [22] as a reference for this optimization problem, we define global energy efficiency (GEE) as the ratio between the sum of all users' rates (SUM-R) and the total consumed power in the network (SUM-P), including the losses in the amplifier and feeding. Then, mathematically, the optimization problem can be written as

$$\begin{aligned} \arg\max_{\mathbf{w}_{m,k}} \quad & \text{GEE} \\ \text{s.t} \quad & \sum_{k} \mathbf{w}_{m,k}^{H} \mathbf{w}_{m,k} \leq P_m, \quad \text{for } m = 1, \ldots, M \end{aligned} \tag{2.34}$$

where the GEE is defined by

$$\text{GEE} = \text{Sum-R}/\text{Sum-P}, \tag{2.35}$$

with

$$\text{Sum-R} = \sum_{m} \sum_{k} \alpha_{m,k} \log_2(1 + \gamma_{m,k}), \tag{2.36}$$

and

$$\text{Sum-P} = \sum_{m} \left(\theta_m + \sum_{k} \mathbf{w}_{m,k}^{H} \mathbf{w}_{m,k} \right), \tag{2.37}$$

where θ_m accounts for the losses in power such as signal processing and battery backup.

The problem in (2.34) is clearly a constrained non-convex optimization. Hence, its hard to solve and find a global maximum. The same approach used in the previous section can be used to find a suboptimal solution for the beamforming vectors. The algorithm will explore the KKT conditions for solving the optimization problem and it will run in a central node. This node has the CSI from all the coordinated BSs, so it calculates all the beamforming vectors and transmits them to the BSs.

2.3.4.2 Algorithm Description

As mentioned, the considered algorithm is based on the same KKT conditions found in Section 2.3.3. Then, we can write the following set of equations

$$\frac{\mathrm{d}\mathcal{L}(\mathcal{T}, \boldsymbol{\lambda})}{\mathrm{d}\mathbf{w}_{m,k}} = 0, \qquad \forall k \in \mathcal{K}, \tag{2.38}$$

$$\sum_{k} \mathbf{w}_{m,k}^{H} \mathbf{w}_{m,k} \leq P_m, \qquad \text{for } m = 1, \ldots, M, \tag{2.39}$$

$$\lambda_m \geq 0, \qquad \text{for } m = 1, \ldots, M, \tag{2.40}$$

$$\lambda_m \left[P_m - \sum_{k} \mathbf{w}_{m,k}^{H} \mathbf{w}_{m,k} \right] = 0, \qquad \text{for } m = 1, \ldots, M. \tag{2.41}$$

Algorithm 3 EE Algorithm for Problem (2.34)

Initialize $l_{\text{in,max}}$,$l_{\text{out,max}}$ and $\mathbf{w}_{m,k}$, $\forall k \in \mathcal{K}$
$l_{\text{out}} = 0$
while not converged or $l_{\text{out}} < l_{\text{out,max}}$ **do**
    Compute Sum-P, $\pi_{m,k}$ and $\mathbf{L}_{m,k}$ from (2.37), (2.43) and (2.26), $\forall k \in \mathcal{K}$
    $l_{\text{in}} = 0$
    while not converged or $l_{\text{in}} < l_{\text{in,max}}$ **do**
        Compute $\mathcal{I}_{m,k}$ according to (2.28)
        for $m = 1, \ldots, M$ **do**
            Compute λ_m and $\beta_{m,k}$, for $i = 1, \ldots, K$, according to (2.41) and (2.32).
            Update $\mathbf{w}_{m,k}$, for $i = 1, \ldots, K$, according to (2.45).
        end for
        $l_{\text{in}} = l_{\text{in}} + 1$
    end while
    $l_{\text{out}} = l_{\text{out}} + 1$
end while

By using similar calculations as those in Section 2.3.3, the KKT condition in (2.38) can be written as

$$[\mathbf{L}_{m,k} + (\pi_{m,k} + \lambda_m)\mathbf{I}]\mathbf{w}_{m,k} = \frac{\alpha_{m,k}\mathbf{h}^H_{(m,k),m}\mathbf{h}_{(m,k),m}\mathbf{w}_{m,k}}{1 + \mathbf{w}^H_{m,k}\mathbf{h}^H_{(m,k),m}\mathbf{h}_{(m,k),m}\mathbf{w}_{m,k} + \mathcal{I}_{m,k}} \times \frac{1}{\text{Sum-P}\ln 2}, \tag{2.42}$$

where a new variable $\pi_{m,k}$ is introduced. It represents the marginal decrease of GEE when there is an increase in the power consumption. Then it can be interpreted as a price to pay when the BS wants to use more power. It is defined by

$$\pi_{m,k} \triangleq \text{Sum-R}/\text{Sum-P}^2, \tag{2.43}$$

where $\mathbf{L}_{m,k}$ is defined in (2.26) and the new $P_{d,m}$ is

$$P_{d,j} \triangleq \frac{\alpha_{m,k}\gamma_{m,k}/(\text{Sum-P}\ln 2)}{1 + \sum_m \sum_k \mathbf{w}^H_{m,k}\mathbf{h}^H_{(d,j),m}\mathbf{h}_{(d,j),m}\mathbf{w}_{m,k}}. \tag{2.44}$$

By the same reasons discussed in Section 2.3.3, the beamforming vectors must have the form

$$\mathbf{w}_{m,k} = \beta_{m,k}\mathbf{B}^{\dagger}_{m,k}\mathbf{h}^H_{m,k}(m). \tag{2.45}$$

The algorithm, therefore, works as follows: assuming the power consumption and prices (interference and power) fixed, the beamforming vectors are computed. Then, the precoders are fixed, and power and prices are updated. The algorithm is summarized in Algorithm 3.

2.3.4.3 Results

In this section we present simulation results to illustrate the performance of the EE CBF algorithm. We consider, again, the same scenario in Section 2.3.2.3 which is described by Table 2.1.

Figure 2.6 – CDF plot of Sum Capacity for EE CBF versus MRT.

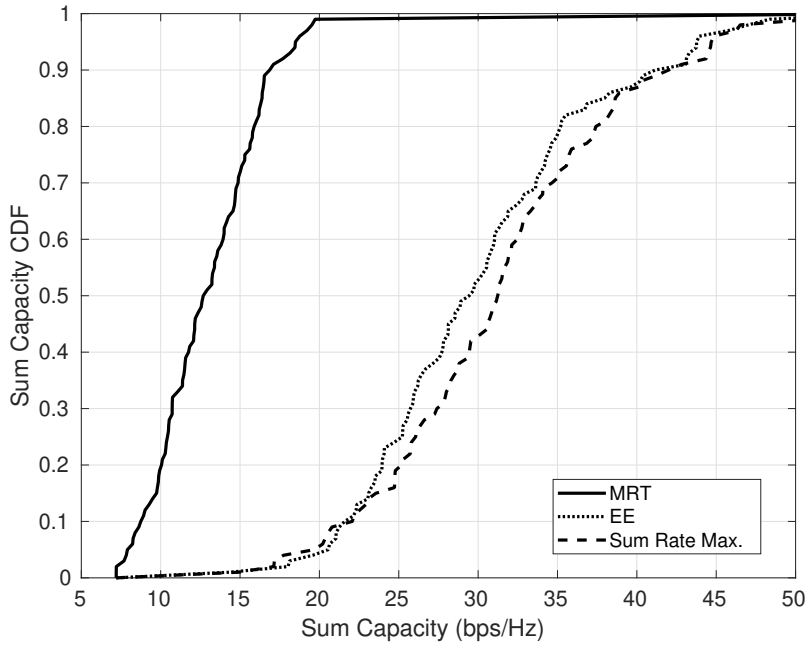

Source: Created by the author.

Figure 2.7 – Energy Efficiency for low power levels at the BSs.

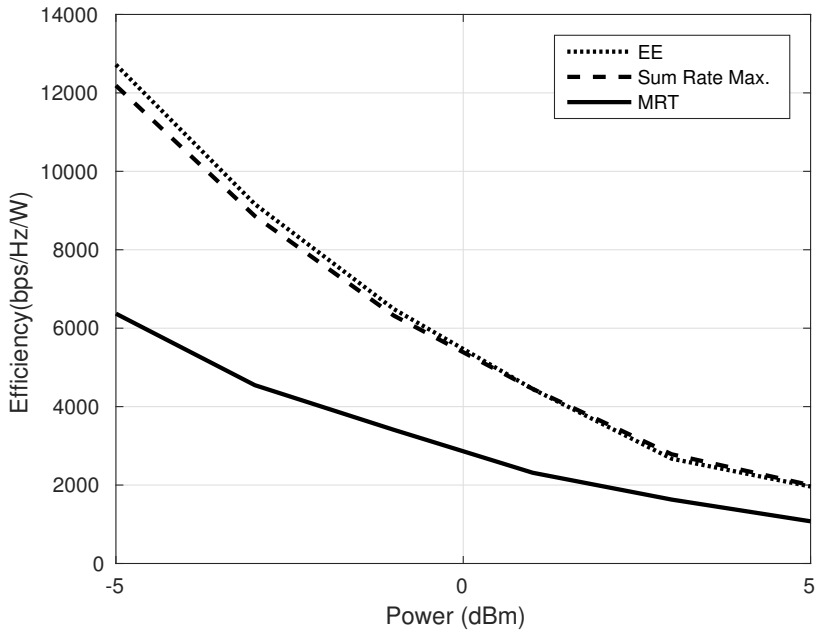

Source: Created by the author.

From Figure 2.6 it can be seem that the EE CBF algorithm outperforms both MRT and rate maximization in achievable sum capacity using the same amount of power. This happens because the EE CBF works in a similar way to the Iterative CBF Rate Maximization algorithm but it takes into account the marginal decrease of the efficiency, than it has a small improvement

in system capacity.

In Figure 2.7 we compare the energetic efficiency for all three approaches. We vary the BS transmission power from -5 dBm to 5 dBm per BS, so that we can compare the results in a region where the interference is not so strong. As expected, the matched channel presents the worst performance among all, because it only cares about the directed channel, so it does not suppress any interference, therefore, it achieves less rate with the same amount of power. From the plot, we can see that for low power levels the EECBF presents better performance.

However the performance gap gets lower when the power increases, which can be seen in Figure 2.8, where we consider a moderate level of power at the BSs [22]. Both algorithms have the same structure for finding the precoders and for allocating power, therefore the low performance gap can be explained. In addition, we can see from the plot that, when we increase the maximum available transmission power the EE decreases. It happens because the EE is a ratio between rate and power, but the rate increases with only the log of the power.

Figure 2.8 – Energy Efficiency EE CBF for moderate power levels at the BSs.

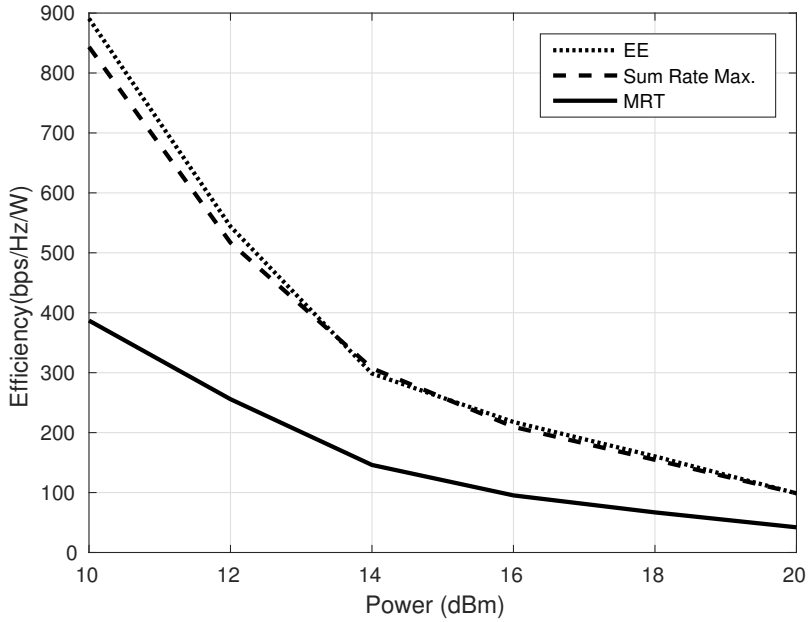

Source: Created by the author.

2.4 Concluding Remarks

In this chapter we presented an overview of the coordinated beamforming, where we described the three BF classical approaches: MRT, ZF and MMSE and three different optimization problems: power minimization [17], sum-rate maximization [18] and energy efficiency [22], which were formulated and solved by using methods known in the literature and assuming a centralized solution.

The centralized approach used by these three works is useful when there is a central unity that can measure all the channels between the BSs and their users. It does not utilize local BS processing, so it saves power at the BSs but requires the CSI from all nodes.

The distributed beamforming approach would be the most suitable choice for the emerging 5G networks, since it takes into account only the local information at each cell for finding the precoders and receive filters.

The decentralized approach is like a medium term between centralized and distributed since a central unity is not required. The precoders are all computed at each BS, but it still needs all interference links among all users to find the optimal solution, which makes the decentralized approach not suitable for 5G.

Therefore, as we are interested in solutions for the next generation of cellular networks, in the next chapters we will explore the distributed beamforming algorithms.

3 PRICING-BASED DISTRIBUTED BEAMFORMING FOR DYNAMIC TIME DIVISION DUPLEXING SYSTEMS

Multi-cell dynamic time division duplexing (TDD) systems make it possible to adapt the number of UL and DL time slots in each cell to the prevailing cell-wide traffic demand. Although dynamic TDD systems can be advantageously deployed in scenarios in which the UL and DL traffic demands are asymmetric and time-varying, dynamic TDD systems give rise to BS-to-BS interference and UE-to-UE interference that negatively impact the system performance.

In this chapter, we propose employing a distributed beamforming scheme to mitigate the BS-to-BS interference and thereby to improve the uplink performance. Specifically, the proposed scheme uses interference pricing to find the appropriate precoder vectors at the BSs, which also improves the SINRs performance in the DL. We compare the performance of the PBA BF scheme with that of ZF BF in an outdoor picocell environment specified by the 3GPP using a realistic system simulator.

We find that the proposed pricing-based (PB) scheme boosts the SINRs in the UL at the expense of a small degradation of the DL SINRs compared with the ZF scheme. On the other hand, the PB BF approach can significantly reduce the DL transmit power levels and thereby improve the overall energy efficiency of the system.

This chapter is structured as follows. In Section 3.1 we present an introduction about dynamic TDD systems. Section 3.2 discusses related works and the contributions of this chapter. The dynamic TDD system model is described in Section 3.3. Section 3.4 formulates the the BF optimization problem and proposes a PBA to solve this problem. An analysis about the convergence, signaling overhead and complexity is also provided. In Section 3.5 we propose a suboptimal approach for the PB problem which converges in less iterations and does not utilize an optimization routine. Simulation results are shown and discussed in Section 3.6 while, finally, in Section 3.7 we present the conclusions for the presented chapter and some perspective for future works.

3.1 Introduction

Multi-cell dynamic TDD systems make it possible to adapt the number of UL and DL time slots in each cell to the prevailing cell-wide traffic demand [3]. LTE systems, standardized by the 3GPP, for example, support the dynamic allocation of subframes to UL and DL transmissions [4]. Such dynamic TDD systems better support asymmetric and fluctuating traffic demands in both homogeneous and heterogeneous environments than systems with fixed subframe allocations [5, 35]. As it is intuitively clear, this gain increases as the traffic asymmetry increases and can reach up to 200 percent packet throughput gains in a 10 MHz system with reasonably realistic assumptions [6].

Next 5G systems will, among another requirements, demand more carrier bandwidth in order to accommodate high data volume. In this case, the frequency division duplex (FDD) may not be the best choice due to the necessity of allocation for both direct and reverse links, therefore, TDD can be the natural solution for next generation networks having a better performance when a large amount of data is transmitted [36].

In order to accommodate the network traffic fluctuations, LTE release 12 has introduced the eIMTA concept [37]. According to this release of 3GPP, there are 7 different available UL-DL configurations on TDD LTE, as shown in Table 3.1. The 'D' and 'U' subframes refer to a DL and UL subframe, respectively, and 'S' is a special subframe related to the guard interval, which can sometimes be used for DL transmission.

Table 3.1 – Dynamic TDD UL-DL configuration on TDD LTE.

UL - DL configuration	Subframe Number									
	0	1	2	3	4	5	6	7	8	9
0	D	S	U	U	U	D	S	U	U	U
1	D	S	U	U	D	D	S	U	U	D
2	D	S	U	D	D	D	S	U	D	D
3	D	S	U	U	U	D	D	D	D	D
4	D	S	U	U	D	D	D	D	D	D
5	D	S	U	D	D	D	D	D	D	D
6	D	S	U	U	U	D	S	U	U	D

Source: Created by the author.

When classic TDD is applied, all BSs within a region choose the same configuration. This strategy works well when the traffic conditions among the BSs are similar, which is not the case for 5G systems. In such systems there are different types of devices, with different types of traffic and requirements for nearby BSs. Therefore, dynamic TDD can be used to improve the network throughput performance when compared to the classic TDD approach [38].

In eIMTA dynamic TDD, the BS can select one of the available configurations (the DL/UL ratio varying from 40/60 to 90/10, depending on the selected mode [4]) for adjusting the UL-DL rate for data transmission. This choice, for a given cell or in a specific subframe, is up to the Operator/Vendor and it can be done based on a smart adaptation to varying traffic loads or in order to mitigate the possible interference between adjacent cells [39].

Table 3.2 summarizes the eIMTA configurations. There are, at least, one subframe for UL and four subframes for DL (if the special subframes are used for DL), and five flexible subframes, 'F', which can be used either for DL or UL transmission, depending on which configuration the BS will choose.

This flexibility of choosing different configurations for nearby BSs leads to a high interference scenario. In order to illustrate this impact, consider a two-cell system, each one with a single user, as shown in Figures 3.1 and 3.2.

Figure 3.1 shows the classic TDD operation, where cell 1 and cell 2 choose configu-

Table 3.2 – Summary of dynamic TDD configurations.

Subframe Number									
0	1	2	3	4	5	6	7	8	9
D	S	U	F	F	D	S/D	F	F	F

Source: Created by the author.

Figure 3.1 – Interference situation on TDD scenario at TTI

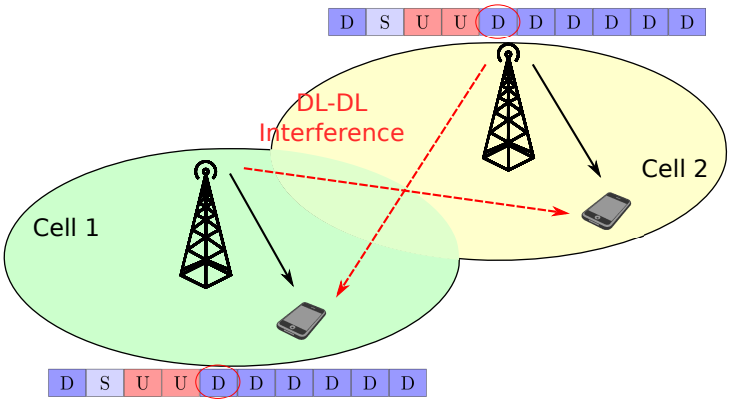

Source: Created by the author.

Figure 3.2 – Interference situation on dynamic TDD scenario at TTI

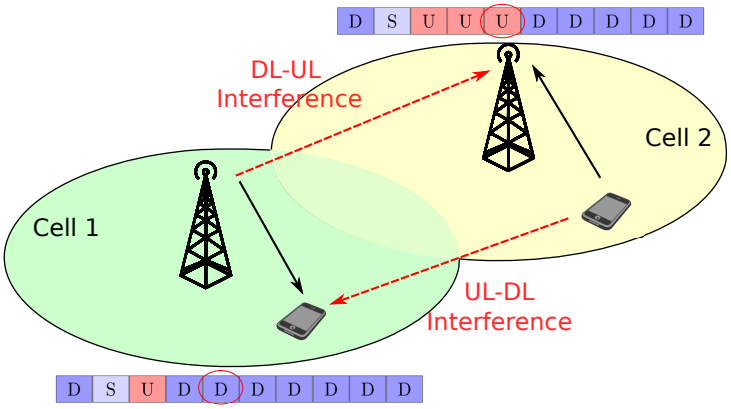

Source: Created by the author.

ration 4 in Table 3.1. By taking as reference the fifth transmission time interval (TTI), both cells are performing DL transmission, a situation in which only one type of interference occurs. This kind of problem has been exhaustively studied in the literature, leading to classic solutions for dealing with interference as presented on Chapter 2.

On the other hand, dynamic TDD systems may give rise to more types of interference, including BS-to-BS and UE-to-UE interference due to conflicting TDD configurations in neighbor cells, synchronization errors, or a lack of synchronism among neighbor cells [6, 7], as shown in Figure 3.2. In order to adapt the cell traffic, each one has chosen different TDD configurations (#5 for cell 1 and #3 for cell 2) leading to downlink-to-uplink interference, between BSs, and uplink-to-downlink interference, between users. As the power for DL transmission is usually

larger than that of the UL mode, the UL suffers more from DL interference. Therefore, the UL is often the bottleneck of the network [40].

Recognizing the engineering tradeoff between adapting the TDD configuration to the current traffic demands and causing more interference in neighbor cells, the 3GPP is currently working on eIMTA schemes [3, 4]. Also, previous works have proposed multi-cell coordination, assisted either by centralized or distributed algorithms to mitigate intercell interference, including BS-to-BS and UE-to-UE interference [6, 35, 41]. However, these works do not make use of the evolving multiple antenna capabilities, including full dimension and massive MIMO transceivers at BSs and the emerging multi-antenna capabilities at UEs.

A related line of research suggests that, in multi-cell MIMO systems, coordinated BF is an efficient technique to mitigate intercell interference and increase the SINR and achievable capacity for cell edge users. Coordinated BF is attractive because it does not require sharing the data symbols across multiple transmission points, as opposed to coordinated multipoint transmissions. Recently, low overhead distributed coordinated BF schemes have been proposed that accurately approximate the performance of centralized algorithms [42, 43]. An alternative and promising approach to designing distributed algorithms for interference management in MIMO systems, based on interference pricing, was proposed by [44]. According to this approach, each receiver announces an interference price, defined as the marginal decrease in capacity due to an increase in interference. Given the interference prices announced by neighboring receivers, and also given knowledge of the corresponding cross-channel matrices, each transmitter can update the transmit power levels and precoding matrices to maximize a utility function that incorporates the own capacity and the cost of the caused interference. However, the overall UL/DL system performance under asymmetric traffic load situations or unequal cell loads has not been studied in these works.

On the other hand, the results reported in [45, 46] indicate that when perfect channel state information at the transmitter (CSIT) is available at the BSs of a massive MIMO system, simple fully distributed per-cell BF schemes can offer performance similar to a more complex centralized or distributed multi-cell optimization. While this is good news for system designers, since it reduces the need for multi-cell coordination, this result is not directly applicable to dynamic TDD and eIMTA systems that need to manage BS-to-BS and UE-to-UE interference, in addition to the multi-cell interference present in both traditional and dynamic TDD systems.

3.2 Related Works and Contribution of the Chapter

Interference management specifically in dynamic TDD systems has been addressed by both the research and system developer communities since the standardization of eIMTA schemes started in the 3GPP [3, 37]. The strategies to deal with dynamic TDD specific interference situations can be categorized as follows:

- Cell clustering based schemes [47, 48, 49];

- PC based schemes [35, 50, 51, 52, 53, 54];
- Interference cancellation and IA based approaches [55];
- Resource allocation [56];
- Coordinated BF algorithms for co-channel interference mitigation [18, 21, 28];
- Interference PB schemes to penalize interference [19, 20, 57, 58, 59, 60, 61];
- Combinations of the above [5].

In cell clustering schemes, neighboring cells are organized in a cluster, such that cells within the cluster choose the same TDD configuration and avoid dynamic TDD interference within the cluster [47, 48, 49]. The 3GPP Technical Report [47] refers to cell clustering as a potential scheme for interference mitigation, but it does not determine what metric should be considered to form the clusters.

In [48], the authors present a centralized clustering algorithm combined with the configuration of DL and UL TDD directions. In [49], the clusters are formed based on a fixed coupling loss and dynamic traffic requirement criteria which are compared with the dynamic cluster based interference mitigation and traffic adaptation scheme. While clustering schemes effectively avoid BS-to-BS and UE-to-UE interference, they limit the capability of traffic adaptation and suffer from border effects between clusters.

PC based schemes developed for dynamic TDD systems employ two distinct approaches to mitigating intercell interference [35, 50, 51, 52, 53, 54]. The first approach allocates higher UL power levels to mobile stations [50], so that they can compensate for the BS-to-BS interference suffered from transmitting neighbor BSs. Obviously, this approach implies increased power consumption at the mobile terminal that can be particularly severe for cell edge users. The second approach reduces the transmit power at the BS side during a BS transmission [51, 52, 53], when a mobile station is performing an UL transmission. The work in [51] proposed a downlink power reduction from 24 dB to 20 dB in the flexible subframes. The authors in [52] propose an adaptive DL PC for a macrocell scenario based on the distance between the BSs. However, this scenario is not representative for next 5G networks in which the cells would be smaller. In [53] the power control proposed scheme reduces the DL power with aperiodic almost blank subframe patterns. A combination of these two approaches is also used in the literature [35, 54] to find the best power allocation equilibrium for DL and UL transmissions. In [35] the authors consider a phanton cell architecture where both DL and UL UEs perform an open loop PC scheme based on a target SINR while in [54] the values for DL power reduction and UL power boost are fixed.

As it will be described on Chapter 5, the IA is a linear precoding technique which is based on the idea of separating the useful signal and interference received in different subspaces. The work in [55] applies joint IA BF to solve the interference problem for dynamic TDD

networks. However, this work considers a three-cell TDD system, which is not a realistic model of systems consisting of a great number of cells.

Another approach to mitigate the interference on dynamic TDD network is based on resource allocation. Reference [56] proposes heuristics to coordinate the transmission among multiple users in different cells without exploiting the spatial dimension to mitigate interference.

Recall from Chapter 2, BF refers to a spatial filtering applied at the transmitter and/or receiver in order to favor some spatial directions over others. Hence, the interference in a multi-antenna scenario can be mitigated by the spatial filter and the system performance can be improved but none of them has considered a dynamic TDD scenario. Many works designed BF algorithms for co-channel interference mitigation. Reference [18] proposes a coordinated linear BF for the multi-cell BS interference channel. By having a set of coordinated BSs, the authors have found the optimum BF vectors that maximize the instantaneous weighted sum-rate. Even though they do not consider a distributed algorithm in their work, they show that the proposed algorithm can be implemented in a distributed way. Reference [21] investigates coordinated BF based on EE for multi-cell MISO systems, which can be applied in a decentralized way. In [28], the authors design a distributed BF algorithm that maximizes the utility function and solves the rate outage constrained problem for a MISO channel, assuming that CSI is known by the transmitters.

Another approach for the MISO-interference channel (MISO-IC) is based on the *interference pricing* idea, according to which users are penalized by the amount of interference they cause which was explored in[19, 20, 57, 58, 59, 60, 61]. In [19], the interference pricing is combined among the users in such a way that the transmitters can improve their own utility functions, which is penalized by the interference caused to other users.

On the other hand, the work in [20] introduces the notion of *interference equilibrium* in which an algorithm based on interference pricing, BF design and power allocation is proposed. The proposed algorithm can be implemented in a distributed way and it was shown to converge to an interference equilibrium point. References [57, 58] also have proposed a PB optimization problem for the MISO-IC, but different from the previews works [57] have formulated a non-cooperative PB game to maximize the for some popular network utilities while [58] have considered an interference channel K par users network having the EE as the utility function. On the other hand, the works in [59, 60, 61] have focused on applying the pricing in cognitive radio networks, while [59] and [61] aim to maximize the MIMO secondary network performance by finding the best set of precoders, [60] used the PB approach to find the best spectrum allocation scheme.

In this chapter, we seek an answer to the question of whether interference PB multi-cell BF can help to mitigate the UL and DL interference in dynamic TDD systems. Although this question is highly relevant from a research and system development perspective, it has not been adequately addressed by previous works, as discussed further in the next section. To this end, we propose a distributed, interference PB optimization problem that takes into account the

specific aspects of multi-cell dynamic TDD systems.

Specifically, we propose a distributed BF algorithm, according to which each BS maximizes a utility function that is a linear combination of a utility function depending on the achieved rate, and a penalty function that takes into account the caused interference at neighboring BSs that are in receiving (UL) mode. The sensitivity of the own utility with respect to the caused interference can be thought of as the 'interference price' that is periodically updated by a coarse scale inter-BS signaling mechanism.

Unlike previous works, in the present chapter we consider a dynamic TDD MISO network where the BSs operate in either DL or UL mode in the 3GPP picocell scenario [37]. We assume perfect CSI at the nodes and assume that all the channels remain constant during a TDD frame (block fading). In this scenario, the UL UEs suffer from interference caused primarily by surrounding BS transmissions. Therefore, our main objective is to ensure a performance gain for UL users by carefully choosing the BS precoders, without the need of increasing the power of UL UEs. To this end, we formulate the problem as an optimization task that involves penalizing the caused interference. To solve this problem, a distributed BF algorithm and associated signaling support are proposed, which find the precoders for DL users. This scheme is tested in a realistic system simulator. Numerical results indicate a performance boost for UL users and significant power saving gains at the BSs at the expense of a small degradation in the DL capacity as compared with the ZF and MRT BF schemes.

We summarize the main contributions of this chapter as follows.

- We describe a system model for multi-user multi-cell MISO dynamic TDD networks and we formulate an optimization problem on which the BS transmission is penalized by the interference caused on UL users;
- We present a PB distributed BF (PBA) for DL BSs to solve this optimization problem which works in two modes, sequential and parallel. We have proved the convergence of sequential approach, we also have detailed the signaling overhead and the complexity analysis for both operation modes. In addition, we have presented the sufficient conditions when the semidefinite relaxation problem yields the rank-one solution;
- It is shown that the UL performance can be improved by the right choice of BS BF and we compare the presented algorithm with the classical MRT and ZF solutions;
- We show that, when increasing the number of antennas, the performance of MRT does not approach ZF in the case of MISO dynamic TDD systems.

3.3 System Model

We consider a multi-cell multi-user MISO network operating in dynamic TDD mode. Each cell has one BS equipped with N_{BS} antennas. BSs operate in either DL or UL mode, and each one serves K single antenna users.

Let $\mathcal{D}$ and $\mathcal{U}$ be the set of BSs, which are in DL and UL mode, respectively, in a given time slot, with $\mathcal{D} \cap \mathcal{U} = \emptyset$. Furthermore, $\mathcal{K} \triangleq \{1, 2, \cdots, K\}$ represents the set of users inside a cell. Our underlying assumption is that the sets $\mathcal{D}$ and $\mathcal{U}$ are formed by some suitable scheduling mechanism executed prior to the dynamic TDD transmission and reception. With this assumption, for a given cell $m \in \mathcal{D}$, the DL received signal for a given user k is given by:

$$y_{m,k}^{\mathrm{DL}} = \underbrace{\sqrt{p_{m,k}}\mathbf{h}_{(m,k),m}\mathbf{w}_{m,k}x_{m,k}}_{\text{useful signal}} + \underbrace{\sum_{\substack{j\in\mathcal{K}\\ j\neq k}} \sqrt{p_{m,j}}\mathbf{h}_{(m,k),m}\mathbf{w}_{m,j}x_{m,j}}_{\text{DL Intracell Interference}} + \underbrace{\sum_{\substack{d\in\mathcal{D}\\ d\neq m}}\sum_{j\in\mathcal{K}} \sqrt{p_{d,j}}\mathbf{h}_{(m,k),d}\mathbf{w}_{d,j}x_{d,j}}_{\text{DL Intercell Interference}} + \underbrace{\sum_{u\in\mathcal{U}}\sum_{l\in\mathcal{K}} \sqrt{q_{u,l}}b_{(m,k),(u,l)}x_{u,l}}_{\text{UE-to-UE Interference}} + \underbrace{z_{m,k}}_{\text{noise}}, \tag{3.1}$$

where $\mathbf{h}_{(m,k),d} \in \mathbb{C}^{1\times N_{\mathrm{BS}}}$ is the channel gain between a BS d and a UE k served by a BS m, $\mathbf{w}_{d,j} \in \mathbb{C}^{N_{\mathrm{BS}}\times 1}$ is the DL transmit BF vector of BS d for DL UE j, $x_{d,j}$ is the data symbol transmitted between nodes d and j (BS-UE or UE-BS depending on the link direction), with $\mathbb{E}[|\mathbf{w}_{d,j}x_{d,j}|^2] = 1$, $b_{(m,k),(u,l)}$ is the interference channel gain between UL UE l belonging to BS u and DL UE k served by BS m, $p_{\{\cdot\}}$ is the transmission power to a DL user, $q_{\{\cdot\}}$ is the transmission power of an UL user, $z_{m,k}$ is the additive white Gaussian noise (AWGN) with zero mean and variance σ_k^2.

Let us consider, without loss of generality, $\mathbf{W}_{m,k} = p_{m,k}\mathbf{w}_{m,k}\mathbf{w}_{m,k}^H$, therefore the achievable rate in the DL direction for a user k in a cell m is given by the Shannon formulation

$$C_{m,k}^{\mathrm{DL}}(\mathbf{W}_{m,k}) = B\log_2(1+\gamma_{m,k}^{\mathrm{DL}}(\mathbf{W}_{m,k})) \quad \text{bps}, \tag{3.2}$$

where B is the system bandwidth and $\gamma_{m,k}^{\mathrm{DL}}(\mathbf{W}_{m,k})$ is the DL SINR, which is defined by

$$\gamma_{m,k}^{\mathrm{DL}}(\mathbf{W}_{m,k}) = \frac{S_{m,k}^{\mathrm{DL}}(\mathbf{W}_{m,k})}{I_{m,k}^{\mathrm{DL}} + \sigma_{m,k}^2}, \tag{3.3}$$

where

$$S_{m,k}^{\mathrm{DL}}(\mathbf{W}_{m,k}) = \mathbf{h}_{(m,k),m}\mathbf{W}_{m,k}\mathbf{h}_{(m,k),m}^H, \tag{3.4a}$$

$$I_{m,k}^{\mathrm{DL}} = \sum_{\substack{j\in\mathcal{K}\\ j\neq k}} \mathbf{h}_{(m,k),m}\mathbf{W}_{m,j}\mathbf{h}_{(m,k),m}^H + \sum_{\substack{d\in\mathcal{D}\\ d\neq m}}\sum_{j\in\mathcal{K}} \mathbf{h}_{(m,k),d}\mathbf{W}_{d,j}\mathbf{h}_{(m,k),d}^H + \sum_{u\in\mathcal{U}}\sum_{l\in\mathcal{K}} q_{u,l}|b_{(m,k),(u,l)}|^2. \tag{3.4b}$$

On the other hand, for cell n operating in UL mode, the received signal related to a given UL UE r can be expressed as:

$$y_{n,r}^{\mathrm{UL}} = \underbrace{\mathbf{v}_{n,r}^H \mathbf{h}_{n,(n,r)}^H \sqrt{q_{n,r}} x_{n,r}}_{\text{useful signal}} + \underbrace{\mathbf{v}_{n,r}^H \sum_{\substack{l\in\mathcal{K}\\ l\neq r}} \sqrt{q_{n,l}} \mathbf{h}_{n,(n,l)}^H x_{n,l}}_{\text{UL Intracell Interference}} + \underbrace{\mathbf{v}_{n,r}^H \sum_{\substack{u\in\mathcal{U}\\ u\neq n}} \sum_{l\in\mathcal{K}} \sqrt{q_{u,l}} \mathbf{h}_{n,(u,l)} x_{u,l}}_{\text{UL Intercell Interference}} +$$

$$+ \underbrace{\mathbf{v}_{n,r}^H \left[\sum_{d\in\mathcal{D}} \left(\mathbf{G}_{n,d} \sum_{j\in\mathcal{K}} \sqrt{p_{d,j}} \mathbf{w}_{d,j} x_{d,j} \right) \right]}_{\text{BS-to-BS interference}} + \mathbf{v}_{n,r}^H \underbrace{\mathbf{z}_{n,r}}_{\text{noise}}, \tag{3.5}$$

where $\mathbf{v}_{n,r} \in \mathbb{C}^{N_{\mathrm{BS}}\times 1}$ is the receiver BF vector of BS n for UL UE r, $\mathbf{G}_{n,d} \in \mathbb{C}^{N_{\mathrm{BS}}\times N_{\mathrm{BS}}}$ is the channel gain between BS n and BS d and $\mathbf{z}_{n,r} \in \mathbb{C}^{N_{\mathrm{BS}}\times 1}$ is a vector with independent AWGN noise.

The capacity for an UL UE r in a cell n is given by:

$$C_{n,r}^{\mathrm{UL}}(\mathbf{v}_{n,r}) = B \log_2(1 + \gamma_{n,r}^{\mathrm{UL}}(\mathbf{v}_{n,r})) \quad \text{bps}, \tag{3.6}$$

where $\gamma_{n,r}^{\mathrm{UL}}(\mathbf{v}_{n,r})$ is the UL SINR expressed by

$$\gamma_{n,r}^{\mathrm{UL}}(\mathbf{v}_{n,r}) = \frac{\mathbf{v}_{n,r}^H S_{n,r}^{\mathrm{UL}}(\mathbf{v}_{n,r}) \mathbf{v}_{n,r}}{\mathbf{v}_{n,r}^H (I_{n,r}^{\mathrm{UL}} + \mathbf{I}_n \sigma_{n,r}^2) \mathbf{v}_{n,r}}, \tag{3.7}$$

where

$$S_{n,r}^{\mathrm{UL}}(\mathbf{v}_{n,r}) = q_{n,r} \mathbf{h}_{n,(n,r)}^H \mathbf{h}_{n,(n,r)}, \tag{3.8a}$$

$$I_{n,r}^{\mathrm{UL}} = \sum_{\substack{l\in\mathcal{K}\\ l\neq r}} q_{n,l} \mathbf{h}_{n,(n,l)}^H \mathbf{h}_{n,(n,l)} + \sum_{\substack{u\in\mathcal{U}\\ u\neq n}} \sum_{l\in\mathcal{K}} q_{u,l} \mathbf{h}_{n,(u,l)}^H \mathbf{h}_{n,(u,l)} + \sum_{d\in\mathcal{D}} \sum_{j\in\mathcal{K}} \mathbf{G}_{n,d} \mathbf{W}_{d,j} \mathbf{G}_{n,d}^H. \tag{3.8b}$$

3.4 Pricing-Based Algorithm (PBA)

3.4.1 Beamforming Problem

In dynamic TDD networks, due to the BS-to-BS interference, the UL reception is strongly affected by the DL transmission of nearby BSs. As we are considering a MISO network, the formulation of the associated optimization problem has to take into account the following requirement: the DL BSs should adjust their beam directions and transmit power in order to limit the BS-to-BS interference.

To this end, we will make use of *interference pricing* [62]. The main idea of this strategy is to enable BSs, that are in DL mode, to take into account the interference they cause at neighbor BSs. This is achieved by penalizing the DL user's utility by the following penalty factor:

$$\pi_{i,j} = -\frac{\partial C_{i,j}}{\partial I_{i,j}} = \frac{B}{\log 2} \left(\frac{1}{I_{i,j}} - \frac{1}{I_{i,j} + s_{i,j}} \right), \tag{3.9}$$

where $\pi_{i,j}$ is the interference pricing associated to the user j connected to the BS i. If i, j is in DL mode, then

$$C_{i,j} \triangleq C_{i,j}^{\mathrm{DL}}(\mathbf{W}_{i,j}), \tag{3.10a}$$

$$s_{i,j} \triangleq S_{i,j}^{\mathrm{DL}}(\mathbf{W}_{i,j}), \tag{3.10b}$$

$$I_{i,j} \triangleq I_{i,j}^{\mathrm{DL}} + \sigma_{i,j}^2. \tag{3.10c}$$

Otherwise, the user i, j is in the UL mode, then

$$C_{i,j} \triangleq C_{i,j}^{\mathrm{UL}}(\mathbf{v}_{i,j}), \tag{3.11a}$$

$$s_{i,j} \triangleq \mathbf{v}_{i,j}^H S_{i,j}^{\mathrm{UL}}(\mathbf{v}_{i,j})\mathbf{v}_{i,j}, \tag{3.11b}$$

$$I_{i,j} \triangleq \mathbf{v}_{i,j}^H (I_{i,j}^{\mathrm{UL}} + \mathbf{I}_n \sigma_{i,j}^2)\mathbf{v}_{i,j}. \tag{3.11c}$$

3.4.2 Optimization Problem

In our BF design we are interested in increasing the UL transmission rate and preserving a reasonable performance for DL UEs by reducing the BS-to-BS interference. A natural and intuitive metric to capture this trade-off is setting the capacity in (3.2) such that the utility function is maximized. By doing this, the prices represent the marginal decrease in the users' capacity relative to the marginal increase in their received DL interference. As a consequence, even if we do not directly formulate at the BS an optimization problem for UL UEs, the prices control the amount of interference received by those users, improving UL performance. Therefore, the PB scheme works in a similar way in the DL as the closed loop PC standardized for LTE [63] works in the UL.

By applying this pricing approach, our main goal is to enforce the DL users to take into account the interference they cause on UL users. The BF vectors are, thus, calculated to find the best balance between the power used to transmit and the caused interference. To capture the trade-off between the useful signal strength in the own cell and the caused interference in neighbor cells, we introduce the system-wide weight parameter $0 \leq \mu \leq 1$, with the help of which the optimization problem for BS m can be written as:

$$\begin{aligned} \underset{\mathbf{W}_{m,k}}{\text{maximize}} \quad & (1-\mu) C_{m,k}^{\mathrm{DL}}(\mathbf{W}_{m,k}) - \mu \mathcal{I}_{m,k}. \\ \text{subject to} \quad & \sum_k \mathrm{Tr}[\mathbf{W}_{m,k}] \leq P_{\max}^{\mathrm{DL}}, \\ & \mathrm{rank}(\mathbf{W}_{m,k}) = 1; \mathbf{W}_{m,k} \succcurlyeq 0, \end{aligned} \tag{3.12}$$

where

$$\mathcal{I}_{m,k} = \sum_{d \in \mathcal{D}} \sum_{j \in \mathcal{K}} \pi_{d,j} \mathrm{Tr}[\mathbf{W}_{m,k} \mathbf{L}_{m,(d,j)}] - \pi_{m,k} \mathrm{Tr}[\mathbf{W}_{m,k} \mathbf{L}_{m,(m,k)}] + \sum_{u \in \mathcal{U}} \sum_{l \in \mathcal{K}} \pi_{u,l} \mathrm{Tr}[\mathbf{W}_{m,k} \mathbf{T}_{m,u}], \tag{3.13}$$

where $\mathbf{H}_{(d,j),m} \triangleq \mathbf{h}^H_{(d,j),m}\mathbf{h}_{(d,j),m}$ and $\mathbf{T}_{m,u} \triangleq \mathbf{G}^H_{m,u}\mathbf{G}_{m,u}$ are Gramian matrices of the interference channels to DL UE j (in BS d) and UL BS u, respectively, due to the DL transmission from BS m to user k.

The optimization problem in (3.12) is complex to solve due to the presence of the rank-1 constraint. Therefore, we consider a modified problem, in which the rank-1 constraint is relaxed, as follows:

$$\begin{aligned} \underset{\mathbf{W}_{m,k}}{\text{maximize}} \quad & (1-\mu)C^{\text{DL}}_{m,k}(\mathbf{W}_{m,k}) - \mu\mathcal{I}_{m,k}; \\ \text{subject to} \quad & \sum_k \text{Tr}[\mathbf{W}_{m,k}] \leq P^{\text{DL}}_{\max}, \\ & \mathbf{W}_{m,k} \succcurlyeq 0. \end{aligned} \tag{3.14}$$

Then, the problem can be solved by CVX optimization tool [64, 65] using SDPT3 solver [66], since the capacity is a concave function with respect to $\mathbf{W}_{m,k}$, and $\text{Tr}(\mathbf{W}_{m,k})$ is convex (see the proof in Appendix A). For problems which involves logarithm, the CVX uses a successive approximation method which approximates the logarithm function by a polynomial function, then the SDPT3 solves the optimization problem via an infeasible primal-dual interior-point al algorithm[1]. These tools, therefore, allow us to find the optimal solution for the suboptimal problem in (3.14). The rank-relaxed problem is optimized over one user at one BS per time, having only one constraint. Therefore (3.14) is not just a relaxation of (3.12) but its tight, i.e., solving the relaxed problem (3.14) is the same to solve the rank-constrained problem (3.12), which will always lead to $\text{rank}(\mathbf{W}_{m,k}) = 1$ [68].

The main idea of the proposed algorithm is to iteratively calculate the BF vectors in a distributed way in each BS until convergence or the algorithm reaches the maximum number of iterations set as an input parameter. The proposed PBA runs either in sequential or parallel mode, if the former is selected, only one BS updates its user precoder per time, while if parallel approach is chosen all the DL BSs update their user's precoder at simultaneously. At the beginning of each iteration, the DL BSs choose a set of random precoders respecting the power constraint. Next, if sequential updating is performed a given BS selects one user and solve the optimization problem in (3.14), otherwise all BSs select one user and (3.14) at the same time. Those steps are repeated until convergence or the algorithm reaches the maximum number of predetermined iterations. The distributed BF price based algorithm is summarized in Algorithm 4.

3.4.3 Algorithm Analysis

3.4.3.1 Convergence

Before the convergence analysis, notice the proposed PBA can run either in sequential or parallel mode. For the parallel implementation, all DL BSs solve the optimization problem at the same based on the previous reported interference prices. For the sequential implementation,

[1] For a detailed description about how the algorithm works, please see [67].

Algorithm 4 Pricing-based distributed BF algorithm.

Initialization: each BS d, with $d \in \mathcal{D}$, chooses a set of random precoders, respecting power constraints. Set $iter = 0$ and a maximum number o iterations $iter_{\max}$
while not converge or $iter < iter_{\max}$ **do**
    Updating DL prices:
    for $d = 1, \cdots, |\mathcal{D}|$ **do**
        for $j = 1, \cdots, K$ **do**
            DL UE d, j calculates $\pi_{d,j}$ according with (3.9).
        end for
    end for
    Updating UL prices:
    for $u = 1, \cdots, |\mathcal{U}|$ **do**
        for $l = 1, \cdots, K$ **do**
            UL BS u calculates $\pi_{u,l}$ according to (3.9).
        end for
    end for
    Price exchange:
    Prices are sent to the DL BSs.
    Updating Precoders:
    BS d selects a user j, based on some criteria, and solves (3.14).
    $\mathbf{w}_{d,j}$ is updated.
    $iter = iter + 1$
end while

Figure 3.3 – Signaling exchange between UEs and BSs. In this figure, BS_1 and BS_2 are on DL mode while BS_3 is on UL mode.

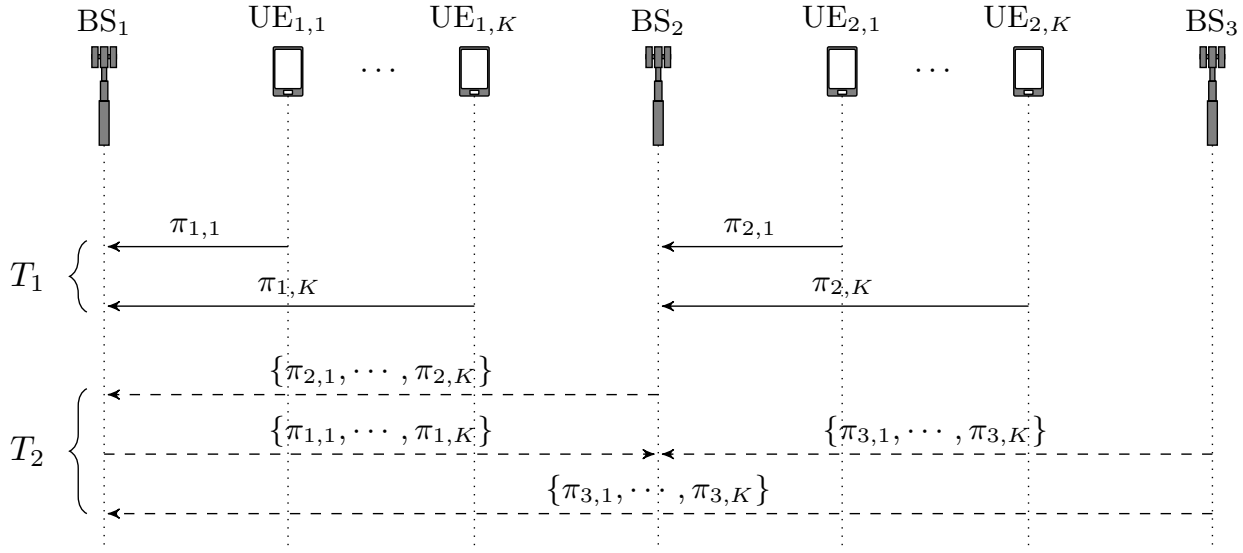

Source: Created by the author.

a BS updates it user's precoder by solving the optimization problem in (3.14) while the other precoders vectors are fixed. After this calculation, the new prices must be updated and exchanged before the new BS performs its update.

The convergence under parallel iterations cannot be proved in a mathematical way

[59], even if simulations show the algorithm converges under some convergence criteria. However, the sequential implementation converges and the proof is shown in Appendix C.

3.4.3.2 Signaling Overhead

To run the PBA, three main steps are needed: (1) measurement of the DL and UL interference prices, (2) interference price exchange between BSs and (3) update the precoder of a given DL UE (m, k).

For step (1) both DL and UL prices are measured at their receivers. For each receiver (i, j), a UE for DL transmission and a BS for UL transmission, two quantities have to be measured, the useful signal power, $s_{i,j}$, and the interference plus noise power (IPNP), $I_{i,j}$. The later is easily measured by the receiver while the former can be obtained by measuring the SINR at the receiver side, then this quantity is multiplied by $I_{i,j}$.

For step (2), the prices measured at the receivers must be forwarded to the DL BS which will solve the optimization problem, this step occurs in two time instances, as illustrated in Figure 3.3. At T_1, the prices are measured according to step (1) for each receiver and at T_2 they are send to the target DL BS. If the algorithm runs in a sequential mode, only the target BS needs to collect the interference prices, if the parallel approach is used, then all the DL BSs must collect the broadcasted interference prices, as illustrated by the Figure 3.3.

Finally, the step (3) consists on run the PBA BF for a given BS m is to solve the optimization problem. The BS will select a user, say (m, k) and it will try to find the best precoder to maximize the user's utility. To this end, the BS m needs the direct channel, $\mathbf{h}_{m,(m,k)}$, IPNP, $I_{m,k}$, and the leakage matrix $\Delta^{\mathrm{DL}}_{m,k} \triangleq \sum_{j=1}^{K} \sum_{d=1}^{|\mathcal{D}|} \pi_{d,j} \mathbf{H}_{m,(d,j)} - \pi_{m,k} \mathbf{H}_{m,(m,k)}$ and $\Delta^{\mathrm{UL}}_{m,k} \triangleq \sum_{l=1}^{K} \sum_{u=1}^{|\mathcal{U}|} \pi_{u,l} \mathbf{T}_{m,u}$. The direct channel can be easily estimated by using the downlink-uplink reciprocity, as we are assuming dynamic TDD scenario. The IPNP is measured at step (1) and the leakage matrix are composed by two terms: the interference prices, already available after step(2), and the channel information. The leakage matrix is composed by two channel terms, the BS-toUE channel, $\mathbf{h}_{m,(d,j)}$, $(d, j) \neq (m, k)$, and the BS-to-BS channel, $\mathbf{G}_{m,u}$. The former can be estimated, as the direct channel, by the downlink-uplink reciprocity, while the $\mathbf{G}_{m,u}$ matrix can be reported by backhaul, for example, after the pilots.

In terms of algorithm implementation, the sequential approach leads to a greater signaling overhead compared with the parallel one. This is due the need to update and exchange the new prices after each BS calculates the new precoder vector, therefore, for each iteration new prices are measured and exchanged $|\mathcal{D}|$ times. For the parallel mode, the interference prices are updated and exchanged just at the end of each iteration.

3.4.3.3 Complexity Analysis

For the PBA, the main complexity relies on the solution of the optimization problem by the CVX. Even if we cannot predict exactly the complexity of the considered problem, according to [66, 67] the SDPT3 solver uses primal-dual interior point algorithm to solve the

problem. Therefore, the most complex operation done is $O(N_{\mathrm{BS}}^3)$, hence the total complexity of the considered PBA BF is approximately $O(N_{\mathrm{iter}}N_{\mathrm{BS}}^3)$, where N_{iter} is the number of iterations the algorithm needs to converge.

3.5 Sub-optimal Distributed Pricing-Based Algorithm (SPBA)

By applying a PB approach, our main goal is to enforce the DL users to take into account the interference they cause on UL users. The BF vectors are, thus, calculated to find the best balance between the power used to transmit and the caused interference.

However, the considered algorithm is still complex in terms of signaling exchanging, iterations to converge and running time. To deal with some of these issues, we propose a SPBA to solve the optimization problem in (3.14) without using the CVX routine to find the precoders and the power allocation for the users.

For a DL UE (m, k), the optimization problem in (3.14) can be written as:

$$\begin{aligned} \underset{\mathbf{w}_{m,k},\, p_{m,k}}{\text{maximize}} \quad & (1-\mu)C_{m,k}^{\mathrm{DL}}(\mathbf{w}_{m,k}, p_{m,k}) - \mu p_{m,k}\mathbf{w}_{m,k}^H \mathbf{L}_{m,k}\mathbf{w}_{m,k}. \\ \text{subject to} \quad & p_{m,k} \leq P_{m,k}^{\max}, \\ & ||\mathbf{w}_{m,k}||^2 = 1, \end{aligned} \tag{3.15}$$

where

$$\mathbf{L}_{m,k} = \sum_{d\in\mathcal{D}}\sum_{j\in\mathcal{K}} \pi_{d,j}\mathbf{h}_{(d,j),m}^H \mathbf{h}_{(d,j),m} - \pi_{m,k}\mathbf{h}_{(m,k),m}^H \mathbf{h}_{(m,k),m} + \sum_{u\in\mathcal{U}}\sum_{l\in\mathcal{K}} \pi_{u,l}\mathbf{G}_{m,u}^H \mathbf{G}_{m,u}, \tag{3.16}$$

is the leakage matrix for the user (m, k).

As the number of interference links are larger than the number of users, the leakage matrix $\mathbf{L}_{m,k}$ has full rank. Therefore, we introduce a new beamforming vector $\tilde{\mathbf{w}}_{m,k} = \mathbf{L}_{m,k}^{1/2}\mathbf{w}_{m,k}$ and $\tilde{\mathbf{h}}_{(m,k),m} = \mathbf{L}_{m,k}^{-1/2}\mathbf{h}_{(m,k),m}$. Now the problem in (3.12) can be written as:

$$\begin{aligned} \underset{\tilde{\mathbf{w}}_{m,k},\, p_{m,k}}{\text{maximize}} \quad & (1-\mu)C_{m,k}^{\mathrm{DL}}(\tilde{\mathbf{w}}_{m,k}, p_{m,k}) - \mu p_{m,k}\tilde{\mathbf{w}}_{m,k}^H \tilde{\mathbf{w}}_{m,k}. \\ \text{subject to} \quad & 0 \leq p_{m,k} \leq P_{m,k}^{\max}, \\ & \tilde{\mathbf{w}}_{m,k}\mathbf{L}_{m,k}^{-1}\tilde{\mathbf{w}}_{m,k}^H = 1, \end{aligned} \tag{3.17}$$

where

$$C_{m,k}^{\mathrm{DL}}(\tilde{\mathbf{w}}_{m,k}, p_{m,k}) = \log_2\left(1 + \frac{p_{m,k}\tilde{\mathbf{h}}_{(m,k),m}\tilde{\mathbf{w}}_{m,k}\tilde{\mathbf{w}}_{m,k}^H\tilde{\mathbf{h}}_{(m,k),m}^H}{I_{m,k}}\right). \tag{3.18}$$

The problem in (3.17) is an optimization problem that consists on finding the best precoder, $\tilde{\mathbf{w}}_{m,k}$, and the best power allocation, $p_{m,k}$, for the user (m, k) in a jointly way. The proposed heuristics consists on solving the optimization problem in a suboptimal way in two steps, first by finding the best beam direction, then, giving the precoders, find the optimal power allocation.

For the beam direction, the approach is to maximize the capacity in (3.18). Therefore, the chosen precoder corresponds to the matched filter, which is $\tilde{\mathbf{w}}_{m,k} = \tilde{\mathbf{h}}^H_{(m,k),m}/||\tilde{\mathbf{h}}^H_{(m,k),m}||$.

After finding the precoder, the new optimization problem is reduced to:

$$\begin{aligned} \underset{p_{m,k}}{\text{maximize}} \quad & (1-\mu)\log_2\left(1+\frac{p_{m,k}\text{Tr}[\tilde{\mathbf{H}}_{m,(m,k)}\tilde{\mathbf{W}}_{m,k}]}{I_{m,k}}\right)-\mu p_{m,k}\tilde{\mathbf{w}}^H_{m,k}\tilde{\mathbf{w}}_{m,k}. \\ \text{subject to} \quad & 0 \leq p_{m,k} \leq P^{\max}_{m,k}. \end{aligned} \tag{3.19}$$

The best power allocation can be found by the bisection method since the first derivative of the cost function is monotonic in terms of $p_{m,k}$. The presented heuristic is described in Algorithm 5.

Algorithm 5 sub-optimal pricing-based algorithm.

Initialization: each BS d, with $d \in \mathcal{D}$, chooses a set of random precoders, respecting power constraints. Set $iter = 0$ and a maximum number of iterations $iter_{\max}$
while not converge or $iter < iter_{\max}$ **do**
    Update DL prices as Algorithm 4
    Update UL prices as Algorithm 4
    Price exchange:
    Prices are sent to the DL BSs.
    Updating Precoders and Power:
    BS d selects a user j, based on some criteria
    Update the user's precoder as $\mathbf{w}_{d,j} = \mathbf{L}^{-1}_{m,k}\mathbf{h}^H_{(m,k),m}$.
    Find the power allocation according to Algorithm 6.
    $iter = iter + 1$
end while

Algorithm 6 Bisection method for power allocation.

set $p_{\min} = 0$, $p_{\max} = P^{\max}_{m,k}$ and $p = (p_{\min} + p_{\max})/2$.
while $|p_{\min} - p_{\max}| > \epsilon$ **do**
    $X_{\min} = (1-\mu)\log_2\left(1+\frac{p_{\min}\text{Tr}[\tilde{\mathbf{H}}_{m,(m,k)}\tilde{\mathbf{W}}_{m,k}]}{I_{m,k}}\right)-\mu p_{\min}\tilde{\mathbf{w}}^H_{m,k}\tilde{\mathbf{w}}_{m,k}.$
    $X_{\max} = (1-\mu)\log_2\left(1+\frac{p_{\max}\text{Tr}[\tilde{\mathbf{H}}_{m,(m,k)}\tilde{\mathbf{W}}_{m,k}]}{I_{m,k}}\right)-\mu p_{\max}\tilde{\mathbf{w}}^H_{m,k}\tilde{\mathbf{w}}_{m,k}.$
    $X_{\text{p}} = (1-\mu)\log_2\left(1+\frac{p\text{Tr}[\tilde{\mathbf{H}}_{m,(m,k)}\tilde{\mathbf{W}}_{m,k}]}{I_{m,k}}\right)-\mu p\tilde{\mathbf{w}}^H_{m,k}\tilde{\mathbf{w}}_{m,k}.$
    if $(X_{\min} - X_{\text{p}})/(p_{\min} - p) > (X_{\max} - X_{\text{p}})/(p_{\max} - p)$ **then**
        $p_{\max} = p$.
    else
        $p_{\min} = p$.
    end if
    $p = (p_{\min} + p_{\max})/2$.
end while

3.6 Numerical Results

We consider a multi-cell dynamic TDD network consisting of 19 cells, out of which 10 cells operate in DL mode and 9 cells operate in UL mode. The system parameters are set according to the recommendations of the 3GPP and correspond to an outdoor picocell environment deployed in 5 MHz bandwidth [47].

The simulation parameters and the BS-to-BS, BS-to-UE and UE-to-UE propagation conditions, including line-of-sight (LoS) and non-line-of-sight (NLoS) conditions are specified in Table 3.3 and Table 3.4 [69]. Table 3.4 shows two distinct propagation scenarios that correspond to LoS and NLoS situations respectively.

We are interested in the UL and DL performance of the system in terms of SINR distribution and overall capacity when the BS takes advantage of MRT and ZF BF and when the system employs the proposed distributed PBA BF. Specifically, we are interested in the achievable performance gains of deploying multiple antennas at the BSs as compared with the performance of a multi-cell single-input single-output (SISO) network. To this end, we consider a scenario with 19 cells and 2 users per cell (a similar approach can be observed in [20]), resulting in 38 users sharing the same resource block within a cluster. Consequently, we can capture the impact of relevant interfering links, including intra-cell, inter-cell and cross-link interferences.

Table 3.3 – Simulation Parameters

Parameter	Value
Number of Cells	19
Users per Cell (K)	2
Cell radius (R)	100 meters
Number of BS Antennas (N_{BS})	[1,4,16]
Number of UE Antennas	1
Downlink Power	24 dBm
Uplink Power	23 dBm
Antenna Gain	0 dB
DL cells	10
UL cells	9
UL receiver Filter	MMSE
Bandwidth (B)	5 MHz

Source: Created by the author.

In order to illustrate and motivate the necessity of protecting the UL BSs from DL interference, consider Figure 3.5. This figure shows the received interference power (averaged over the central UL BS) terms and compares it with the interference power received from surrounding BSs and surrounding UEs considering the first and second interference rings in a 19 cells scenario as a function of the number of users per cell. For DL transmission we consider the ZF BF to illustrate that the conventional beamforming strategy is not enough to manage the BS-to-BS interference in the dynamic TDD scenario. The UL receiver is chosen to be the MMSE

Table 3.4 – Propagation Characteristics.

Outdoor Pico BS to outdoor Pico BS
LOS: if $R < 2/3$km: PL(R) = 98.4 + 20log$_{10}$(R), R km if $R \geq 2/3$km: PL(R) = 101.9 + 40log$_{10}$(R), R km
Outdoor Pico BS to UE and **UE to Outdoor Pico BS**
LOS: PL(R) = 103.8 + 20.9log$_{10}$(R), R km NLOS: PL(R) = 145.4 + 37.5log$_{10}$(R), R km Prob$_{\text{LOS}}$(R) = 0.5 − min(0.5, 5exp(−0.156/R)) + min(0.5, 5exp(−R/0.03)).
UE to UE
If $R < 50$m: PL(R) = 98.45 + 20log$_{10}$(R), R km If $R \geq 50$m: PL(R) = 55.78 + 40log$_{10}$(R), R m.

Source: Created by the author.

Figure 3.4 – Interference situation on TTI 5.

(a) Central UL cell and 18 DL interfering cells.

(b) Central UL cell and 18 UL interfering cells.

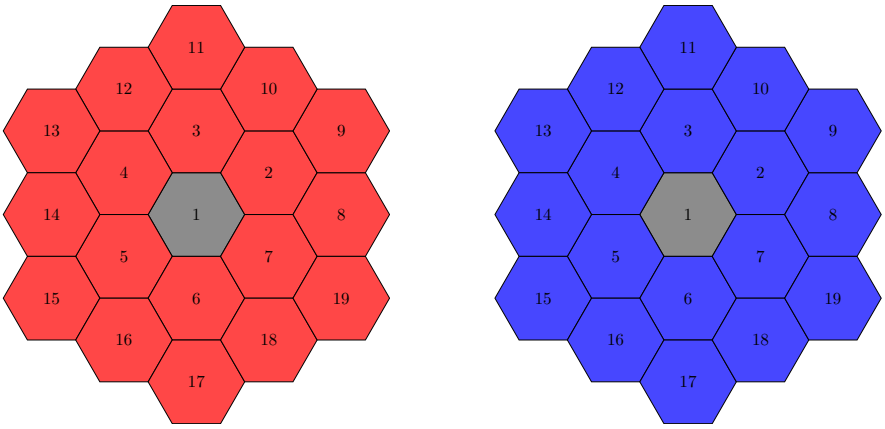

Source: Created by the author.

to mitigate the interference received by the central cell. This figure indicates that the average BS-to-BS interference is stronger than the UE-to-BS, even for 8 users per cell. This happens due two main reasons, (i) in the 3GPP pico-cell scenario, the average path-loss between BSs is smaller than the average path-loss between a UE and a BS, (ii) the DL transmit power is greater than the UL transmit power. Those two combined reasons lead to a greater interference coming from the DL BSs than the UL UEs.

Figure 3.5 – Interference behavior for UL users in a dynamic TDD scenario with 19 cells and 8 antennas in each BS. DL BSs use ZF BF and UL BSs use the MMSE receiver filter.

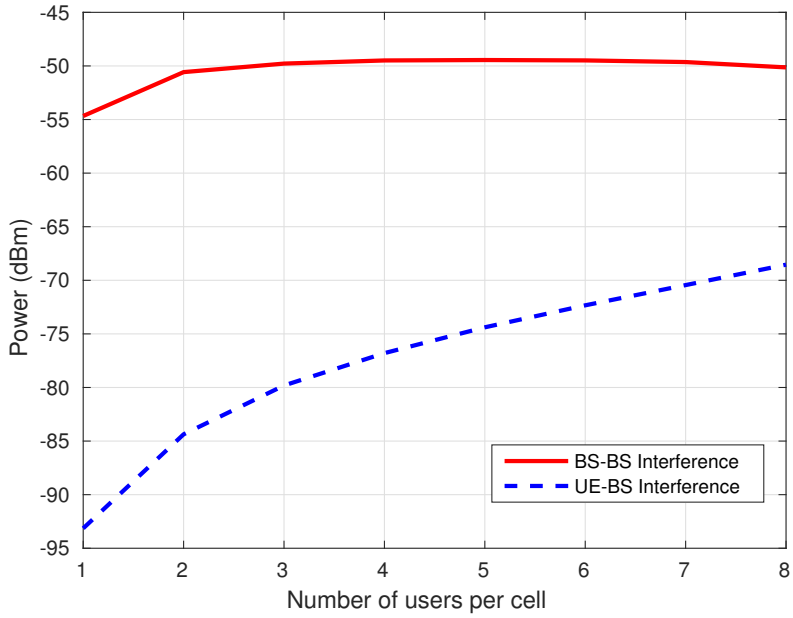

Source: Created by the author.

3.6.1 Classical Pricing Problem ($\mu = 0.5$)

In this subsection we consider the case $\mu = 0.5$, which corresponds to a fixed pricing scheme in which the capacity of the own link and the caused interference are equally weighed.

Figure 3.6 presents the CDF of the DL SINR, The baseline for this result is the case in which all 19 cells operate in DL mode using ZF BF ("All DL"). In the dynamic TDD case, as expected, the worst performance is experienced when the BSs do not employ BF. As it can be seen in Figure 3.6, enabling the dynamic TDD operation without BF is basically not a viable option: dynamic TDD causes around 20 dB performance loss to the median user and only about 20% of the users reach higher than 5 dB DL SINR. Applying MRT improves the DL performance, but the SINR is still poor as compared with the case in which all cells operate in DL mode. This result confirms the intuitive expectation that MRT is not a viable option in interference limited situations.

The performance of the PB distributed BF and the ZF approaches is superior not only to the MRT case, but also to the baseline case ("All DL"). This is a very promising result and suggests that even with a low number of BS antennas, dynamic TDD can be a feasible alternative to traditional TDD networks. To understand why both approaches can effectively deal with the negative effects of the new types of interference in dynamic TDD systems, and also to understand the performance difference between ZF and distributed pricing, recall that the objective of ZF is to cancel the intracell interference. In contrast, according to the PB strategy, the BSs take into account the interference that they cause both to the UEs that are in reception

Figure 3.6 – Comparison of donwlink SINR for different BF strategies in a dynamic TDD scenario. The “All DL" curve represents the system behavior if all users were operating on DL mode.

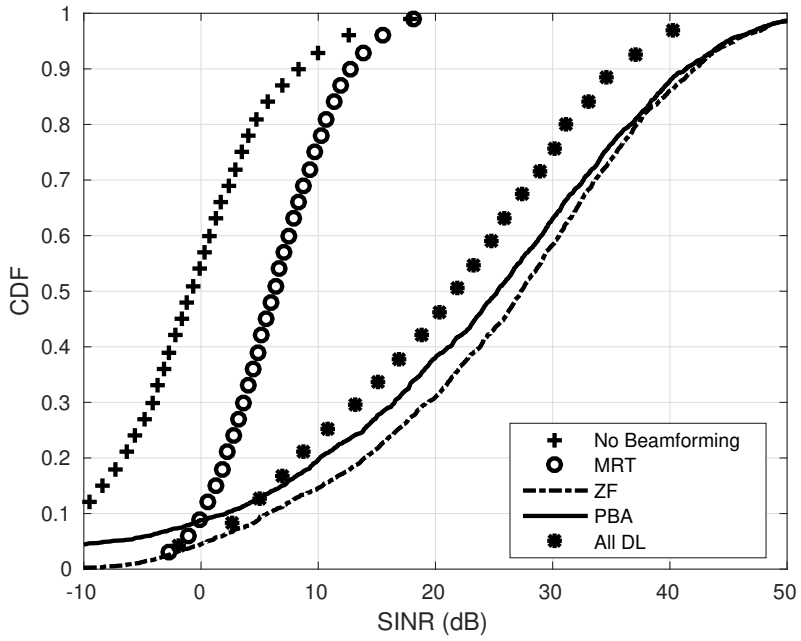

Source: Created by the author.

mode and to neighbor BSs. In other words, the distributed PB strategy takes into account the BS-to-BS interference when selecting the DL precoder vector, which makes precoder selection slightly inferior to that of ZF precoding.

Figure 3.7 compares the UL SINR performance of the BF schemes discussed above. In this figure, the baseline is when all users are in UL mode (“All UL"). As expected, without BF at the BSs, also the UL performance suffers from the aggressive interference that is inherently present in dynamic TDD systems (“No Beamforming"). When BSs apply the PBA scheme, the UL SINR significantly improves compared with using ZF. This is due to the ability of the pricing algorithm to take into account the interference that the DL BSs transmissions cause in the UL. With distributed pricing, the DL power is reduced, which increases the UL performance.

Figure 3.8 compares the power consumption for DL transmissions with distributed PBA and ZF BF approaches. ZF BF always uses full power to perform DL transmissions, since using full power is beneficial for maximizing the own cell performance [70]. In contrast, the distributed PBA scheme tends to reduce the transmit power to limit the caused interference.

Notice that the PB scheme occasionally uses less than 28 dBm of power, and can use up to the maximum sum power (34 dBm). This fluctuation is due to the closed loop interference PB PC: At some iterations, the interference channel can be severe, causing the pricing algorithm to reduce the transmission power to limited the associated penalty. The opposite can be inferred when the DL BSs use close to the maximum power level: when the interference channel is weak, high transmit power is used to increase the DL utility.

Figure 3.7 – Comparison of UL SINR for different BF strategies in a dynamic TDD scenario. The “All UL" curve represents the system behavior if all users were operating on UL mode.

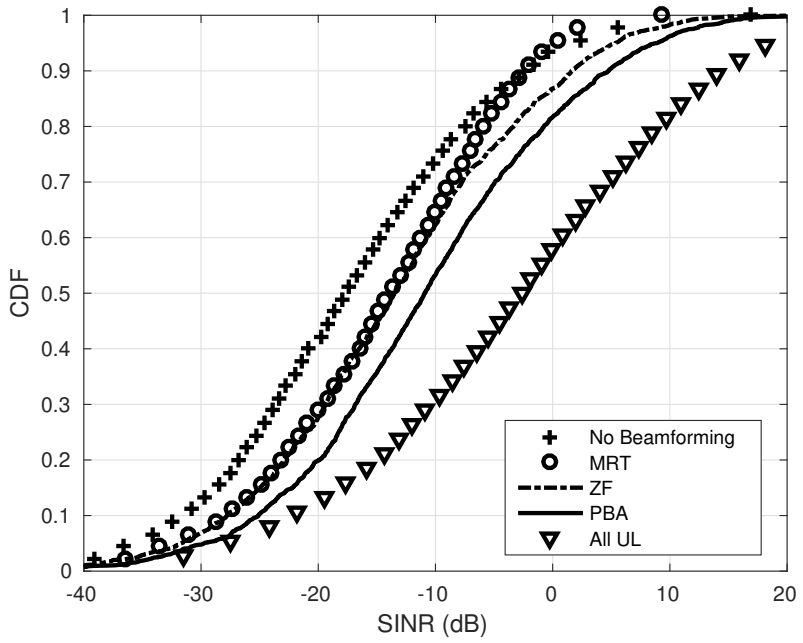

Source: Created by the author.

Figure 3.8 – Comparison of total consumed power in DL for PBA and ZF strategies.

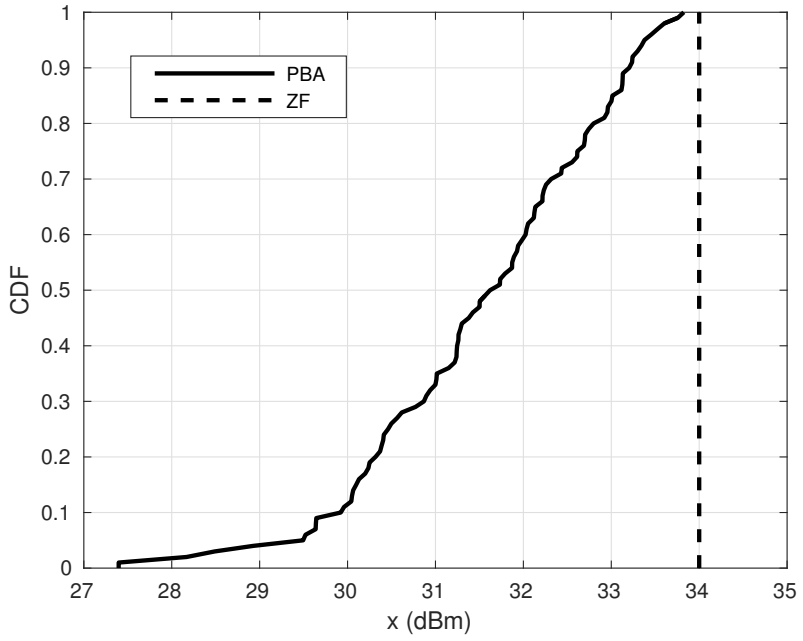

Source: Created by the author.

To gain insight about the relation of the transmit power and achieved DL capacity, Figure 3.9 shows an energy efficiency plot which is defined by the ratio (in bits per second)

Figure 3.9 – Energy efficiency CDF in bits/Joule for both PBA and ZF BF approaches.

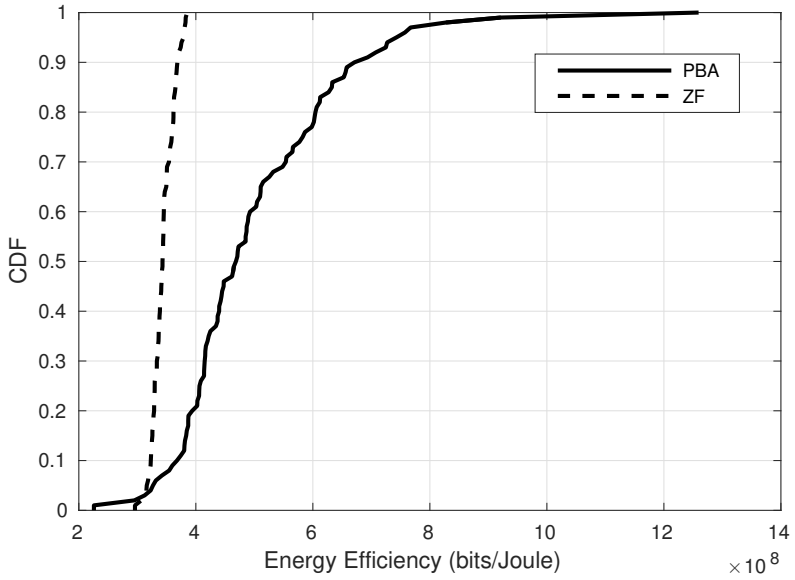

Source: Created by the author.

between the achievable rate and the consumed power (in Joules) at a BS [21]. The distributed PBA achieves higher capacity per Joule of energy compared with ZF BF. The reason for this is that the pricing approach reduces the interference by using less transmit power, while maintaining high capacity for DL UEs.

Figure 3.10 and Figure 3.11 show capacity results as a function of the number of BS antennas. In the DL, as expected, ZF achieves higher transmission rates than the PB scheme, since the pricing algorithm has the characteristic of improving the performance of UL UEs at the expense of a somewhat reduced DL performance. An important insight is that the performance of MRT does not approach that of ZF as the number of antennas increases. This is due to the MISO dynamic TDD scenario, in which interference at DL UEs coming from single antenna UL UEs is not mitigated.

For UL transmissions, with a small number of BS antennas, the PB approach boosts the capacity for UL UEs by adjusting the DL precoders. However, this gap tends to decrease when the number of antennas gets higher, this phenomenon happens due the increasing of the degrees of freedom for the ZF BF and the MMSE filter design. When the number of antennas at BSs gets high, the BSs have enough degrees of freedom to perform close-to-optimum DL BF and UL receiving filter. Since there are only 2 users per cell in our simulations, when the number of antennas at BSs is higher than 12, the UL performance gap tends to disappear. onsequently, ZF BF is a viable option.

Figure 3.12 and Figure 3.13 show the impact of the number of users when the number of antennas at BSs is 16. For the DL capacity, Figure 3.12, it can be observed the PB strategy has a performance gap when compared with ZF BF. As the number of users gets near to the number of antennas, the degrees of freedom decrease and the interference cannot be fully

Figure 3.10 – Mean DL capacity in bps for DL BF strategies when the number of BS antennas increases.

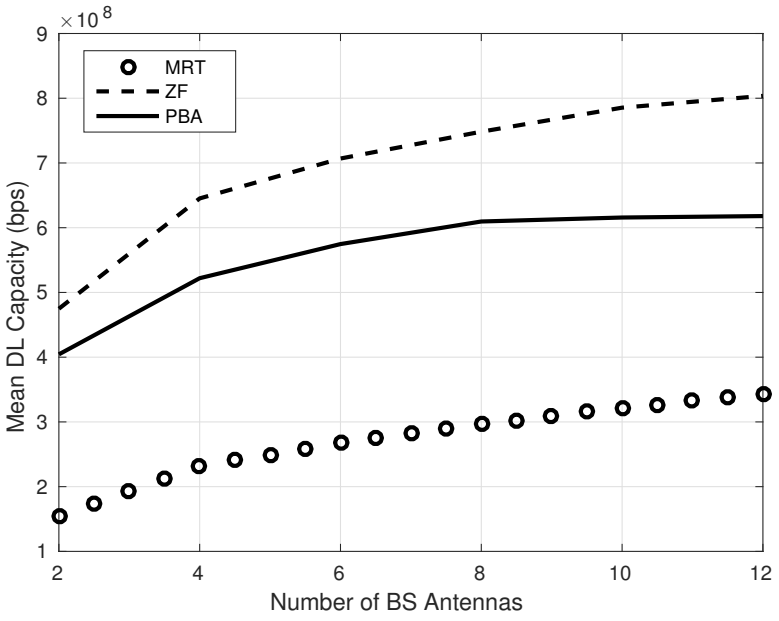

Source: Created by the author.

Figure 3.11 – Mean UL capacity in bps for DL BF strategies when the number of BS antennas increases.

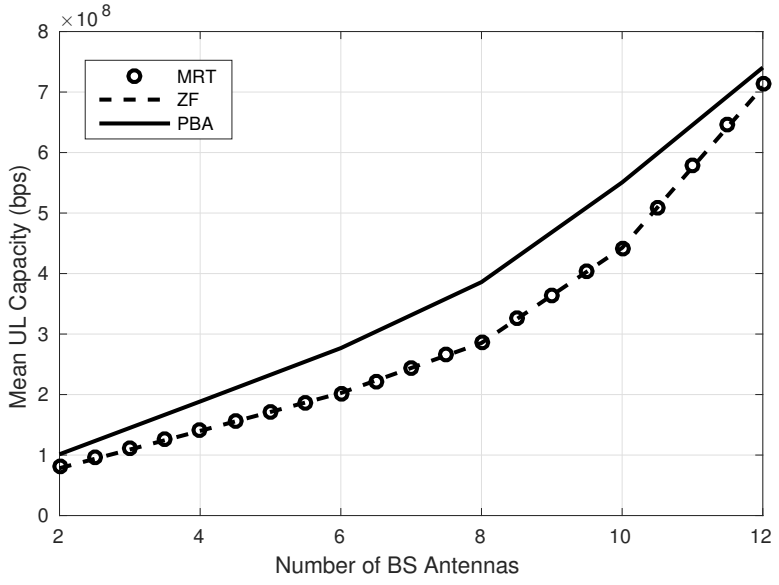

Source: Created by the author.

mitigated. Therefore, the PB approach approximates the ZF performance. For the UL case, as Figure 3.13 shows, the opposite occurs. When the degrees of freedom is high enough, the PB and ZF strategies have similar performance, and both approach the “All UL" case, since the minimum mean square error receiver can effectively cancel the interference. When the number of users increases, the degrees of freedom decreases, and the UL performance for PB approach

Figure 3.12 – Mean DL capacity in function of number of users per cell for 16 antennas BS.

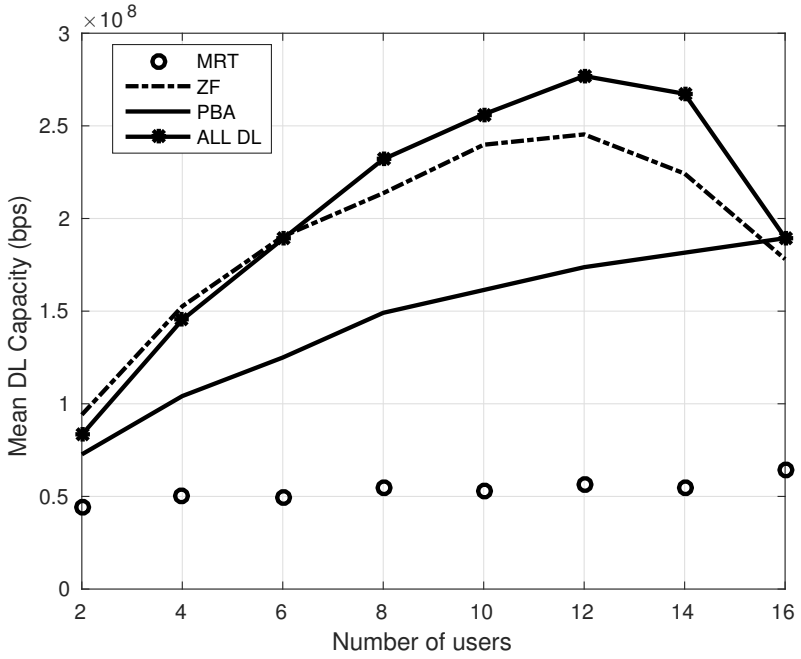

Source: Created by the author.

Figure 3.13 – Mean UL capacity in function of number of users per cell for 16 antennas BS.

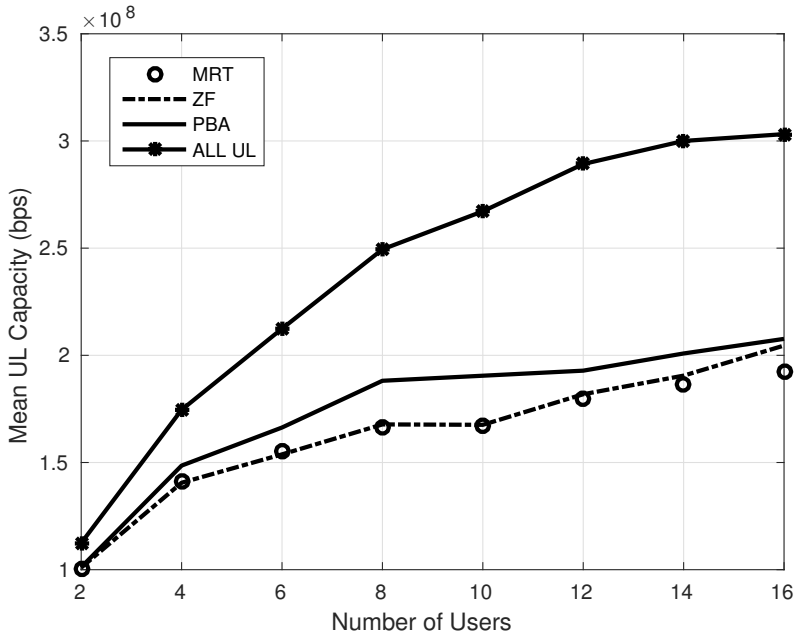

Source: Created by the author.

outperforms ZF. This is true until the number of users start to reach the same number of antennas. With lower number of degrees of freedom, ZF BF performs similarly to the considered PB scheme.

The convergence behavior of proposed PB algorithm for both implementations is

Figure 3.14 – Number of iterations to PBA converges for a 19 cells scenario, where 10 cells are in the DL transmission mode while 9 cells are in the UL mode. The BSs are equipped with 8 antennas.

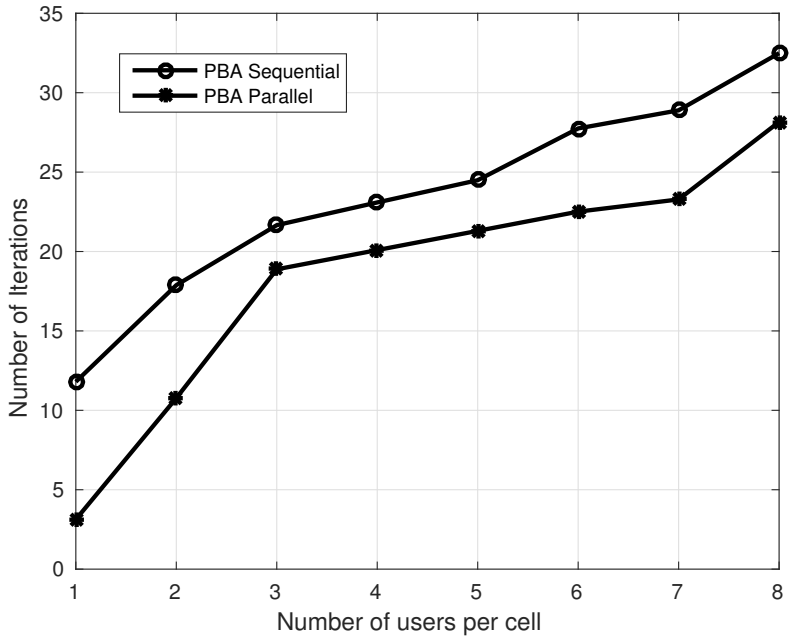

Source: Created by the author.

showed in Figure 3.14. For an algorithm to converge, the normalized difference in terms of objective function between two consecutive iterations should be less than a predetermined threshold ϵ. In our simulations we set $\epsilon = 1\%$. It can be observed that, even if the convergence for the parallel implementation of the proposed PB cannot be proved, it converges faster than the sequential precoders updating.

3.6.2 Impact of Interference Pricing Adjustment

Recall from (3.12), that the penalty term μ determines the weight of the caused interference as compared with the DL utility. Therefore, when μ is set to a low value (close to 0), the BSs tend to ignore the caused interference, including BS-to-BS and BS-to-UE interference, and try to maximize the own cell capacity. On the other hand, when μ is set to a high value (close to 1), the BSs aim at minimizing the caused interference at the expense of the capacity achieved in the own cell.

To gain insight in the impact of setting μ on both the DL and UL capacity and the number of antennas, Figure 3.15 plots the DL and UL mean SINR as a function of μ. Intuitively, as μ increases from a low value, the BSs reduce their transmit power levels, and adapt their beams to avoid causing interference to receiving BSs and UEs. The effect of reducing the interference is visible on both the DL and the UL capacity curves.

Notice that as μ increases beyond around 0.5, the DL SINR starts decreasing, since

Figure 3.15 – DL and UL capacity behavior when the μ parameter varies from 0 to 1.

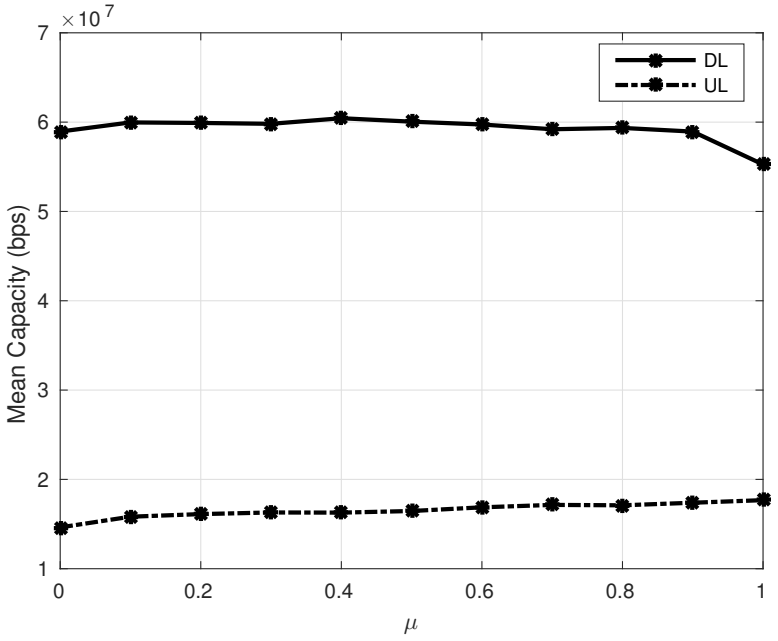

Source: Created by the author.

the system aims at minimizing the caused interference and it effectively becomes noise limited. On the other hand, since the UL SINR always benefits from penalizing the BS-to-BS interference.

3.6.3 SPBA Results

Table 3.5 presents the simulation run time results, in seconds, for the PBA and SPBA per algorithm iteration over 1,000 simulations. We used a Intel(R) Core(TM) i5-2450M CPU @ 2.50GHz machine to run each algorithm with the same channel realizations. For the PBA, the rum time was calculated as the total time to run the CVX optimization tool while for the SPBA it was calculated as the total time to find both precoders and power allocation.

Table 3.5 – Run time, in seconds, for PBA and SPBA.

	Minimum run time	Maximum run time	Mean run time
PBA	1.0781	2.6766	1.4755
SPBA	0.0016	0.0034	0.0027

Source: Created by the author.

As expected, the SPBA runs faster than the optimum PBA since the precoders are found by a closed form solution and the bisection method does not evolve any complex operation. As discussed in Section 3.4.2, the CVX uses a primal-dual interior point algorithm which involves more calculations, then more time to run, than the proposed heuristic method.

Figure 3.16 and 3.17 show the downlink and uplink SINR performance, respectively, using three different BF approaches: the classical ZF, the proposed PBA and the proposed SPBA.

In terms of downlink, the proposed heuristic achieves almost the same performance of the PBA and ZF BF. This result can be explained by the choice of the beam direction which tries to maximize the user's capacity but it also takes into account the leakage interference matrix to the other users which balances the user's maximization and interference minimization on the downlink. In terms of uplink, the heuristic uplink performance is worse than the PBA but it is still better than the ZF approach. This can also be explained by the choice of the beam direction. The best precoder for the SPBA takes into account the leakage matrix which contains the interference terms, therefore it has a better performance than ZF since it does not care about the uplink interference. However, the transmit downlink precoders is not optimized to avoid interference to other users since it consider the direct channel to find the precoders, which leads a worse performance than the PBA scheme.

Figure 3.16 – Comparison of downlink SINR for different BF strategies in a dynamic TDD scenario.

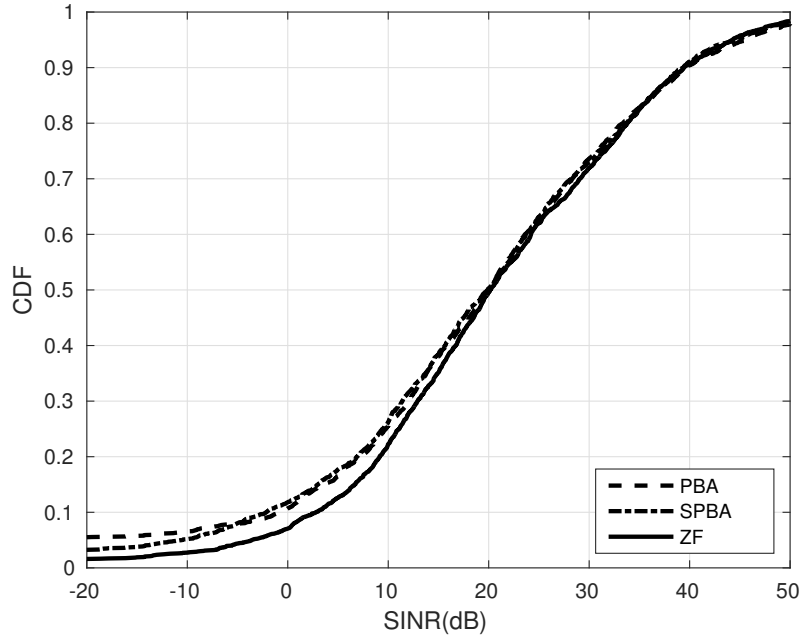

Source: Created by the author.

To analyze the impact of the power allocation method Figures 3.18 and 3.19 show the total consumed power and the energy efficiency for the three considered BF schemes. For the ZF scheme, we use a total power constraint to perform DL transmissions, since using full power is beneficial for maximizing the own cell performance [70]. In contrast, the distributed PBA scheme tends to reduce the transmit power to limit the caused interference, due to the pricing mechanism and the heuristic calculates the transmit power by Algorithm 6. As expected, the heuristic utilizes more power than the PBA scheme since the optimal beamforming is not done but it still has a power saving comparing to the ZF leading to a better performance also in terms of energy efficiency for downlink users.

Figure 3.17 – Comparison of uplink SINR for different BF strategies in a dynamic TDD scenario.

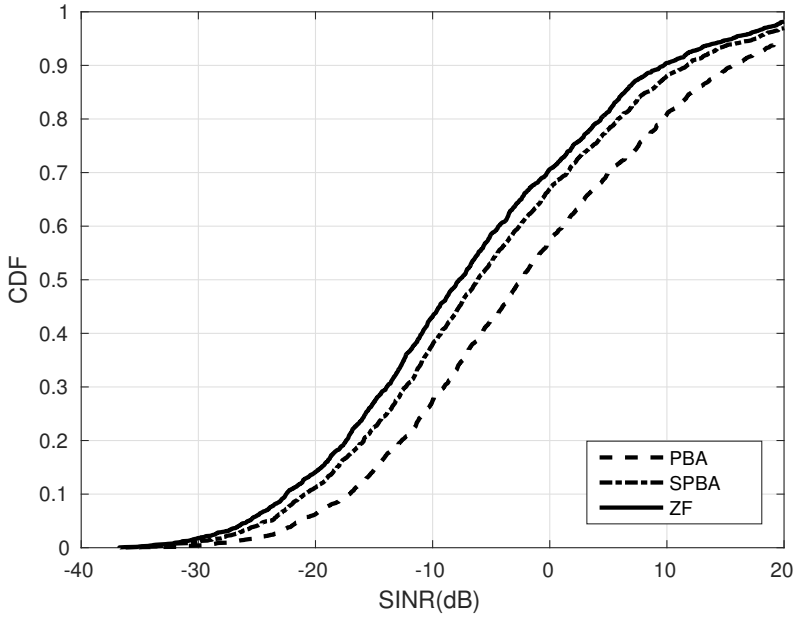

Source: Created by the author.

Figure 3.18 – Comparison of total consumed power in DL for PBA BF, ZF BF and the SPBA strategies.

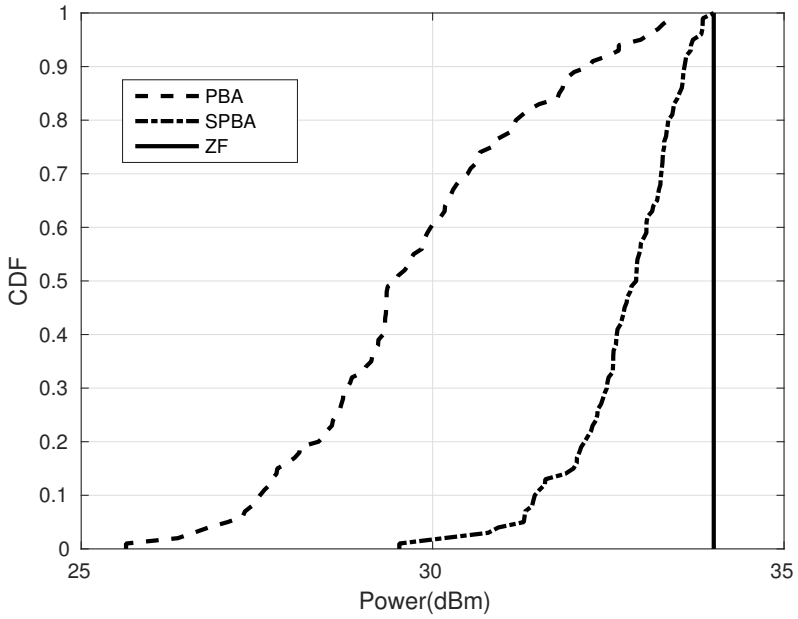

Source: Created by the author.

The convergence behavior of the proposed SPBA approach is shown in Figure 3.20 and Figure 3.21 where the $\epsilon = 1\%$ threshold was used for convergence criterion. It can be observed that the SPBA converges faster than both PBA approaches due the suboptimal scheme adopted when the number of users is greater than one. With one user, the parallel approach takes

Figure 3.19 – Energy efficiency CDF in bits/Joule for PBA BF, ZF BF and heuristic approaches.

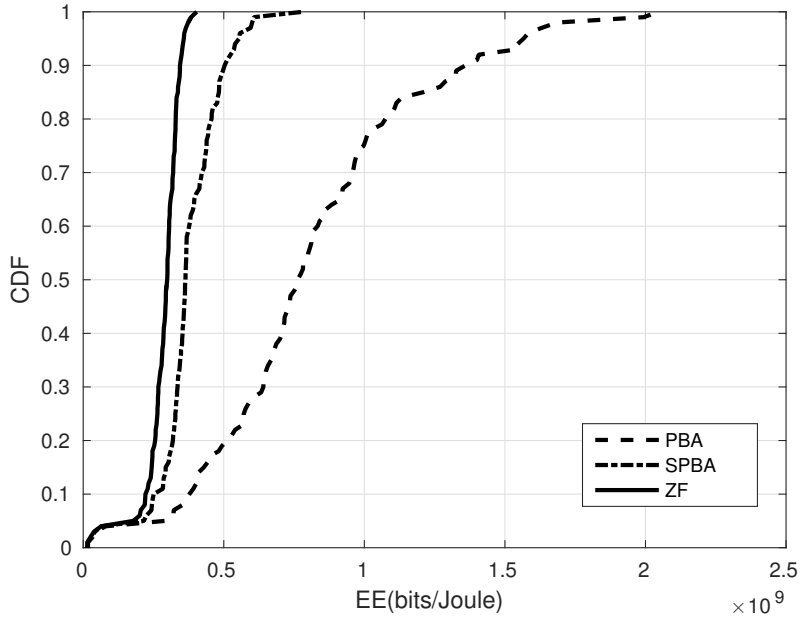

Source: Created by the author.

into account all the users in each iteration, which makes the algorithm to converge fast. For more than two users, the number of possible choices increases for the parallel approach leading to more iterations for convergence.

Figure 3.20 – Mean number of iterations for DL capacity convergence ($N_t = 8$).

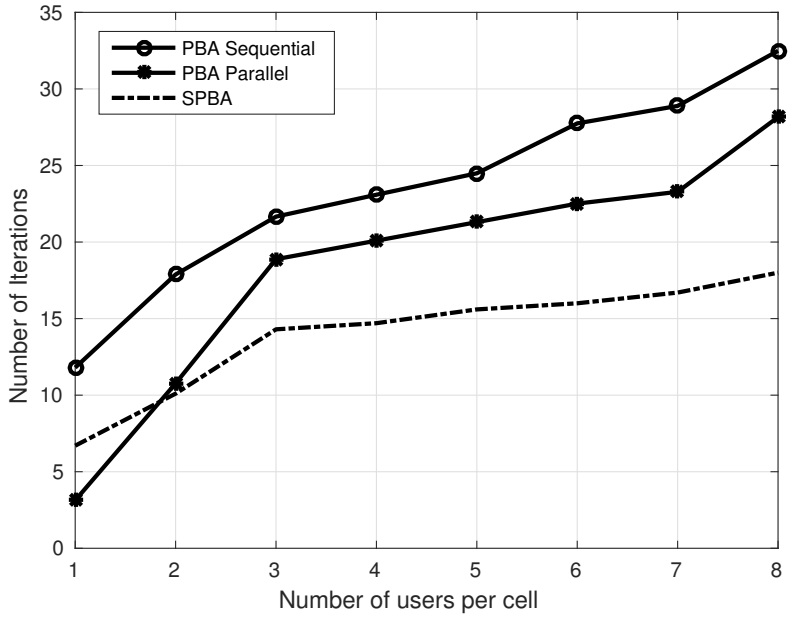

Source: Created by the author.

Figure 3.21 – Convergence behavior for a given channel realization ($N_t = 4$).

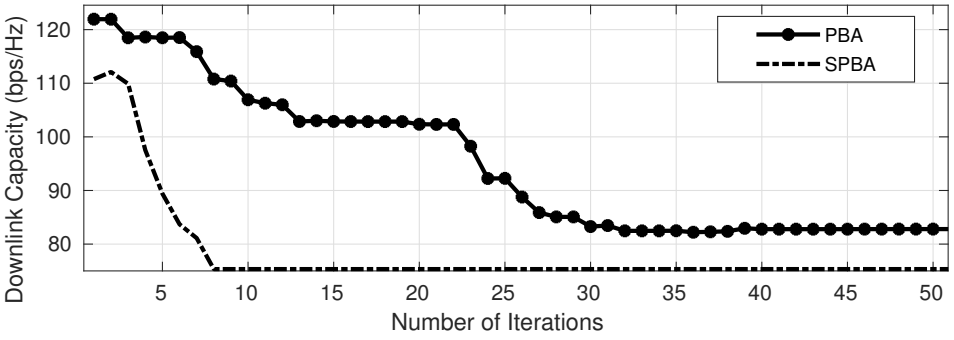

Source: Created by the author.

3.7 Concluding Remarks

In this chapter, we have considered a multi-cell multi-user MISO dynamic TDD network and proposed PB BF to mitigate the inherent BS-to-BS and UE-to-UE interference in such networks. We formulated an optimization problem that captures the dynamic TDD specific interference situations and proposed a distributed algorithm to solve this problem.

The major findings of this chapter are as follows:

- The proposed distributed PBA BF, which penalizes the DL transmission, is an effective way of improving the UL performance at the cost of minor degradation in the DL performance.
- We proposed a signaling scheme that enables the DL BSs to solve a local optimization problem, which leads to an overall system performance improvement.
- The proposed PBA reduces the DL consumed power at the BSs, while improves the UL SINR.
- To deal with the complexity of the PBA, we proposed the SPBA which solves the optimization problem in a sub-optimum way and converges in less iterations. The SPBA has a similar behavior to the PBA for DL direction while on UL it is outperformed by the PBA but yet having a better performance than the ZF BF.

Our results appear to suggest that ZF and PBA BF outperforms MRT, even when increasing the number of antennas, because both ZF and PBA BF can better deal with the new type of interference situations

4 PRICING-BASED BEAMFORMING FOR MIMO DYNAMIC TDD SCENARIO

This chapter aims to extend the results of the previous dynamic TDD MISO problem for multi-antenna UEs. We rewrite the system model and the optimization problem and we show the equivalence between the single stream MIMO problem and the previous MISO scenario. We also show some plots to illustrate the impact on the system behavior when the UEs have multiple antenna capabilities at the consider dynamic TDD scenario.

It is organized as follows. In Section 4.1 a brief introduction about MIMO networks is presented. Section 4.2 presents the considered system model while the PB beamforming for MIMO systems is described in Section 4.3. The SPBA for MIMO networks is described in Section 4.4 while Section 4.5 presents the obtained results bot both PBA and SPBA strategies. Finally, in Section 4.6 we present a conclusion and possible future works.

4.1 Introduction

It is well known in the scientific community that MIMO systems achieve more spectral efficiency with the same power consumption when compared to SISO and MISO systems [71, 72, 73]. For a single cell single user scenario, the capacity of a $N_{\mathrm{BS}} \times N_{\mathrm{UE}}$ increases linearly with $\min(N_{\mathrm{BS}}, N_{\mathrm{UE}})$ regarding to SNR values [74].

With multiple antennas on both BS and UE sides, one can take advantage of spatial gain due the multiple paths created by the MIMO scenario which reduces the fading sensitivity and increases the system capacity, reliability and its coverage. This MIMO feature is refereed as *spatial diversity* in the literature [30].

In order to recover the transmitted signal through the multi-path transmission and eliminate any other effects produced by the wireless channel, a receiver filter based on the channel properties and transmit CSI can be implemented at the receive side.

Therefore, the precoders and receiver filter can be jointly designed at the BSs based on some optimization criterion. The most common approaches are the MMSE criterion [75, 76, 77], ZF constraints [77, 78] and SNR maximization [79, 80]. The joint optimization, however, leads to two main problems: the high complexity of filters computation and low potential for simplify one of the communication sides [81].

Another possible strategy is to optimize the precoders and receive filters in a separated way. However, this not lead to an optimal solution since they are both part of a coupled optimization problem.

Then, the most used solution is to optimize the transmit precoders and the receiver filters in a iterative way, where one of them is fixed while the other is optimized based on some optimization criterion. When the optimum value for the former is found, it is fixed and the latter can be optimized. This procedure is done until reach some convergence criterion. This

procedure can be implemented in a distributed way, since each BS needs to calculate its own transmit/receive filter pairs. Another advantage is the possibility for all calculations to be done at BS side where the reverse CSI can be obtained via pilot training sequences from the uplink users by taking advantage of reciprocity on TDD systems [45, 82].

In this chapter, differently from the previous, we consider a multi-cell multi-user MIMO network operating in dynamic TDD mode. Each cell has one BS equipped with N_{BS} antennas which transmits a single stream. BSs operate in either DL or UL mode, and each one serves K users equipped with N_{UE} antennas.

4.1.1 Related Works

We also have pointed in Chapter 3 the advantages of using dynamic TDD systems for new 5G networks. However, for the best of our knowledge, there are only few works which apply a MIMO beamforming strategy for such systems. The work in [83] proposes a decentralized beamforming in order to maximize the network weighed sum rate. The proposed framework, however, did not considerate the impact of BS-to-BS interference, where we have shown on Chapter 3 that is greater than the UE-to-UE interference on 3GPP pico-cell scenario. As also discussed on Chapter 3, the work in [55] has considered a MIMO dynamic TDD scenario, however, the proposed solution is restricted to a 3-users scenario, limiting the number of cases that the proposed technique can be applied. A more recent work done by [84] has proposed a decentralized approach to minimize BS power transmission while keep the DL users above a predetermined SINR level.

Different from other MIMO works, in this chapter we analyze a multi-antenna UE performance for the PB algorithm described on Chapter 3. We formulate a system model for the single stream MISO problem and we show an equivalence of the solution for the MIMO and MISO problems.

4.2 System Model

Making the same assumptions of Chapter 3, for a given cell $m \in \mathcal{D}$, the post processed DL received signal for a given user k is given by:

$$
\begin{aligned}
y_{m,k}^{\mathrm{DL}} = \underbrace{\sqrt{p_{m,k}}\mathbf{v}_{m,k}^{H}\mathbf{H}_{(m,k),m}\mathbf{w}_{m,k}x_{m,k}}_{\text{useful signal}} + \underbrace{\mathbf{v}_{m,k}^{H}\sum_{\substack{j\in\mathcal{K}\\ j\neq k}}\sqrt{p_{m,j}}\mathbf{H}_{(m,k),m}\mathbf{w}_{m,j}x_{m,j}}_{\text{DL Intracell Interference}} + \\
\underbrace{+\mathbf{v}_{m,k}^{H}\sum_{\substack{d\in\mathcal{D}\\ d\neq m}}\sum_{j\in\mathcal{K}}\sqrt{p_{d,j}}\mathbf{H}_{(m,k),d}\mathbf{w}_{d,j}x_{d,j}}_{\text{DL Intercell Interference}} + \underbrace{\mathbf{v}_{m,k}^{H}\sum_{u\in\mathcal{U}}\sum_{l\in\mathcal{K}}\sqrt{q_{u,l}}\mathbf{B}_{(m,k),(u,l)}\mathbf{w}_{l,u}x_{u,l}}_{\text{UE-to-UE Interference}} + \\
+\mathbf{v}_{m,k}^{H}\underbrace{\mathbf{z}_{m,k}}_{\text{noise}},
\end{aligned}
\tag{4.1}
$$

where $\mathbf{B}_{(m,k),(u,l)} \in \mathbb{C}^{N_{\mathrm{UE}} \times N_{\mathrm{UE}}}$ is the interference channel matrix between UL UE l belonging to BS u and DL UE k served by BS m.

Let us consider, without loss of generality, $\mathbf{W}_{m,k} = p_{m,k}\mathbf{w}_{m,k}\mathbf{w}_{m,k}^H$ for downlink and $\mathbf{W}_{l,u} = q_{l,u}\mathbf{w}_{l,u}\mathbf{w}_{l,u}^H$ for uplink, therefore the capacity in the DL direction for a user k in a cell m is given by the Shannon formulation in (3.2), where $\gamma_{m,k}^{\mathrm{DL}}(\mathbf{W}_{m,k})$ for a MIMO system is given by

$$\gamma_{m,k}^{\mathrm{DL}}(\mathbf{W}_{m,k}) = \frac{S_{m,k}^{\mathrm{DL}}(\mathbf{W}_{m,k})}{\mathbf{v}_{m,k}^H I_{m,k}^{\mathrm{DL}} \mathbf{v}_{m,k} + \sigma_{m,k}^2}, \tag{4.2}$$

where

$$S_{m,k}^{\mathrm{DL}}(\mathbf{W}_{m,k}) = \mathbf{v}_{m,k}^H \mathbf{H}_{(m,k),m} \mathbf{W}_{m,k} \mathbf{H}_{(m,k),m}^H \mathbf{v}_{m,k}, \tag{4.3a}$$

$$I_{m,k}^{\mathrm{DL}} = \sum_{\substack{j \in \mathcal{K} \\ j \neq k}} \mathbf{H}_{(m,k),m} \mathbf{W}_{m,j} \mathbf{H}_{(m,k),m}^H + \sum_{\substack{d \in \mathcal{D} \\ d \neq m}} \sum_{j \in \mathcal{K}} \mathbf{H}_{(m,k),d} \mathbf{W}_{d,j} \mathbf{H}_{(m,k),d}^H + \sum_{u \in \mathcal{U}} \sum_{l \in \mathcal{K}} \mathbf{B}_{(m,k),(u,l)} \mathbf{W}_{u,l} \mathbf{B}_{(m,k),(u,l)}^H. \tag{4.3b}$$

On the other hand, for cell n operating in UL mode, the received signal related to a given UL UE r can be expressed as:

$$\begin{aligned} y_{n,r}^{\mathrm{UL}} = & \mathbf{v}_{n,r}^H \underbrace{\mathbf{H}_{n,(n,r)}^H \sqrt{q_{n,r}} \mathbf{w}_{n,r} x_{n,r}}_{\text{useful signal}} + \mathbf{v}_{n,r}^H \underbrace{\sum_{\substack{l \in \mathcal{K} \\ l \neq r}} \sqrt{q_{n,l}} \mathbf{H}_{n,(n,l)}^H \mathbf{w}_{n,r} x_{n,l}}_{\text{UL Intracell Interference}} + \mathbf{v}_{n,r}^H \underbrace{\sum_{\substack{u \in \mathcal{U} \\ u \neq n}} \sum_{l \in \mathcal{K}} \sqrt{q_{u,l}} \mathbf{H}_{n,(u,l)}^H \mathbf{w}_{u,l} x_{u,l}}_{\text{UL Intercell Interference}} + \\ & + \mathbf{v}_{n,r}^H \underbrace{\left[\sum_{d \in \mathcal{D}} \left(\mathbf{G}_{n,d} \sum_{j \in \mathcal{K}} \sqrt{p_{d,j}} \mathbf{w}_{d,j} x_{d,j} \right) \right]}_{\text{BS-to-BS interference}} + \mathbf{v}_{n,r}^H \underbrace{\mathbf{z}_{n,r}}_{\text{noise}}, \end{aligned} \tag{4.4}$$

where $\mathbf{G}_{n,d} \in \mathbb{C}^{N_{\mathrm{BS}} \times N_{\mathrm{BS}}}$ is the channel gain between BS n and BS d. Therefore, the UL capacity is given by (3.6) where the UL SINR for the MIMO system is expressed as:

$$\gamma_{n,r}^{\mathrm{UL}}(\mathbf{v}_{n,r}) = \frac{S_{n,r}^{\mathrm{UL}}(\mathbf{v}_{n,r})}{\mathbf{v}_{n,r}^H (I_{n,r}^{\mathrm{UL}} + \mathbf{I}_n \sigma_{n,r}^2) \mathbf{v}_{n,r}}, \tag{4.5}$$

where

$$S_{n,r}^{\mathrm{UL}}(\mathbf{v}_{n,r}) = \mathbf{v}_{n,r}^H \mathbf{H}_{n,(n,r)}^H \mathbf{W}_{n,r} \mathbf{H}_{n,(n,r)} \mathbf{v}_{n,r}, \tag{4.6a}$$

$$I_{n,r}^{\mathrm{UL}} = \sum_{\substack{l \in \mathcal{K} \\ l \neq r}} \mathbf{H}_{n,(n,l)}^H \mathbf{W}_{n,r} \mathbf{H}_{n,(n,l)} + \sum_{\substack{u \in \mathcal{U} \\ u \neq n}} \sum_{l \in \mathcal{K}} \mathbf{H}_{n,(u,l)}^H \mathbf{W}_{u,l} \mathbf{H}_{n,(u,l)} + \sum_{d \in \mathcal{D}} \sum_{j \in \mathcal{K}} \mathbf{G}_{n,d} \mathbf{W}_{d,j} \mathbf{G}_{n,d}^H. \tag{4.6b}$$

4.3 Pricing-Based Beamforming for MIMO system

4.3.1 Optimization Problem

Based on the *interference pricing* idea used on the previous chapter where the users are penalized by the amount of interference they cause on other users, we will design the downlink beamforming for the dynamic TDD MIMO network.

According to this approach, each receiver announces an interference price, defined as the marginal decrease in the user's capacity due to an increase in perceived interference. Given the interference prices announced by neighboring receivers, and also given knowledge of the corresponding cross-channel matrices, each transmitter can update the transmit power levels and precoding matrices to maximize a utility function. The pricing equations for the MIMO case can be written as:

$$\pi_{i,j} = -\frac{\partial C_{i,j}}{\partial I_{i,j}} = \frac{B}{\log 2}\left(\frac{1}{I_{i,j}} - \frac{1}{I_{i,j}+s_{i,j}}\right), \tag{4.7}$$

where $\pi_{i,j}$ is the interference pricing associated to the user j connected to the BS i. If i, j is in the DL mode, then

$$C_{i,j} \triangleq C_{i,j}^{\mathrm{DL}}(\mathbf{W}_{i,j}), \tag{4.8a}$$
$$s_{i,j} \triangleq S_{i,j}^{\mathrm{DL}}(\mathbf{W}_{i,j}), \tag{4.8b}$$
$$I_{i,j} \triangleq \mathbf{v}_{i,j}^{H} I_{i,j}^{\mathrm{DL}} \mathbf{v}_{i,j} + \sigma_{i,j}^{2}. \tag{4.8c}$$

Otherwise, the user i, j is in the UL mode, then

$$C_{i,j} \triangleq C_{i,j}^{\mathrm{UL}}(\mathbf{v}_{i,j}), \tag{4.9a}$$
$$s_{i,j} \triangleq S_{i,j}^{\mathrm{UL}}(\mathbf{v}_{i,j}), \tag{4.9b}$$
$$I_{i,j} \triangleq \mathbf{v}_{i,j}^{H}(I_{i,j}^{\mathrm{UL}} + \mathbf{I}_n \sigma_{i,j}^{2})\mathbf{v}_{i,j}. \tag{4.9c}$$

As only one stream is considered for each user, the optimization problem for the MIMO problem can be written in the same way as the previous chapter. Therefore, the MIMO optimization problem is

$$\begin{aligned} \underset{\mathbf{W}_{m,k}}{\text{maximize}} \quad & (1-\mu) C_{m,k}^{\mathrm{DL}}(\mathbf{W}_{m,k}) - \mu \mathcal{I}_{m,k}. \\ \text{subject to} \quad & \sum_{k} \mathrm{Tr}[\mathbf{W}_{m,k}] \leq P_{\max}^{\mathrm{DL}}, \\ & \mathrm{rank}(\mathbf{W}_{m,k}) = 1; \mathbf{W}_{m,k} \succcurlyeq 0, \end{aligned} \tag{4.10}$$

where

$$\begin{aligned} \mathcal{I}_{m,k} = & \sum_{d\in\mathcal{D}} \sum_{j\in\mathcal{K}} \pi_{d,j} \mathrm{Tr}[\mathbf{W}_{m,k} \mathbf{L}_{(d,j),m}] - \\ & - \pi_{m,k} \mathrm{Tr}[\mathbf{W}_{m,k} \mathbf{L}_{m,(m,k)}] + \sum_{u\in\mathcal{U}} \sum_{l\in\mathcal{K}} \pi_{u,l} \mathrm{Tr}[\mathbf{W}_{m,k} \mathbf{T}_{m,u}], \end{aligned} \tag{4.11}$$

where $\mathbf{L}_{(d,j),m} \triangleq \mathbf{H}_{(d,j),m} \mathbf{H}_{(d,j),m}^{H}$ and $\mathbf{T}_{m,u} \triangleq \mathbf{G}_{u,m} \mathbf{G}_{u,m}^{H}$ are Gramian matrices of the interference channels to the DL UE j (in BS d) and the UL BS u, respectively, due to the DL transmission from BS m to user k.

Here, due the complexity of problem (4.10), we relax the rank-1 constraint as done in the previous chapter. Then, the modified problem, can be written as follows:

$$\begin{aligned} \underset{\mathbf{W}_{m,k}}{\text{maximize}} \quad & (1-\mu)C_{m,k}^{\text{DL}}(\mathbf{W}_{m,k}) - \mu \mathcal{I}_{m,k}; \\ \text{subject to} \quad & \sum_{k} \text{Tr}[\mathbf{W}_{m,k}] \leq P_{\max}^{\text{DL}}, \\ & \mathbf{W}_{m,k} \succcurlyeq 0. \end{aligned} \tag{4.12}$$

As we are interested on calculating the best precoder (beam direction and power allocation) for downlink users, the UL precoders and the receive filters for DL and UL are fixed. The optimization problem, then, is the same as that of (3.14). Therefore, the beamforming algorithm for the MIMO case is similar to Algorithm 4 in Chapter 3. The main difference is that the UL receive filters can be updated during the DL beamforming calculation or after the DL convergence on the PBA for MISO case. The algorithm for the MIMO case is based on the iterative approach where we must update, at least, the DL receive filters for each algorithm iteration due the pricing calculation. Therefore, the DL beamforming is calculated while the receive filter is fixed and, at the end of each iteration, the updated precoder is fixed while the DL receive filter is updated.

4.3.2 Algorithm Analysis

4.3.2.1 Signaling Aspects

The pricing signaling for the MIMO case follows the same procedure of the previous MISO discussed on Chapter 3. The discussion about the parallel and sequential implementation also holds for the MIMO case in terms of signaling.

The key point on signaling for the MIMO PBA is the knowledge of the interfering channels ($\mathbf{L}$ and $\mathbf{G}$) and receive filters $\mathbf{v}_{m,k}$ for a DL BS m to update prices and beamformers, and the transmit precoders $\mathbf{w}_{m,k}$ for UE k in order to update its receive filter. In order to have all these informations available on their respective node, we consider that all network nodes (BS or UE) use orthogonal training sequences[1] in forward and backward direction [83, 85].

This procedure, together with the channel reciprocity, allows the knowledge of the effective channels information, i.e., the precoded pilots after sending by the channel, at each node of interest[2].

4.3.2.2 Complexity Analysis

For the MIMO PBA, the main complexity relies on the solution of the optimization problem by the CVX as on the MISO case in Chapter 3. As the BS estimates the effective

[1] Also known as pilot symbols.

[2] The number of orthogonal pilots sequence for this procedure depends on the number of UEs and the number of antennas in each one [83].

channel (which is a vector due the one stream transmission), the most complex operation is only dependent on the number of BS antennas. Therefore, as the MISO case, the most complex operation done is $O(N_{\mathrm{BS}}^3)$ [66, 67], hence the total complexity of the considered PBA BF for MIMO system is approximately $O(N_{\mathrm{iter}}N_{\mathrm{BS}}^3)$, where N_{iter} is the number of iterations the algorithm needs to converge.

4.4 Sub-optimal Distributed Pricing-Based Algorithm (SPBA) for MIMO systems

As done in the previous section for the PBA, now we will analyze the MIMO formulation for the proposed SPBA. The problem we want to solve is (4.12) for a single stream transmission per user.

Once again, we are only interested to find the best set of precoders and power allocation for the DL transmission, therefore the UEs receive filter is kept fixed for the MIMO SPBA algorithm. By using the same approach of the previous chapter, for a DL UE (m, k), the optimization problem in (4.12) can be written as:

$$\begin{aligned} \underset{\mathbf{w}_{m,k},\, p_{m,k}}{\text{maximize}} \quad & (1-\mu)C_{m,k}^{\mathrm{DL}}(\mathbf{w}_{m,k}, p_{m,k}) - \mu p_{m,k}\mathbf{w}_{m,k}^H \mathbf{L}_{m,k}\mathbf{w}_{m,k}. \\ \text{subject to} \quad & p_{m,k} \leq P_{m,k}^{\max}, \\ & ||\mathbf{w}_{m,k}||^2 = 1, \end{aligned} \tag{4.13}$$

where

$$\mathbf{L}_{m,k} = \sum_{d\in\mathcal{D}}\sum_{j\in\mathcal{K}} \pi_{d,j}\mathbf{H}_{(d,j),m}^H \mathbf{H}_{(d,j),m} - \pi_{m,k}\mathbf{H}_{(m,k),m}^H \mathbf{H}_{(m,k),m} + \sum_{u\in\mathcal{U}}\sum_{l\in\mathcal{K}} \pi_{u,l}\mathbf{G}_{m,u}^H \mathbf{G}_{m,u}, \tag{4.14}$$

is the leakage matrix for the user (m, k).

Following the same steps as previous chapter, we introduce a new beamforming vector $\tilde{\mathbf{w}}_{m,k} = \mathbf{L}_{m,k}^{1/2}\mathbf{w}_{m,k}$ and $\tilde{\mathbf{h}}_{(m,k),m} = \mathbf{L}_{m,k}^{-1/2}\mathbf{v}_{m,k}^H \mathbf{H}_{(m,k),m}$, where $\mathbf{v}_{m,k}^H$ is the fixed DL receive filter. Therefore, the DL precoders are chosen the same way as for the MISO case, i.e., $\tilde{\mathbf{w}}_{m,k} = \tilde{\mathbf{h}}_{(m,k),m}^H / ||\tilde{\mathbf{h}}_{(m,k),m}^H||$ and the power $p_{m,k}$ is found via bisection method.

As we have to calculate the equivalent channel, $\mathbf{v}_{m,k}^H \mathbf{H}_{(m,k),m}$, to update the DL precoders, the DL receive filters need to be updated at each iteration of the MIMO SPBA. Therefore, we can use the Algorithm 5 to update the DL precoders for MIMO systems where we only introduce a new step (DL receive filter update) at the end of each iteration.

4.5 Results

The considered scenario is the same used in the previous chapter: a dynamic TDD network with 19 cells (10 cells operating in DL mode and 9 cells operation in UL mode) with 2 users sharing the same frequency resource. The simulation parameters are described on Tables 3.3 and 3.4. The precoders and receiver filter for both DL and UL are summarized on Table 4.1.

Table 4.1 – Precoders and receiver filter for MIMO dynamic TDD simulations.

	Precoder	Receiver Filter
DL	PB BF	MMSE
UL	MRT	MMSE

Source: Created by the author.

4.5.1 PBA results

Figures 4.1 and 4.2 show the DL and UL performance, respectively, when the number of UE antennas increases. From both plots, we can see the performance of the considered PB scheme increases with the number of UE antennas. This happens due to the addition of the MMSE receiver filter on the DL UEs, which mitigates part of the interference that was not suppressed by the pricing algorithm.

For the UL case, the addition of more antennas on the UE side, combined with the MRT precoder, results in a directive beam from the user to the BS, increasing the received SNR. The interference that the MRT cause can cause to other UL users is compensated by the MMSE receivers and the PBA.

Figure 4.1 – Comparison of PBA downlink SINR for different UE antenna configurations.

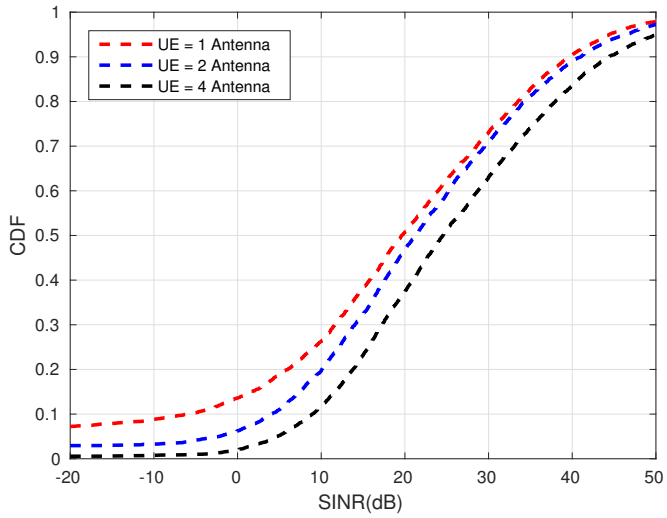

Source: Created by the author.

Figure 4.3 shows the power consumption for different UE antenna configurations. As expected, when the number of antennas at the UE side increases, the BSs use less power for the DL transmission due the MMSE receive filters at the UE side, which increases the network spectral efficiency.

Figure 4.2 – Comparison of PBA uplink SINR for different UE antenna configurations.

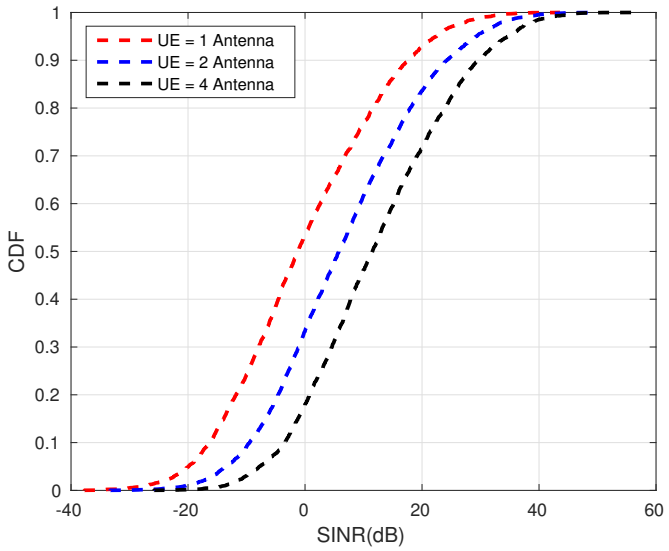

Source: Created by the author.

Figure 4.3 – Comparison of consumed power for different UE antenna configurations.

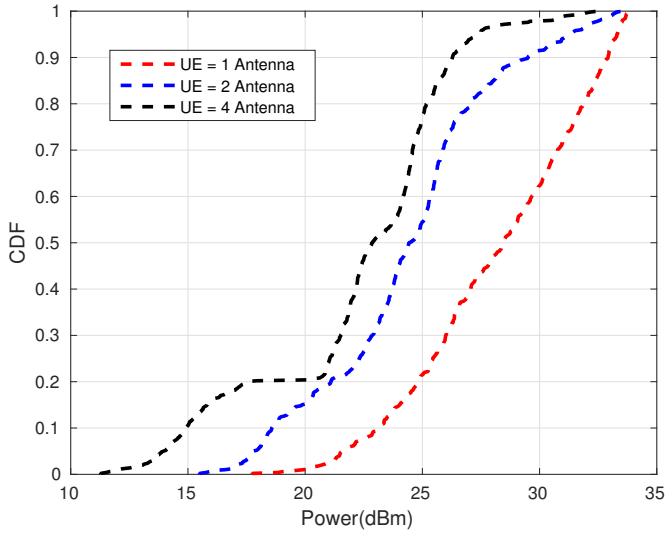

Source: Created by the author.

4.5.2 SPBA results

In this section we present the MIMO results for the SPBA. As observed for the PBA, when the number of antennas at the UE side increases we have a performance gain of both DL and UL transmissions as can be seen on Figures 4.4 and 4.5.

Figures 4.6 and 4.7 show a comparison between the PBA and SPBA for multi-antenna UE. In Figure 4.6 the DL behavior for the MIMO dynamic TDD is shown where we can see that the proposed heuristic has a tight gap to the optimal PBA. This happens because we

Figure 4.4 – Comparison of SPBA downlink SINR for different UE antenna configurations.

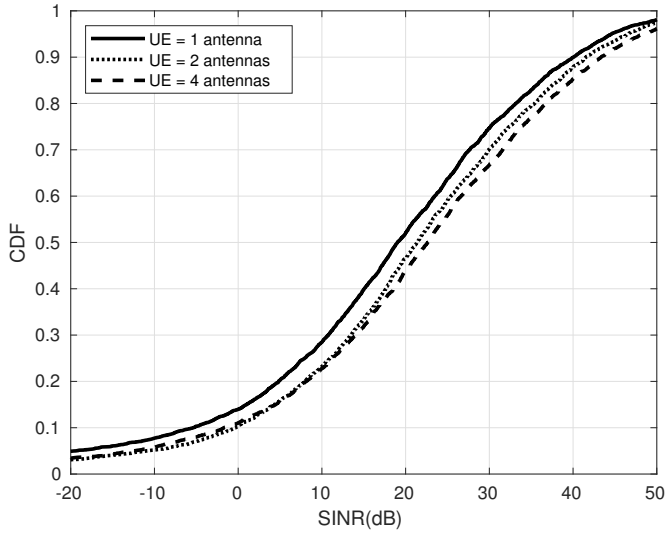

Source: Created by the author.

Figure 4.5 – Comparison of SPBA uplink SINR for different UE antenna configurations.

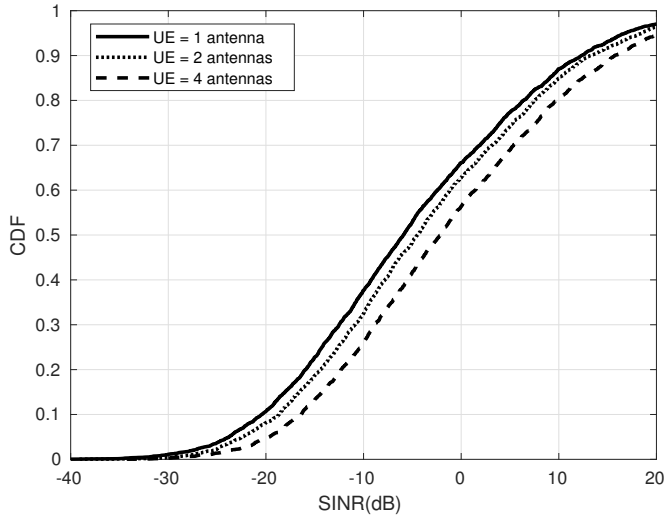

Source: Created by the author.

design the DL precoders as the matched channel of the equivalent channel which increases the DL SINR. We also take into account the leakage matrix to the DL users, where we reduce both DL and UL interference, boosting the DL performance.

For the UL scenario, Figure 4.7, the gap between the PBA and SPBA increases when the number of UE antennas gets high. The reason is the same that explains the low gap between the two algorithms for the DL transmission. The DL precoder is not optimize to suppress the DL-UL interference, even if we take into account the interference leakage matrix. As the number of antennas

Figure 4.6 – Comparison of downlink SINR between the two proposed price approaches for different UE antenna configurations.

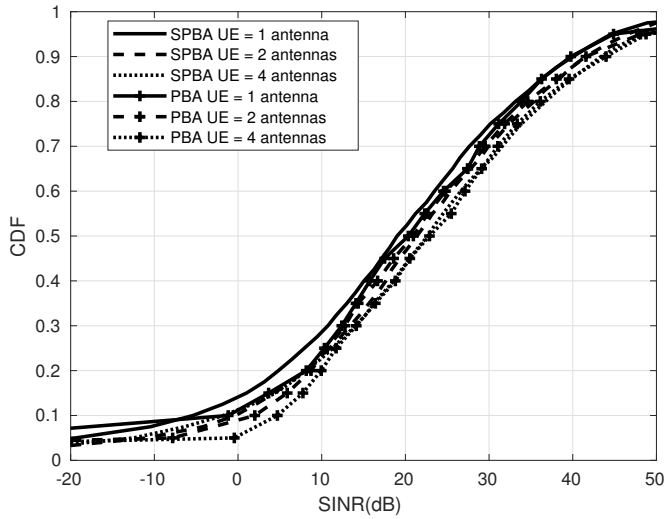

Source: Created by the author.

Figure 4.7 – Comparison of uplink SINR between the two proposed price approaches for different UE antenna configurations.

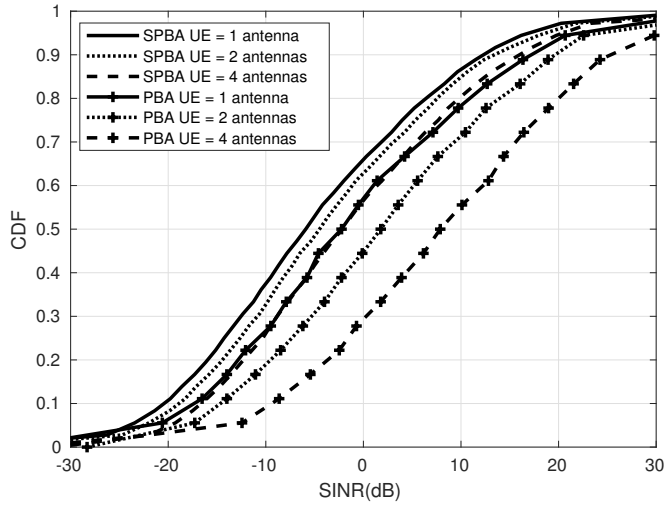

Source: Created by the author.

4.6 Conclusions

In this chapter we have extended the results of previous PBA for MIMO systems. When the UEs have multi-antenna capabilities, the network performance increases by exploiting the spatial diversity. For one stream transmission, the MIMO problem is similar to the previous pricing MISO optimization problem, since only the DL side is considered for the optimization problem, while the UL precoders are chosen to be a previous fixed solution. The main difference between the two algorithms (MISO and MIMO) is that, for MIMO systems, the DL receive

filters need to be updated in each pricing algorithm iteration, leading to a new equivalent channel for DL precoder which includes a new signaling step.

The obtained results are consistent with the considered scenario and they open a branch for future works, where one can develop a complete framework which takes account both DL and UL transmission for precoders and receive filters design.

Another possible next step is to consider a multiple stream scenario taking advantage of the multiplex gain and, therefore, increasing the network throughput. However, the interference will increase and another precoder/receive filter strategy should be considered to manage it properly.

5 GREEDY ALGORITHM FOR STREAM SELECTION IN A MIMO INTERFERENCE CHANNEL

In this chapter we continue the interference management for MIMO systems. We are now interested on finding the maximum number of streams users in a MIMO network that can be sent without loss at data rate transmission (throughput). We propose a GSSA (greedy stream selection algorithm) for a $M \times N$ K-user MIMO-IC. The proposed algorithm tries to find the "best stream" allocation by removing streams with low SINR until the system capacity cannot be increased.

This chapter is organized as follows. Section 5.1 presents the state of art and the objective of the present chapter. In Section 5.2 the IA problem and the considered system model are presented. In Section 5.3 the degrees of freedom (DoF) and feasibility concepts are described while in Section 5.4 the classical IA algorithms are presented. Section 5.5 presents the GSSA and the motivation behind this algorithm. Section 5.6 provides the analysis of the considered GSSA by comparing it with fixed IA solutions and exhaustive search by means of Monte Carlo simulations. And, finally, in Section 5.7, some conclusions are drawn.

5.1 Introduction

We have seen on previous chapters that beamforming and power control are an effective way to deal with interference. So far, we have analyzed a precoder design and power control algorithms for dynamic TDD systems: a MISO scenario on Chapter 3 and a single stream MIMO scenario on Chapter 4.

We now are interested on a multi-stream MIMO networks. For that kind of scenario, an interference management strategy is to assume that the transmitters can cooperate with each other by performing a joint transmission. By doing this, the whole system can be seen as a multi-user MIMO scenario. A well-known algorithm for such case is block diagonalization (BD) [86], which is employed in coordinated multi-point (CoMP) communications.

However, because BD is a joint transmission strategy it requires all transmitters to have the data that must be sent to each receiver. The existence of a communication link is not always possible, thus an approach that can send data without any transmitter interfering on each other has emerged. The *IA* [11, 12] is a linear preconding technique which is based on the idea that the multiple transmitters in a network try to align the interference at the unintended receivers into a reduced dimensional subspace. The subspace orthogonal to the interference subspace is free from interference and can be used for correctly decoding the desired information.

The DoF, by its turn, represents how the capacity of a system grows with the log of the SNR [12]. For an IC, it can be seen as the total number of streams that can be sent by the users, thus increasing the DoF of a system implies at higher throughput for the users. In order to maximize the sum rate capacity of the interference channel, some works have exploit how to

perform a stream selection strategy [87, 88, 89, 90]. In [87] the authors used a pricing method for the stream allocation for the max-SINR algorithm. By their turn, in [88], the authors proposed a stream allocation solution and a precoder design based on a procedure that selects the stream with less interference by choosing the beams recursively. In [89] this work was extended by modifying the algorithm presented in [88] for different initialization points. [90] has extended the work on [89] by proposing a precoder/decoder design to reduce the amount of CSI exchanged by the users pairs.

Different from previous chapter, we will make an use of an interference management algorithm to develop a low-complexity algorithm for stream selection in a MIMO-interference channel (MIMO-IC).

Let $(M, N, d)^K$ characterizes a K-user MIMO-IC network, where M is the number of transmit antennas, N is the number of receive antennas and d is the number of DoF or streams each user wants to send. We seek to answer the following question "given the $(M, N, d)^K$ MIMO-IC, what is the best number of streams for each user to transmit which maximizes the network throughput ?"

To this end, we have proposed a greedy algorithm to answer this question. The proposed algorithm runs with the MMSE-IA precoder and its performance is compared with the exhaustive search by Monte Carlo simulations in two different scenarios. The first scenario is refereed as symmetric attenuation scenario which no path loss is considered among the network nodes. In the second one, the signal strength is a function of the distance, thus more streams are allowed to be transmitted.

The results show that the GSSA outperforms, in both scenarios, any fixed solution and it achieves a good sum capacity performance when compared with the best stream allocation (exhaustive search), but with less computational complexity.

5.2 Interference Alignment

In Section 5.1, we have defined the IA as a spatial filtering where we divide the user's space in two subspaces: one for the desired signal, named 'desired signal subspace', and other for the interference, named 'interference subspace'. It is done by designing properly the precoders and receiver filters for each user in the network.

The way IA is applied is dependent on many variables such as scenario and domain [91]. The scenario considered in this thesis is the $M \times N$ K-user MIMO-IC [11, 92, 93], as shown in Figure 5.1. In our model, K is the number of interfering users that are sharing the same resource and $\mathbf{H}_{ki} \in \mathbb{C}^{N \times M}$ is the channel matrix between the transmitter i and receiver k. For each user, the transmitter is equipped with M antennas and the receiver is equipped with N antennas.

Figure 5.1 – System model for a $M \times NK$-user MIMO-IC.

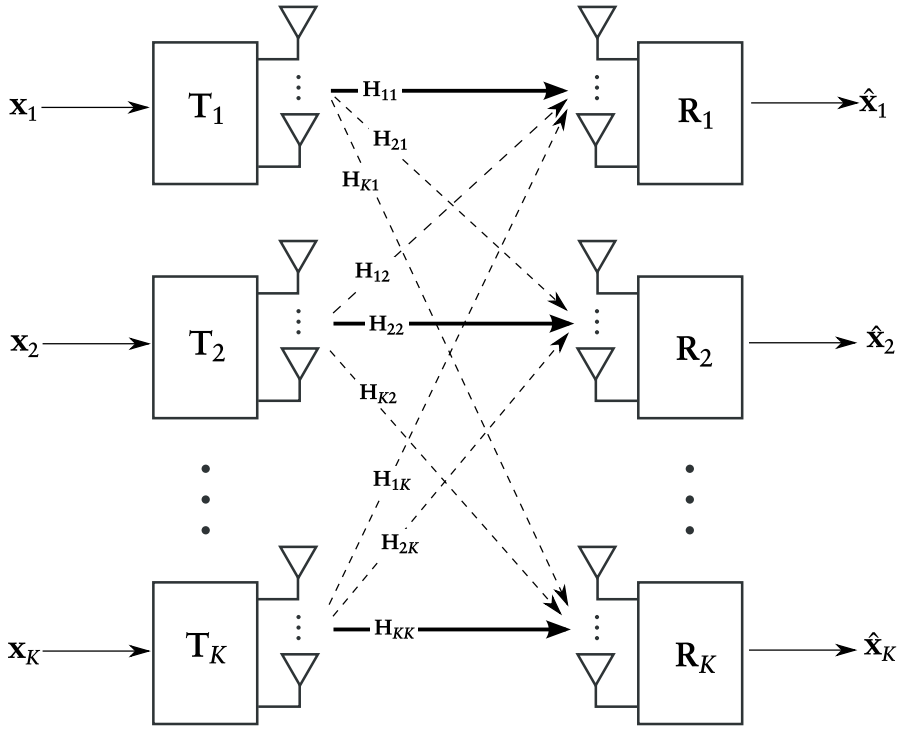

Source: Created by the author.

For a given user k, the received signal $\mathbf{y}_k$ can be written as

$$\begin{aligned}\mathbf{y}_k &= \sum_{i=1}^{K} \mathbf{H}_{ki}\mathbf{W}_i\mathbf{x}_i + \mathbf{n}_k \\ &= \underbrace{\mathbf{H}_{kk}\mathbf{W}_k\mathbf{x}_k}_{\text{usefull signal}} + \underbrace{\sum_{\substack{i=1 \\ i\neq k}}^{K} \mathbf{H}_{ki}\mathbf{W}_i\mathbf{x}_i}_{\text{interference}} + \mathbf{n}_k,\end{aligned} \tag{5.1}$$

where $\mathbf{x}_k \in \mathbb{C}^{d_k \times 1}$ is the transmit signal of the k-th user, and d_k is the number of degrees of freedom allocated for the user k (number of streams that the user k will transmit to its receiver). $\mathbf{W}_k \in \mathbb{C}^{M \times d_k}$ is the precoder of the k-th transmitter and $\mathbf{z}_k \in \mathbb{C}^{N \times 1}$ is the complex white Gaussian noise vector with distribution $\mathcal{CN}(\mathbf{0},\ N_0\mathbf{I})$ at the k-th receiver.

By applying a receiver filter $\mathbf{V}_k \in \mathbb{C}^{d_k \times N}$ at the received signal, we have

$$\mathbf{V}_k^H\mathbf{y}_k = \mathbf{V}_k^H\mathbf{H}_{kk}\mathbf{W}_k\mathbf{x}_k + \overbrace{\mathbf{V}_k^H \sum_{\substack{i=1 \\ i\neq k}}^{K} \mathbf{H}_{ki}\mathbf{W}_i\mathbf{x}_i}^{\varphi} + \mathbf{V}_k^H\mathbf{n}_k. \tag{5.2}$$

It can be noted in (5.2) that φ represents the interference from the unintended users. If the summation term is in the null space of $\mathbf{V_k}$, φ will be equal to zero. Thus, the interference

alignment condition can then be mathematically written as

$$\mathbf{V}_k^H \mathbf{H}_{ki} \mathbf{W}_i = \mathbf{0}, \quad \forall k \neq i, \tag{5.3a}$$

$$\text{rank}(\mathbf{V}_k^H \mathbf{H}_{kk} \mathbf{W}_k) = d_k. \tag{5.3b}$$

For an example, consider a 3-user MIMO-IC scenario, where each user has 2 antennas illustrated in Figure 5.2. For this case, the precoders have to satisfy the following equations

Figure 5.2 – System model for 2×2 3-user MIMO-IC.

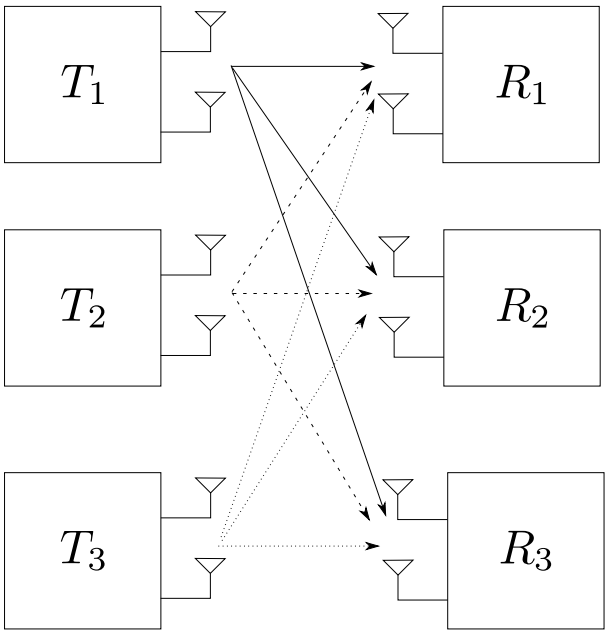

Source: Created by the author.

$$\text{span}(\mathbf{H}_{12}\mathbf{W}_2) = \text{span}(\mathbf{H}_{13}\mathbf{W}_3) \tag{5.4a}$$

$$\text{span}(\mathbf{H}_{32}\mathbf{W}_2) = \text{span}(\mathbf{H}_{31}\mathbf{W}_1) \tag{5.4b}$$

$$\text{span}(\mathbf{H}_{21}\mathbf{W}_1) = \text{span}(\mathbf{H}_{23}\mathbf{W}_3) \tag{5.4c}$$

where span($\mathbf{X}$) indicates the subspace spanned by the columns of a matrix $\mathbf{X}$. Each of those equations correspond a condition of alignment, i.e., the separation of the desired signal and the interference signal in two different subspaces for each receiver, where is illustrated by Figure 5.3, where U_k represents the desired signal subspace for user k and I_k represents the interference subspace for this same user.

It is important to note that, if each user has N antennas, then d_k represents the dimension of the desired signal subspace and $N - d_k$ is the dimension of the interference subspace.

Figure 5.3 – After applying the precoders and receive filters, the receive space is divided into desired signal subspace, U, and interference subspace, I.

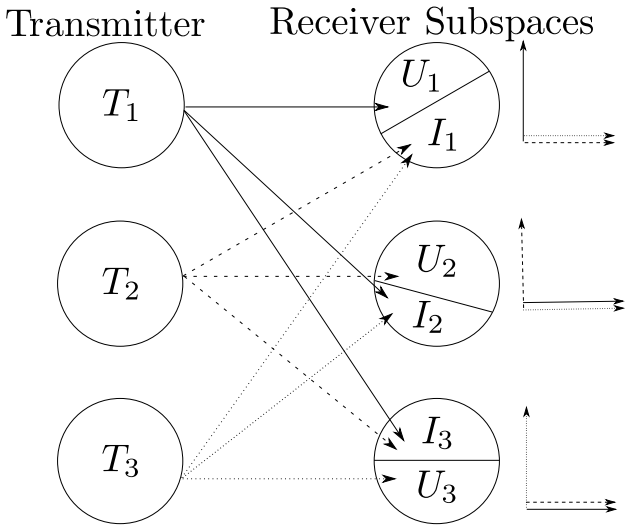

Source: Created by the author.

5.3 Degrees of Freedom and IA Feasibility

5.3.1 Degrees of Freedom

The DoF can be understood as the maximum multiplex gain of a MIMO system [94], which can be viewed as how many data streams can be sent by an user. When IA is applied in a MIMO-IC, part of the dimensions available is used for align the unintended signal, therefore the DoF does not represent $\min(M, N)$ as a point-to-point MIMO communication.

In the example of Figure 5.3, there is one dimension for the interference and one for the desired user signal, therefore, the total do DoF is equal to one. However, for more general scenarios, determinate how many DoF is available is still an open problem [91].

For an $M \times N$ MIMO-IC, the work in [95] has provided an inner bound and outer bound for the total of DoF that can be achieved. This number is related to the following ratio

$$R = \lfloor \frac{\max(M, N)}{\min(M, N)} \rfloor, \tag{5.5}$$

where $\lfloor \dot{\rfloor}$ is the floor operator. This work shows if $K \leq R$, the total number of DoF is equal to $K \min(M, N)$, otherwise it is $K \min(M, N) \frac{R}{R+1}$, which is achievable by IA.

5.3.2 IA Feasibility

The feasibility of an IA system is related to find an IA solution such it can separate the desired signal and the interference into two different subspaces. Finding whenever the IA problem is feasible or not helps to draw some informations about the DoF for a MIMO-IC. It was presented on Section 5.2 that finding an IA solution is related to solve Equations (5.3a) and (5.3b). Therefore, the IA problem can be seen as a system of equations and the feasibility

problem can be solved by comparing the number of equations and the number of variables in this system [96, 97].

To determine the number of equations for IA, consider the Equations (5.3a) and (5.3b) rewritten in the following way

$$\left(\mathbf{v}_k^{[m]}\right)^H \mathbf{H}_{ki}\mathbf{w}_i^{[n]} = \mathbf{0}, \quad \forall k \neq i, \forall n \in \{1, 2, \cdots, d_i\} \quad \text{and} \quad \forall m \in \{1, 2, \cdots, d_k\}, \tag{5.6}$$

where $\mathbf{w}_i^{[n]}$ and $\mathbf{v}_k^{[m]}$ are the transmit and receive beamforming, respectively for each stream. Therefore, the number of equations, N_e can be determined as [97]

$$N_e = \sum_{\substack{i,k \\ i \neq k}} d_i d_k. \tag{5.7}$$

Applying the precoder $\mathbf{w}_i^{[n]}$ produces $d^{[k]}(M^{[k]} - d^{[k]})$ variables while applying the receiver filter $\mathbf{v}_k^{[m]}$ produces $d^{[k]}(N^{[k]} - d^{[k]})$ variables [97], therefore the total number of variables, N_v is

$$N_v = d^{[k]}(M^{[k]} + N^{[k]} - 2d^{[k]}). \tag{5.8}$$

If symmetric systems $(M, N, d)^K$ are taken into consideration, the IA is feasible if these conditions are satisfied [97, 98]:

$$N_v \geq N_e \tag{5.9a}$$

$$M + N - (K+1)d \geq 0. \tag{5.9b}$$

If any of these cannot be satisfied, the system is infeasible and an IA solution cannot be found.

5.4 IA Algorithms

In the literature, there are many works that have developed algorithms to solve the interference alignment problem such as [11, 24, 25, 99, 100, 101, 102, 103, 104]. Next we will describe the IA classical algorithms.

5.4.1 Closed-Form Solution

The closed-form solution for the IA problem only exists for few cases [91]. For the 3-user case, the close-form solution is known and it is determined when the Equations (5.4a)-(5.4c) are satisfied an then it is applied the proper receive filter [100, 101]. As there are

many possibilities to solve (5.4a)-(5.4c), we need to restrict the solutions. To this end, the new set of equations to be satisfied can be written as

$$\text{span}(\mathbf{H}_{12}\mathbf{W}_2) = \text{span}(\mathbf{H}_{13}\mathbf{W}_3) \tag{5.10a}$$

$$\mathbf{H}_{32}\mathbf{W}_2 = \mathbf{H}_{31}\mathbf{W}_1 \tag{5.10b}$$

$$\mathbf{H}_{21}\mathbf{W}_1 = \mathbf{H}_{23}\mathbf{W}_3 \tag{5.10c}$$

These equations are equivalent to [101]

$$\text{span}(\mathbf{W}_1) = \text{span}(\mathbf{E}\mathbf{W}_1) \tag{5.11a}$$

$$\mathbf{W}_2 = \mathbf{H}_{32}^{-1}\mathbf{H}_{31}\mathbf{W}_1 \tag{5.11b}$$

$$\mathbf{W}_3 = \mathbf{H}_{23}^{-1}\mathbf{H}_{21}\mathbf{W}_1, \tag{5.11c}$$

where $\mathbf{E} = \mathbf{H}_{31}^{-1}\mathbf{H}_{32}\mathbf{H}_{12}^{-1}\mathbf{H}_{13}\mathbf{H}_{23}^{-1}\mathbf{H}_{21}$. Therefore, $\mathbf{V}_1$ is any combination of n eigenvectors of $\mathbf{E}$ and $\mathbf{W}_2$ and $\mathbf{W}_3$ can be found by solving (5.11b) and (5.11c), respectively.

The next step is to calculate the receive filters $\mathbf{V}_k$. This is done by applying a ZF such as

$$\mathbf{V}_1 = \text{null}([\mathbf{H}_{12}\mathbf{W}_2]) = \text{null}([\mathbf{H}_{13}\mathbf{W}_3]) \tag{5.12a}$$

$$\mathbf{V}_2 = \text{null}([\mathbf{H}_{21}\mathbf{W}_1]) = \text{null}([\mathbf{H}_{23}\mathbf{W}_3]) \tag{5.12b}$$

$$\mathbf{V}_3 = \text{null}([\mathbf{H}_{31}\mathbf{W}_1]) = \text{null}([\mathbf{H}_{32}\mathbf{W}_2]), \tag{5.12c}$$

where, null($\mathbf{X}$) represents the null space of a matrix $\mathbf{X}$.

5.4.2 IA-MMSE

A pure IA algorithm that solves (5.3a) and (5.3b) is considered suboptimal for low SNR values, since it takes account only the rank of the equivalent channel. The MMSE algorithm seeks a more general objective where IA is just a part of it. For the considered IA problem the MSE is given by

$$\text{MSE} = \sum_{k=1}^{K} \mathbb{E}\|\mathbf{V}_k^H\mathbf{y}_k - \mathbf{x}_k\|^2. \tag{5.13}$$

Replacing (5.2) in (5.13), we have

$$\text{MSE} = \sum_{k=1}^{K} \mathbb{E}\|\mathbf{V}_k^H\left(\mathbf{H}_{kk}\mathbf{W}_k\mathbf{x}_k + \sum_{i=1,i\neq k}^{K}\mathbf{H}_{ki}\mathbf{W}_i\mathbf{x}_i + \mathbf{n}_k\right) - \mathbf{x}_k\|^2. \tag{5.14}$$

Hence, the MMSE optimization problem is given by

$$\min_{\{\mathbf{V}_k\};\{\mathbf{V}_k\}} \sum_{k=1}^{K} \text{tr}\,(\mathbf{V}_k^H(\sum_{i=1}^{K}\mathbf{H}_{ki}\mathbf{V}_i\mathbf{W}_i^H\mathbf{H}_{ki}^H + N_0\mathbf{I})\mathbf{V}_k) - 2\mathbb{R}\{\text{tr}\,(\mathbf{V}_k^H\mathbf{H}_{kk}\mathbf{W}_k)\}$$

$$\text{subject to } \text{tr}(\mathbf{W}_i^H\mathbf{W}_i) \leq P_i; \qquad \forall i \in \{1,\ldots,K\}, \tag{5.15}$$

where P_i is the power for each transmitter.

Following the solution for this optimization problem given in [99], the receive filter $\mathbf{V}_k$ can be calculated as

$$\mathbf{V}_k = \left(\sum_{i=1}^{K} \mathbf{H}_{ki} \mathbf{W}_i \mathbf{W}_i^H \mathbf{H}_{ki}^H + N_0 \mathbf{I} \right)^{-1} \mathbf{H}_{kk} \mathbf{W}_k, \tag{5.16}$$

and the precoder $\mathbf{V}_i$ is given by

$$\mathbf{W}_i = \left(\sum_{k=1}^{K} \mathbf{H}_{ki}^H \mathbf{V}_k \mathbf{V}_k^H \mathbf{H}_{ki} + \mu_i \mathbf{I} \right)^{-1} \mathbf{H}_{ii}^H \mathbf{V}_i, \tag{5.17}$$

where $\mu_i \geqslant 0$ is the Lagrangian multiplier and it can be found via Newton iterations [105]. This approach is clearly an iterative procedure, thus, in practice, the transmitters first initialize their precoders considering the constraint in (5.15), then they use (5.16) and (5.17) to calculate the precoders and receiver filters until convergence.

5.4.3 Max-SINR

Differently from the previous IA-MMSE, the max-SINR proposed in [25] seeks to maximize the post-processed SINR. This algorithm is based on the TDD reciprocity, where the direct and reverse links have the following relationship:

$$\overrightarrow{\mathbf{W}}_k = \mathbf{V}_k \tag{5.18a}$$

$$\overrightarrow{\mathbf{V}}_k = \mathbf{W}_k \tag{5.18b}$$

$$\overrightarrow{\mathbf{H}}_{k,i} = \mathbf{H}_{k,i}^H \quad \forall k, i \in \{1, 2, \cdots, K\}, \tag{5.18c}$$

where $\overrightarrow{\mathbf{X}}$ indicates the reverse direction for a matrix $\mathbf{X}$.

The SINR for the ℓ-th stream of the k-th user is given by:

$$\mathrm{SINR}_{k\ell} = \frac{\mathbf{V}_k^{[\star\ell]H} \mathbf{H}_{kk} \mathbf{W}_k^{[\star\ell]} \mathbf{W}_k^{[\star\ell]H} \mathbf{H}_{kk}^H \mathbf{V}_k^{[\star\ell]}}{\mathbf{V}_k^{[\star\ell]H} \mathbf{B}_{k\ell} \mathbf{V}_k^{[\star\ell]}}, \tag{5.19}$$

where $\mathbf{B}_{k\ell}$ is the interference-plus-noise covariance matrix, which is given by

$$\mathbf{B}_{k\ell} = \sum_{i=1}^{K} \sum_{d=1}^{d_i} \left(\mathbf{H}_{ki} \mathbf{W}_i^{[\star d]} \mathbf{W}_i^{[\star d]H} \mathbf{H}_{ki}^H - \mathbf{H}_{kk} \mathbf{W}_k^{[\star\ell]} \mathbf{W}_k^{[\star\ell]H} \mathbf{H}_{kk}^H + \sigma_n^2 \mathbf{I}_{N_k} \right). \tag{5.20}$$

If the precoder $\mathbf{W}_k$ is fixed, the receive filter $\mathbf{V}_k$ which maximizes (5.19) is [25]

$$\mathbf{V}_k^{[\star\ell]} = \frac{\mathbf{B}_{k\ell} \mathbf{H}_{kk} \mathbf{W}_k^{[\star\ell]}}{\| \mathbf{B}_{k\ell} \mathbf{H}_{kk} \mathbf{W}_k^{[\star\ell]} \|}. \tag{5.21}$$

The max-SINR is summarized in Algorithm 7.

Algorithm 7 IA max-SINR algorithm.

1: Initialize the precoders $\mathbf{W}_k$ respecting power constraints for all $k \in K$.
2: Calculate $\mathbf{B}_{k\ell}$ for all k and ℓ, according with (5.20).
3: Find the receive filters using (5.21).
4: Reverse the transmission directions using (5.18a)-(5.18c).
5: Calculate $\overrightarrow{\mathbf{B}}_{k\ell}$ for all k and ℓ.
6: Calculate $\overrightarrow{\mathbf{V}}_{k\ell}$ for all k and ℓ.
7: Reverse all links and update $\mathbf{W}_k$ using (5.18b).
8: Repeat all the steps until convergence.

5.5 Greedy Stream Selection Algorithm (GSSA)

As aforementioned in Section 5.1, there are many efforts for increasing the rate of the users. In a MIMO scenario, we can take advantage of the multiple antennas and transmit multiple streams as many as the number of antennas available. However, in a interference scenario, transmitting more streams means to increase the level of interference in the whole system which can lead to a decreasing of the total throughput instead of get more data rate if the interference caused is too high.

The choice, then, is to set a fixed stream allocation that leads to a feasible solution or try to find the best stream allocation by performing an exhaustive search by trying all the possibilities and choose the best one. In the first strategy, even if we find the best number of streams that can be transmitted by checking the feasibility conditions of the system, it does not take account the time changes of the channel, thus this leads to a perform losses when the channel varies along the time. In a scenario with many transmitter/receiver pairs, find the best stream allocation by performing an exhaustive search is not recommended, due the high number of possibilities of choice. In this section, therefore, we present an algorithm with low complexity that can find a good stream allocation for the scenario described at Figure 5.1 which outperforms the fixed strategy solution and approximates to the best allocation one.

5.5.1 Algorithm Description

In order to find a good "stream allocation" we have developed a greedy algorithm, whose main idea is to remove streams based on the post-processing SINR value. In other words, we compare all streams of all users, remove the worst one, and then repeat the process until the sum capacity of the system is no longer increased by this process. Each time a stream is removed, the previous IA solution is used as a starting point and a new IA solution is found for the new stream configuration.

The algorithm is initialized by setting the number of streams for each user to the maximum allowed value[1]. After running the IA algorithm for the first time, we will have the set

[1] This value can be at most $\min(M, N)$ streams, but in this chapter we will use $\min(M-1, N-1)$ to leave at least one dimension where the interference from the unintended transmitters can be aligned.

of precoders and receiving filter and thus we will be able to compute the post-processing SINR.

After calculating the post-processing SINR of all streams of all users we can calculate the sum capacity of the whole system. The stream with the lowest SINR is then removed and the corresponding precoder is updated by removing the column related with the removed stream.

These resulting precoders are used as initialization for the next run of the IA algorithm, which will likely converge faster than the previous run. This stream reduction continues until each user has only one stream left or the sum capacity of the system does not improve after the removal of the lowest SINR stream, in which case the solution before the last stream removal is used. The GSSA is summarized in Algorithm 8.

Algorithm 8 GSSA (greedy stream selection algorithm).

1: **Initialization:** Set the maximum number of streams equal to $\min(M-1, N-1)$ for each user and set the precoders for the users, respecting the power constraints.
2: Run the IA algorithm;
3: **Store for each user:** the number of streams, SINR for each stream (Eq. (5.19)), precoders (Eq. (5.17)), receiver filters (Eq. (5.16)), and the sum capacity of the system;
4: Remove the user stream with lower SINR;
5: **if** user has only one stream **then**
6: Remove the lowest SINR among the remaining users.
7: **if** all the users have only one stream **then**
8: End the algorithm.
9: **end if**
10: **end if**
11: Run the IA algorithm (now the initialization is done with the resulting precoders of step 4) and store the new configuration (as in step 3);
12: **while** New Sum Capacity > Old Sum Capacity **do**
13: Repeat step 4;
14: Repeat step 11;
15: **end while**

5.5.2 Algorithm Analysis

5.5.2.1 Signaling Aspects

To run the GSSA algorithm, two main steps are needed: (1) the IA algorithm and (2) the stream selection. For the former, the information needed to be exchange is dependent on the algorithm used to perform the alignment. For the latter, the BS needs to store the number of streams, precoders and receiver filter for its user and the SINR for each stream for all the network users to decide which BS needs to remove one user's stream and also to calculate the system sum capacity. Hence, each BS needs to send a vector containing the SINR for each stream of its user which decreases at each iteration, since one stream is removed.

5.5.2.2 Complexity

In order to motivate the use of the greedy approach, we compare the number of iterations needed to determine the best stream allocation for the optimal and the proposed GSSA. The exhaustive search needs to evaluate all the possible stream configurations, then the number of iterations needed to find the best solution is $O(\min(M, N)^K)$. The proposed GSSA eliminates some stream configurations during its execution, then, the maximum number of iterations is $O((\min(M, N)) \times K)$.

5.6 Numerical Results

In this section we present simulation results to illustrate the performance of the proposed GSSA. For comparison, we include simulation results for different fixed stream allocation as well as the "best stream allocation" result, which is selected by running the IA algorithm for each possible configuration and choosing the one that yields the highest sum capacity.

The scenario is composed by $K = 3$ transmitter/receiver pairs[2], as can be seen in Figure 5.4. Each transmitter is placed at the center of a cell and its corresponding receiver is placed at a random position in the same cell. The numbers between brackets in the plots represent the number of streams for each user, e.g., [1 2 1] represents one stream for user 1, two streams for user 2 and one stream for user 3. The simulation parameters are summarized in Table 5.1.

Table 5.1 – Simulation Parameters.

Parameter	Value
Number of Monte Carlo Simulations	10,000
Cell Radius	1 km
Number of antennas	3 or 5 at each node
User position	randomly placed inside its cell
Modulation	4-PSK
Path Loss Model (in dB with d in km)	$128.1 + 37.6 \log_{10}(d)$
Noise Power	$N_0 = -116.4$ dBm
Transmission Power	Adjusted to match SNR at the border of the cell

Source: Created by the author.

[2] Best stream allocation can be found by an exhaustive search here because we are limiting the simulation to only 3 transmitter/receiver pairs.

Figure 5.4 – 3 cells scenario. Each cell has one transmit/receiver pair. The dots represent the users that are randomly placed within the cell. The transmitters are placed in the center of each cell.

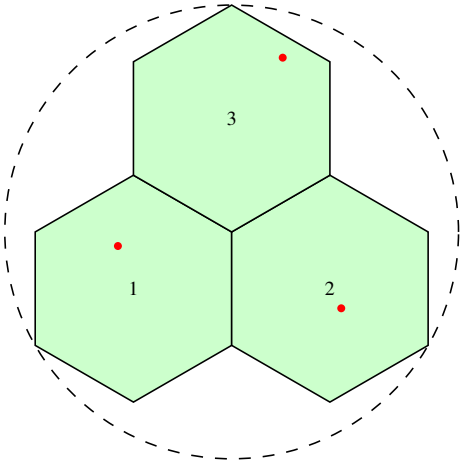

Source: Created by the author.

5.6.1 No Path Loss Case

Initially we simulate the case where all links, direct and interfering links, have similar path losses[3]. More specifically, we do not include path loss calculation in the simulation and each link is modeled as a random Gaussian matrix with zero mean and an identity covariance matrix. Since all interfering links have similar power with respect to the direct channel this case corresponds to the fully connected interference alignment in the literature and maximum performance is attained (at the high SNR regime) when the total number of streams respects the feasibility conditions addressed in [106, 107].

Figure 5.5 shows the sum capacity versus SNR for the different streams configurations when each node has 3 antennas. It can be seen that the proposed GSSA outperforms the case of best fixed solution [1 1 2][4]. The reason is that the fixed solution is an average of the sum capacity over the realizations for each SNR value, whereas the proposed algorithm tries to find the best solution at each channel realization.

Table 5.2 shows the percentages for which each stream configuration was chosen by the GSSA. The noise is the main concern in the low SNR regime (from 0 dB to 10 dB), thus the proposed algorithm often chooses the [1 1 1] solution (over than 80% of choice) as the one with better capacity, as can be seen more clearly in Figure 5.6 (represented by 3 streams bar plot), which is a feasible solution according to (5.9b). Sending more streams turns the IA solution unfeasible since for transmit more streams a user needs to divide its limited transmit power among the streams used for transmission.

On the other hand, for high SNR regime (from 10 dB to 30 dB), the interference

[3] This configuration does not represent a realistic scenario. It corresponds, for instance, to a scenario that all the transmitters are close from each other and all receivers have the same distance to its transmitter.

[4] In this scenario with 3 users and 3 antennas at each node IA is feasible if two users transmit one stream and one user transmit two streams, but no more. On average, performance of [1 1 2], [1 2 1] and [2 1 1] are the same.

Figure 5.5 – Sum capacity versus SNR for the case with no path loss and 3 transmit/receive antennas.

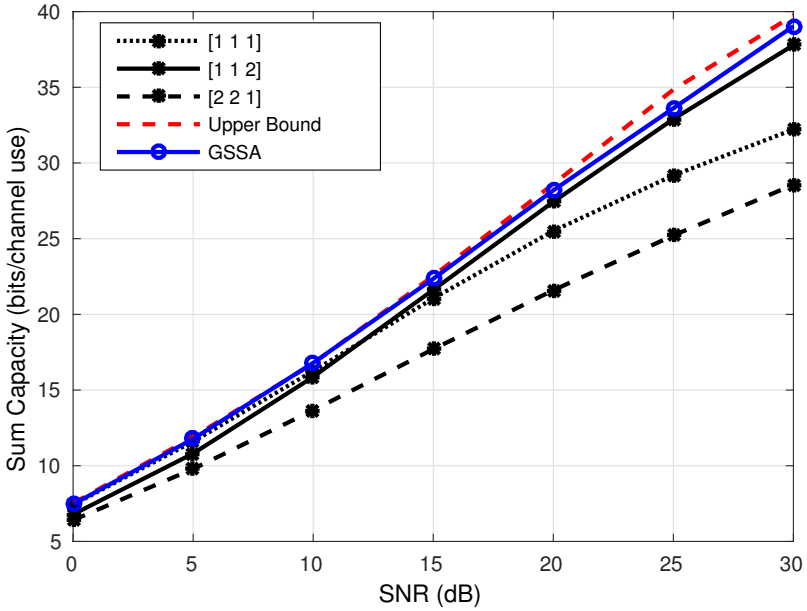

Source: Created by the author.

Table 5.2 – Selection percentage for each configuration in No Path Loss case for Tx = Rx = 3 antennas.

Streams \ SNR	0 dB	5 dB	10 dB	15 dB	20 dB	25 dB	30 dB
[111]	83.5%	64%	41.6%	20.2%	6.5%	1.7%	0.9%
[112]	4.7%	10.7%	18.4%	26.2%	31.5%	33.6%	33%
[121]	4.7%	11.5%	19.2%	25.8%	30%	32%	32.5%
[211]	5.4%	11.4%	19.1%	27.3%	31.9%	32.6%	33.6%
[221]	0.7%	0.7%	0.4%	0.1%	0.06%	0.02%	0%
[212]	0.7%	0.9%	0.4%	0.2%	0.02%	0.02%	0%
[122]	0.7%	0.7%	0.4%	0.2%	0%	0.01%	0%
[222]	0.2%	0.1%	0.5%	0%	0.02	0.05%	0%

Source: Created by the author.

is the main concern, since the transmit power is much higher than the noise power. Therefore, the GSSA avoids any stream allocation which would send more streams than what is possible while keeping IA feasible. That means the [1 1 1] configuration could be the best choice[5] in the high SNR regime. However, note that Equation (5.9b) only holds for full symmetric system (all users having the same transmit and receive antennas and number of streams sent), therefore when $d = 2$, where each user transmit two streams (the [2 2 2] case), the IA solution is unfeasible. Figure 5.6 indicates that an asymmetric stream transmission, with one user sending two streams

[5] Note from Equation (5.9b), the feasibility constraint for a symmetric system indicates that the IA solution for this case would be [1 1 1] with $d = 1$ stream per user.

Figure 5.6 – Percentage of choice for the total number of streams sent for the no path loss case with 3 transmit/receive antennas.

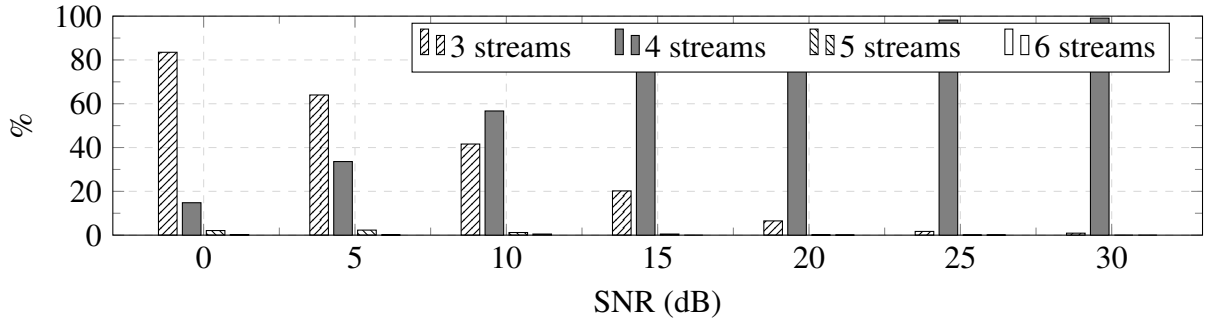

Source: Created by the author.

while the others send just one (total of 4 streams transmitted), is preferable than the symmetric case. It happens because the transmit power is greater than the noise power, so the user can still split its power into two streams and achieve a good rate, while it keeps one dimension to align the interference because other users use only one stream. If another user wants to transmit two streams, the one dimensional subspace will not be enough to align the interference and it will make the system unfeasible.

5.6.2 Path Loss Case

In practice, heterogeneous path loss between the users and BSs induces a scenario between the fully connected interference topology and the *partially connected interference topology* in [108, 109]. The users can take advantage of this configuration by sending more streams, thus improving the system capacity. In order to analyze the performance of the proposed GSSA in the presence of heterogeneous path loss we simulate the symmetric case with 3 and 5 transmit/receive antennas and an asymmetric case where the transmitter is equipped with 5 antennas and the receiver is equipped with 3 antennas. The results are illustrated, respectively, in Figure 5.7, Figure 5.9 and Figure 5.11 where we show the system capacity versus SNR values.

Compared with Figure 5.5, a configuration with a total of 5 or even 6 streams can work well in the heterogeneous path loss case, while in the previous case with uniform path loss they would perform badly. From the plot, we can conclude that the proposed GSSA reaches again a performance closer to the upper bound. Table 5.3 shows the percentages for which each stream configuration was chosen by the GSSA and can be used to explain the behavior in Figure 5.7.

Interestingly, the results in Table 5.3 seem like the opposite of the results in Table 5.2. In this scenario, as the transmit power is low and there is path loss among the interfering links, the interference caused by the unintended transmitters, at a given receiver, is much smaller than no path loss case. Thus, for low SNR regime, all the users can use the maximum number of allowed streams, two in our simulation here, and still achieve good performance, therefore, the full stream case (6 transmitted streams) is selected in more than 80% of simulations as shown in Figure 5.8.

Figure 5.7 – Sum capacity versus SNR for path loss case and 3 transmit/receive antennas.

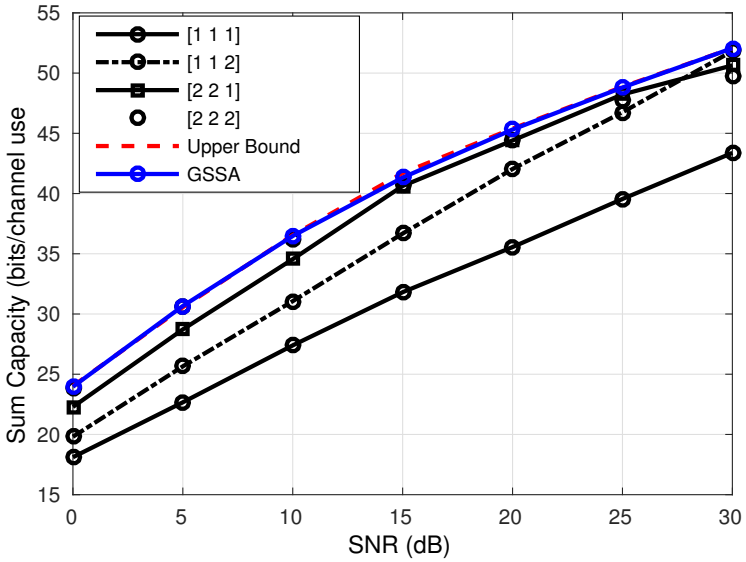

Source: Created by the author.

Table 5.3 – Selection percentage for each configuration in Path Loss case for Tx = Rx = 3 antennas.

SNR / Streams	0 dB	5 dB	10 dB	15 dB	20 dB	25 dB	30 dB
[111]	0%	0%	0%	0%	0%	0%	0%
[112]	0.05%	0.05%	0.04%	0.3%	2%	6.8%	11.5%
[121]	0.07%	0.01%	0.03%	0.3%	1.6%	7.3%	16.1%
[211]	0.1%	0.04%	0.03%	0.3%	1.7%	7.8%	16.5%
[221]	2.1%	1.7%	2.3%	5%	8.6%	7.7%	5.6%
[212]	4%	4%	7.2%	14.7%	22.5%	19.8%	12.2%
[122]	2.6%	1.8%	2.5%	5.3%	9%	8.1%	5.5%
[222]	91%	92.4%	87.9%	74.1%	54.6%	42.5%	32.6%

Source: Created by the author.

On the other hand, as the SNR gets higher, the transmission power and the interference increase. However, the relative difference in terms of path losses does not change, since it only depends on the distances between the nodes. As the interference gets high, the choice percentage for the [2,2,2] case by the GSSA algorithm decreases since there must be a free dimension to perform the align. This phenomenon is shown in Figure 5.8 where we can see the increase of choices for 4 and 5 streams cases. Then, the [2 1 1], [1 2 1] and [1 1 2] solutions are choose more often for high SNR regime.

This behavior can also be seen in Figure 5.9 and in Table 5.4, where now we have 5 transmit/receive antennas. From Table 5.4, it can be observed that the GSSA chooses configurations with high number of streams (at least 6 streams), due the low transmit power

Figure 5.8 – Percentage of choice for the total number of streams sent for the path loss case with 3 transmit/receive antennas.

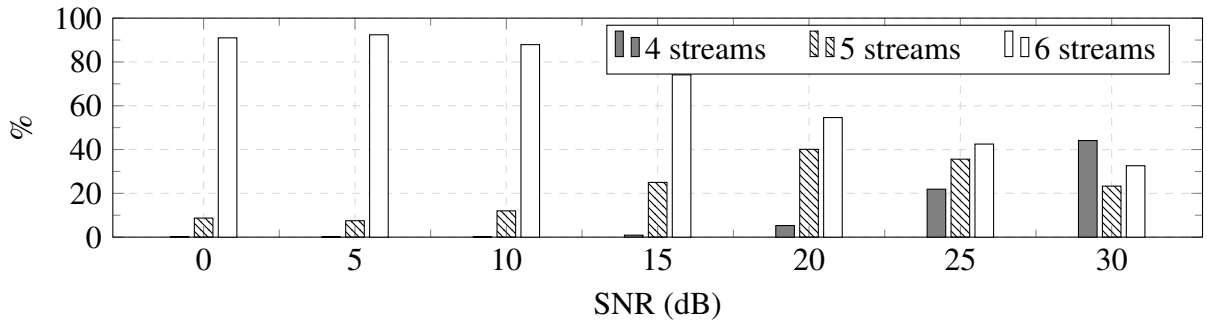

Source: Created by the author.

which leads small interference among the users as in 3 antenna case.

The GSSA is a suboptimal approach, then, sometimes, it does not choose a good stream configuration as for the case when the SINR is 30 dB. For the considered scenario, (5 transmit/receive antennas), the best pattern of streams to transmit cannot be determined, since the path loss between all three users has to be taken into account to determinate how many interference links are strong and have influence on the received SINR.

However, its performance is always better or, at least, equal to any fixed solution, as observed in Figure 5.9. Therefore, the behavior of the algorithm goes towards the behavior in the homogeneous path loss case, which can be considered a kind of a lower bound on the number of streams that can be sent in the non-homogeneous path loss case.

Figure 5.9 – Sum capacity versus SNR for path loss case and 5 transmit/receive antennas.

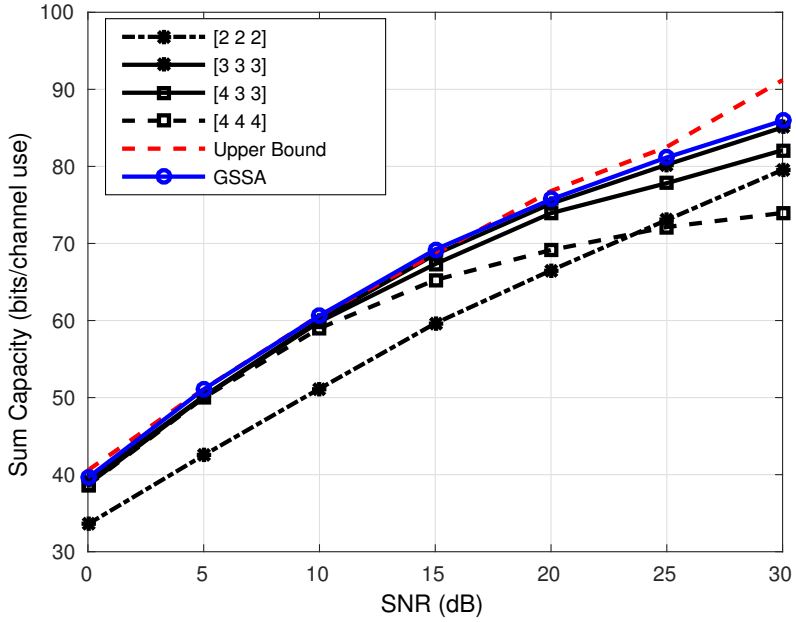

Source: Created by the author.

Table 5.4 – Selection percentage for each configuration in Path Loss case for Tx = Rx = 5 antennas.

SNR / Streams	0 dB	5 dB	10 dB	15 dB	20 dB	25 dB	30 dB
[223]	0%	0%	0%	0%	0.5%	3.4%	9.3%
[232]	0%	0%	0%	0%	0.5%	5.4%	13.5%
[233]	0%	0%	0%	0%	2.7%	4.5%	4%
[234]	0%	0%	0%	0%	0.3%	0.7%	1.5%
[242]	0%	0%	0%	0%	0%	0%	1%
[244]	0%	0%	0%	0%	0%	0%	1%
[322]	0%	0%	0%	0%	0.7%	4.2%	13.5%
[323]	0%	0%	0%	1%	2.3%	3.3%	3%
[324]	0%	0%	0%	0%	0.5%	0.6%	1.1%
[331]	0%	0%	0%	0%	0%	0%	1%
[332]	0%	0%	0%	2.3%	10.5%	16.3%	9.1%
[333]	20.4%	10.3%	13.9%	19.5%	19.9%	16.3%	10%
[334]	8.6%	5.7%	5.3%	5.3%	5.5%	5%	3.1%
[342]	0%	0%	1%	2.6%	5.5%	3.8%	4.5%
[343]	14.2%	11.8%	12.4%	14.3%	11.1%	8.6%	7%
[344]	9.5%	8.7%	7%	4%	3%	3%	2%
[422]	0%	0%	0%	0%	0%	0%	1%
[423]	0%	0%	0%	0%	0.9%	0.8%	0.5%
[432]	0%	0%	0%	2.4%	5.4%	4%	4%
[433]	11.1%	10.9%	10.8%	14%	10.7%	7.8%	5%
[434]	8.4%	8.3%	5.6%	3%	3.2%	3.4%	1.4%
[442]	0%	0.8%	1.7%	4%	4.5%	3.8%	2%
[443]	14.4%	21.1%	27.9%	19%	10.4%	4.3%	1.5%
[444]	13.4%	22.4%	14.4%	8.6%	1.9%	0.8%	0%

Source: Created by the author.

Figure 5.10 – Percentage of choice for the total number of streams sent for the path loss case with 5 transmit/receive antennas.

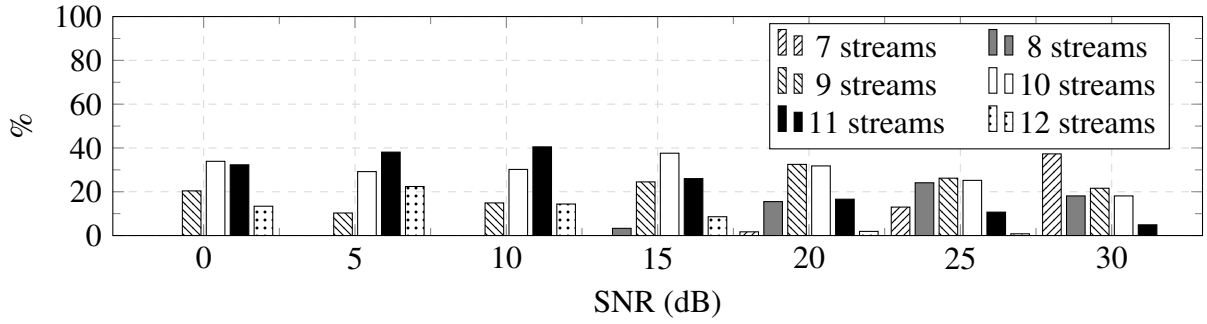

Source: Created by the author.

In order to illustrate that the proposed GSSA works for any case of antenna configuration, we present in Figure 5.11 a simulation where we consider an asymmetric scenario with 5 antennas at the transmitter side and 3 antennas at the receiver side and in Table 5.5 the percentage of choice for each stream configuration over 10000 simulations.

Figure 5.11 – Sum capacity versus SNR asymmetric case. The transmitter has 5 antennas while the receiver is equipped with 3 antennas.

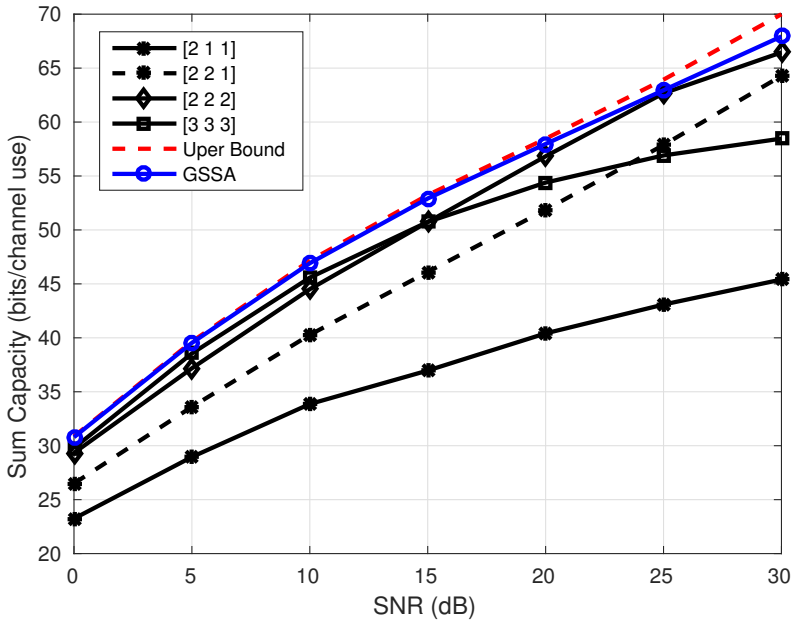

Source: Created by the author.

Figure 5.12 – Percentage of choice for the total number of streams sent for the path loss asymmetric case with 5 transmit antennas and 3 receive antennas.

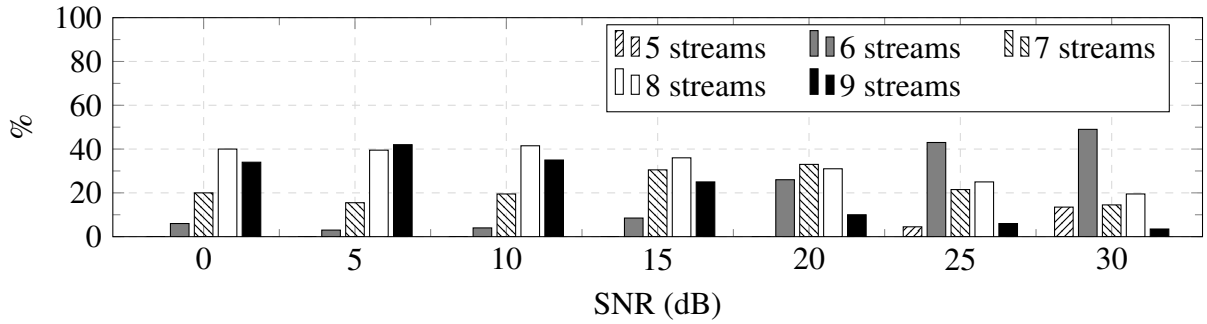

Source: Created by the author.

As observed in the other configurations, the proposed GSSA outperforms any fixed stream allocation and it presents a performance close to the optimum case. As the number of streams is limited by the min(M, N), the [3 3 3] is the highest stream configuration that can be used.

Table 5.5 – Selection percentage for each configuration in Path Loss case for Tx = 5 and Rx = 3 antennas.

Streams \ SNR	0 dB	5 dB	10 dB	15 dB	20 dB	25 dB	30 dB
[122]	0%	0%	0%	0%	0%	1%	5%
[123]	0%	0%	0%	0%	0%	2%	4%
[132]	0%	0%	0%	0%	1%	2%	3.5%
[212]	0%	0%	0%	0%	0%	2%	4.5%
[213]	0%	0%	0%	0%	0%	2%	3%
[221]	0%	0%	0%	0%	0%	1.5%	4%
[222]	6%	3%	4%	8.5%	21%	30%	29%
[223]	5%	4%	4%	8.5%	11%	9.5%	7.5%
[231]	0%	0%	0%	0%	2%	3%	3%
[232]	7%	5.5%	7.5%	10%	11%	6%	3%
[233]	10%	8%	10%	9%	10%	8.5%	6%
[312]	0%	0%	0%	0%	1%	1.5%	3%
[321]	0%	0%	0%	0%	1%	2.5%	3.5%
[322]	8%	6%	8%	11%	10%	5.5%	3.5%
[323]	11%	10%	10%	10%	8.5%	6.5%	6.5%
[331]	0%	0%	0%	1%	1%	0.5%	0.5%
[332]	19%	21.5%	21.5%	17%	12.5%	10%	7%
[333]	34%	42%	35%	25%	10%	6%	3.5%

Source: Created by the author.

For low SNR regime, we can see from Table 5.5 and Figure 5.12 that the best choices are the full stream configuration ([3 3 3]) or 8 streams in total ([3 3 2] or [3 2 3]), which is in accordance with the previous results, since the path loss existence reduces a major part of the interference between the users, therefore users can use full multiplex gain. For high SNR regime, the number of streams needs to be reduced due the increasing of interference between the users, therefore the GSSA selects the [2 2 2] (6 streams in total) stream configuration more often than the others, while the percentage of choices for the [3 3 3] case is drastically reduced.

5.7 Concluding Remarks

The IA is a powerful technique to deal with the interference problem because it separates the useful signal and the interference into two orthogonal subspaces, so the user can transmit its signal without any interference.

One of the problems for the IA technique is how to determine the DoF. The DoF is related to the multiplexing gain of a MIMO system and it can be translated by the number of streams that can be sent for each user in the network. Even [95] has determined an inner and an outer bound for the number of streams that can be sent over the IA channel, the exactly value cannot be determined and it is related to the channel properties.

In practical scenarios, the path loss is non homogeneous which relaxes the size of the

interference subspace needed to perform the alignment, without a floor at the high SNR regime. This allows the transmission of more streams than would normally be possible in a way similar to what is discussed in [108, 109].

Therefore, a GSSA was proposed in order to select the best stream allocation that maximizes the system throughput by taking into account the channel particularities. By comparing the proposed GSSA with an exhaustive search, we illustrated that the greedy algorithm outperforms any fixed solution and it can achieve a good performance compared with the best solution, but with less computational complexity for symmetric and asymmetric scenarios. Thus, the proposed GSSA can determine the DoF for the IA.

6 CONCLUSIONS AND FUTURE WORKS

In this thesis we have addressed the interference management aspects for 4th Generation (4G) cellular networks and beyond. We saw that the interference is one of the major problems for cellular network and it needs to be mitigate in order to maximize the system throughput and guarantee QoS for network users. The problems of interest were those of precoding design, power allocation and stream selection to improve system's capacity. Specific conclusions for each chapter are given below.

In **Chapter 2**, an overview about CBF was done where we have compared the classic BF approaches (MRT, ZF and MMSE) with three different centralized solutions [17, 18, 22] each one with respect to a particular optimization problem. Those works achieve the optimum solution of their respective problem by assuming a central unity that knows the CSI of the network links and calculates the respective BF and power allocation. However, for 5G networks, these kind of solutions are not suitable due the number of network nodes and the amount of information needed to be feedback to the BSs and UEs. Therefore, we concluded that distributed algorithms would be the best solution for next generation network and we made use of this information on the next chapters.

In **Chapter 3**, a BF solution for a multi-cell multi-user MISO dynamic TDD network was proposed. We have shown by simulation plots that the BS-to-BS interference, which affects the UL transmission is more prejudicial than the UE-to-UE which affects the DL transmission. To combat the BS-to-BS and protect the UL transmission, we came up with two distributed algorithms for DL transmission based on the pricing idea which penalizes the user according to the amount of interference it causes at others users: the PBA which solves a relaxed optimization problem via CVX solver and the SPBA, a less complex heuristic, which solves the same problem in less iterations with a small performance loss. The proposed algorithms have gains on power saving for DL and throughput for UL when compared to the classical MRT and ZF BF. The main findings of this chapter also include a signaling scheme so the problem can be treated and solved in a distributed way.

In **Chapter 4**, we have extended the results on Chapter 3 for MIMO systems. We have formulated the dynamic TDD pricing interference problem for a single stream transmission and we found a similar optimization framework to the previous chapter. From the results, we have seen that equipping the UEs with multiple antennas increases both DL and UL performance while saving power for DL transmission when the proposed PBA is applied.

In **Chapter 5**, we saw that, for interference limited scenarios in IA problems, there is a trade-off between the number of streams sent by users and the network total throughput since more streams indicates more date rate but it also increases the interference. Therefore, we have proposed a GSSA which finds the best stream configuration in order to maximize the network capacity. Our algorithm is less complex than the optimal solution (exhaustive search) with a tight

performance gap and it outperforms any fixed solution for symmetric and asymmetric scenarios.

Future Research

In our thesis, we have considered that each cell chooses its transmission direction based on a previous schedule for dynamic TDD networks. One can investigate and propose novel schedule schemes based on some metric such as QoS or throughput requirements and comparing with the fixed schemes. With this regard, some questions emerge, such as:

- What is the impact on signaling and complexity for the transmission selection algorithm?
- How the cells can shift their directions? What is the impact of this shifting?
- Is the seven eIMTA DL-UL configuration enough to meet new QoS requirements?
- Does the schedule affects the interference management?

It is known that multi-antenna UE will be used on 5G networks jointly with massive MIMO on BSs. Therefore, one can consider another metric of optimization or include QoS constraint such as user's satisfaction. Also, one can investigate the system behavior for millimeter wave channel. With this regard, some questions emerge, such as:

- What is the gain of massive MIMO on dynamic TDD scenarios?
- What is the impact of the number of streams on dynamic TDD scenarios?
- Does the GSSA work for dynamic TDD systems?
- How tight is the gap for the GSSA algorithm and the optimum solution for dynamic TDD systems?
- Since DL and UL users have different requirements, how many antennas are necessary to keep a certain QoS for DL and UL users?

Regarding the IA approach, it is still to be applied in 5G scenarios [110, 111], therefore one can explore classical IA algorithms for new 5G networks and propose new IA solutions.

REFERENCES

1 ERICSSON. **More than 50 Billion Connected Devices - Taking Connected Devices to Mass Market and Profitability**. 2011. Available from: <http://www.akos-rs.si/files/Telekomunikacije/Digitalna_agenda/Internetni_protokol_Ipv6/More-than-50-billion-connected-devices.pdf>. Visited on: 20 Apr. 2018.

2 OSSEIRAN, A. et al. **The Foundation of the Mobile and Wireless Communications System for 2020 and Beyond: Challenges, Enablers and Technology Solutions**. In: PROC. Vehicular Technology Conference. [S.l.: s.n.], June 2013. p. 1–5. DOI: 10.1109/VTCSpring.2013.6692781.

3 SHEN, Z. et al. Dynamic uplink-downlink configuration and interference management in TD-LTE. **IEEE Communications Magazine**, v. 50, n. 11, p. 51–59, Nov. 2012. ISSN 0163-6804. DOI: 10.1109/MCOM.2012.6353682.

4 3GPP. **Evolved Universal Terrestrial Radio Access (E-UTRA): Physical channels and modulation**. [S.l.], Mar. 2010. (Release 9, TR 36.211).

5 DING, M. et al. **Dynamic TDD transmissions in homogeneous small cell networks**. In: PROC. International Conference on Communications Workshops. [S.l.: s.n.], June 2014. p. 616–621.

6 ELBAMBY, M. et al. **Dynamic Uplink-Downlink Optimization in TDD-based Small Cell Networks**. In: PROC. International Symposium on Wireless Communications Systems. [S.l.: s.n.], Aug. 2014. p. 939–944.

7 RAHMAN, M. I. et al. **Study on UE-to-UE interference Between TDD Systems**. In: PROC. IEEE Vehicular Technology Conference Spring. [S.l.: s.n.], May 2012. p. 1–5.

8 ADEDIRAN, Y.; LASISI, H.; OKEDERE, O. Interference management techniques in cellular networks: A review. Ed. by Kun Chen. **Cogent Engineering**, Cogent OA, v. 4, n. 1, p. 1294133, 2017. DOI: 10.1080/23311916.2017.1294133.

9 HOSSAIN, E. et al. Evolution toward 5G multi-tier cellular wireless networks: An interference management perspective. **IEEE Wireless Communications**, v. 21, n. 3, p. 118–127, June 2014.

10 VEEN, B. D. V.; BUCKLEY, K. M. Beamforming: a versatile approach to spatial filtering. **IEEE ASSP Magazine**, v. 5, n. 2, p. 4–24, Apr. 1988. ISSN 0740-7467.

11 CADAMBE, V.; JAFAR, S. Interference alignment and the degrees of freedom of the K user interference channel. **IEEE Trans. Inf. Theory**, v. 54, n. 8, p. 3425–3441, 2008.

12 JAFAR, S. A. Interference Alignment - A New Look at Signal Dimensions in a Communication Network. **Foundations and Trends in Communications and Information Theory**, v. 7, n. 1, p. 1–134, 2011. ISSN 1567-2190. DOI: 10.1561/0100000047.

13 COSTA, M. Writing on Dirty Paper. **IEEE Transactions on Information Theory**, v. 29, n. 3, p. 439–441, May 1983. ISSN 0018-9448. DOI: 10.1109/TIT.1983.1056659.

14 EREZ, U.; BRINK, S. ten. A Close-to-Capacity Dirty Paper Coding Scheme. **IEEE Transactions on Information Theory**, v. 51, n. 10, p. 3417–3432, Oct. 2005. ISSN 0018-9448. DOI: 10.1109/TIT.2005.855586.

15 SUN, Y. et al. Near-Capacity Dirty-Paper Code Design: A Source-Channel Coding Approach. **IEEE Transactions on Information Theory**, v. 55, n. 7, p. 3013–3031, July 2009. ISSN 0018-9448. DOI: 10.1109/TIT.2009.2021319.

16 YU, W.; LAN, T. Transmitter Optimization for the Multi-Antenna Downlink With Per-Antenna Power Constraints. **IEEE Transactions on Signal Processing**, v. 55, n. 6, p. 2646–2660, June 2007.

17 DAHROUJ, H.; YU, W. Coordinated beamforming for the multicell multi-antenna wireless system. **IEEE Transactions on Wireless Communications**, v. 9, n. 5, p. 1748–1759, May 2010.

18 VENTURINO, L.; PRASAD, N.; WANG, X. Coordinated Linear Beamforming in Downlink Multi-cell Wireless Networks. **IEEE Transactions on Wireless Communications**, v. 9, n. 4, p. 1451–1461, Apr. 2010. ISSN 1536-1276. DOI: 10.1109/TWC.2010.04.090553.

19 ZHANG, C. et al. **A Beamforming Algorithm Based on Interference Pricing for the MISO Interference Channel**. In: PROC. IEEE Vehicular Technology Conference. [S.l.: s.n.], Sept. 2010. p. 1–5. DOI: 10.1109/VETECF.2010.5594261.

20 ESCUDERO GARZÁS, J. et al. Interference Pricing Mechanism for Downlink Multicell Coordinated Beamforming. **IEEE Transactions on Communications**, v. 62, n. 6, p. 1871–1883, June 2014.

21 HUANG, Y.; XU, J.; QIU, L. **Energy Efficient Coordinated Beamforming For Multicell MISO Systems**. In: PROC. IEEE Global Communications Conference. [S.l.: s.n.], Dec. 2013. p. 2526–2531.

22 VENTURINO, L.; BUZZI, S. **Energy-efficient coordinated beamforming in downlink OFDMA cellular networks**. In: PROC. in Statistical Signal Processing. [S.l.: s.n.], June 2014. p. 492–495.

23 CADAMBE, V.; JAFAR, S. Interference Alignment and Degrees of Freedom of the K-User Interference Channel. **IEEE Transactions on Information Theory**, v. 54, n. 8, p. 3425–3441, Aug. 2008. ISSN 0018-9448. DOI: 10.1109/TIT.2008.926344.

24 SHEN, H.; LI, B.; LUO, Y. **Precoding Design Using Interference Alignment for the Network MIMO**. In: PROC. International Symposium on Personal, Indoor and Mobile Radio Communications. [S.l.: s.n.], Sept. 2009. p. 2519–2523. DOI: 10.1109/PIMRC.2009.5449875.

25 GOMADAM, K.; CADAMBE, V.; JAFAR, S. **Approaching the Capacity of Wireless Networks through Distributed Interference Alignment**. In: PROC. IEEE Global Telecommunications Conference. [S.l.: s.n.], Nov. 2008. p. 1–6.

26 PETERS, S.; HEATH, R. Cooperative Algorithms for MIMO Interference Channels. **IEEE Transactions on Vehicular Technology**, v. 60, n. 1, p. 206–218, Jan. 2011. ISSN 0018-9545. DOI: 10.1109/TVT.2010.2085459.

27 _____. **Interference Alignment via Alternating Minimization**. In: PROC. International Conference on Acoustics, Speech and Signal Processing. [S.l.: s.n.], Apr. 2009. p. 2445–2448. DOI: 10.1109/ICASSP.2009.4960116.

28 LI, W.-C. et al. Coordinated Beamforming for Multiuser MISO Interference Channel Under Rate Outage Constraints. **IEEE Transactions on Signal Processing**, v. 61, n. 5, p. 1087–1103, Mar. 2013. ISSN 1053-587X. DOI: 10.1109/TSP.2012.2231080.

29 ZUFERI, W. et al. **Performance evaluation of uncoordinated beamforming over cognitive radio network**. In: PROC. International Symposium on Telecommunication Technologies. [S.l.: s.n.], Nov. 2012. p. 181–186.

30 GOLDSMITH, A. **Wireless Communications**. New York, NY, USA: Cambridge University Press, 2005. ISBN 0521837162.

31 BJÖRNSON, E.; BENGTSSON, M.; OTTERSTEN, B. Optimal Multiuser Transmit Beamforming: A Difficult Problem with a Simple Solution Structure [Lecture Notes]. **IEEE Signal Processing Magazine**, v. 31, n. 4, p. 142–148, July 2014. ISSN 1053-5888. DOI: 10.1109/MSP.2014.2312183.

32 WIESEL, A.; ELDAR, Y. C.; SHAMAI, S. Zero-Forcing Precoding and Generalized Inverses. **IEEE Transactions on Signal Processing**, v. 56, n. 9, p. 4409–4418, Sept. 2008.

33 SERBETLI, S.; YENER, A. Transceiver optimization for multiuser MIMO systems. **IEEE Transactions on Signal Processing**, v. 52, n. 1, p. 214–226, Jan. 2004.

34 3GPP. **Evolved Universal Terrestrial Radio Access (E-UTRA); Radio Frequency (RF) requirements for LTE Pico Node B**. [S.l.], May 2011. (Release 9, TR 36.931).

35 YU, B. et al. **Dynamic TDD Support in the LTE-B Enhanced Local Area Architecture**. In: PROC. IEEE Globecom International Workshop on Heterogeneous and Small Cell Networks (HetSNets). [S.l.: s.n.], Dec. 2012. p. 585–591.

36 SUSITAIVAL, R. et al. **Internet Access Performance in LTE TDD**. In: PROC. Vehicular Technology Conference. [S.l.: s.n.], May 2010. p. 1–5.

37 3GPP. **TS 36.300 - Evolved Universal Terrestrial Radio Access (E-UTRA) and Evolved Universal Terrestrial Radio Access Network (E-UTRAN) Overall Description (Release 12)**. [S.l.: s.n.], 2015.

38 KHORYAEV, A. et al. **Performance analysis of dynamic adjustment of TDD uplink-downlink configurations in outdoor picocell LTE networks**. In: PROC. International Congress on Ultra Modern Telecommunications and Control Systems and Workshops. [S.l.: s.n.], Oct. 2012. p. 914–921.

39 PAULI, V.; LI, Y.; SEIDEL, E. **Dynamic TDD for LTE-A and 5G**. [S.l.: s.n.], Sept. 2015. Available from: <http://l4ka.org/publications/>.

40 YU, B.; ISHII, H.; YANG, L. **System Level Performance Evaluation of Dynamic TDD and Interference Coordination in Enhanced Local Area Architecture**. In: VEHICULAR Technology Conference. [S.l.: s.n.], June 2013. p. 1–6. DOI: 10.1109/VTCSpring.2013.6692777.

41 VENKATASUBRAMANIAN, V. et al. **On the Performance Gain of Flexible UL/DL TDD with Centralized and Decentralized Resource Allocation in Dense 5G Deployments**. In: PROC. IEEE Annual International Symposium on Personal, Indoor and Mobile Radio Communications. [S.l.: s.n.], Sept. 2014. p. 1840–1845.

42 TÖLLI, A.; PENNANEN, H.; KOMULAINEN, P. Decentralized Minimum Power Multi-cell Beamforming with Limited Backhaul Signalling. **IEEE Transactions on Wireless Communications**, v. 10, n. 2, p. 570–580, Feb. 2011.

43 ASGHARIMOGHADDAM, H.; TÖLLI, A.; RAJATHEVA, N. **Decentralized Multi-cell Beamforming via Large System Analysis in Correlated Channels**. In: PROC. European Signal Processing Conference (EUSIPCO). [S.l.: s.n.], Sept. 2014. p. 341–345.

44 SHI, C. et al. **Distributed Interference Pricing for the MIMO Interference Channel**. In: PROC. IEEE International Conference on Communications (ICC). [S.l.: s.n.], June 2009. p. 1–5.

45 MARZETTA, T. L. Noncooperative Cellular Wireless with Unlimited Numbers of Base Station Antennas. **IEEE Transactions on Wireless Communications**, v. 9, n. 11, p. 3590–3600, Nov. 2010.

46 YIN, H. et al. A Coordinated Approach to Channel Estimation in Large-Scale Multiple-Antenna Systems. **IEEE Journal on Selected Areas in Communications**, v. 31, n. 2, p. 264–273, Feb. 2013.

47 3GPP. **Evolved Universal Terrestrial Radio Access (E-UTRA): Further enhancements to LTE Time Division Duplex (TDD) for Downlink-Uplink (DL-UL) interference management and traffic adaptation**. [S.l.], June 2012. (Release 11, TR 36.828).

48 SUN, F.; ZHAO, Y.; SUN, H. **Centralized Cell Cluster Interference Mitigation for Dynamic TDD DL/UL Configuration with Traffic Adaptation for HTN Networks**. In: PROC. IEEE Vehicular Technology Conference. [S.l.: s.n.], Sept. 2015. p. 1–5.

49 TAO, M. et al. **Realtime dynamic clustering for interference and traffic adaptation in wireless TDD system**. In: PROC. Symposium on Computational Intelligence in Production and Logistics Systems. [S.l.: s.n.], Dec. 2014. p. 128–133. DOI: 10.1109/CIPLS.2014.7007171.

50 SHARP. **R1-132350: UL power control based interference mitigation for eIMTA**. [S.l.: s.n.], May 2013.

51 _____. **R1-132350: DL power control based interference mitigation for eIMTA**. [S.l.: s.n.], May 2013.

52 LEE, H.; CHO, D.-H. **Combination of Dynamic-TDD and Static-TDD Based on Adaptive Power Control**. In: PROC. IEEE Vehicular Technology Conference. [S.l.: s.n.], Sept. 2008. p. 1–5. DOI: 10.1109/VETECF.2008.387.

53 JIANG, L.; LEI, M.; DU, J. **Cross-Subframe Co-Channel Interference Mitigation Scheme for LTE-Advanced Dynamic TDD System**. In: PROC. IEEE Vehicular Technology Conference. [S.l.: s.n.], June 2013. p. 1–5.

54 TAKAHASHI, H.; YOKOMAKURA, K.; IMAMURA, K. **A Transmit Power Control Based Interference Mitigation Scheme for Small Cell Networks Using Dynamic TDD in LTE-Advanced Systems**. In: PROC. IEEE Vehicular Technology Conference. [S.l.: s.n.], May 2014. p. 1–5. DOI: 10.1109/VTCSpring.2014.7022802.

55 NA, C.; HOU, X.; JIANG, H. **Interference alignment based dynamic TDD for small cells**. In: PROC. IEEE Globecom Workshops. [S.l.: s.n.], Dec. 2014. p. 700–705. DOI: 10.1109/GLOCOMW.2014.7063514.

56 AL-RAWI, M.; JANTTI, R. **A dynamic TDD inter-cell interference coordination scheme for Long Term Evolution networks**. In: PROC. International Symposium on Personal Indoor and Mobile Radio Communications. [S.l.: s.n.], Sept. 2011. p. 1590–1594.

57 XU, W.; WANG, X. Pricing-Based Distributed Downlink Beamforming in Multi-Cell OFDMA Networks. **IEEE Journal on Selected Areas in Communications**, v. 30, n. 9, p. 1605–1613, Oct. 2012.

58 PAN, C. et al. Pricing-Based Distributed Energy-Efficient Beamforming for MISO Interference Channels. **IEEE Journal on Selected Areas in Communications**, v. 34, n. 4, p. 710–722, Apr. 2016.

59 NGUYEN, D. N.; KRUNZ, M. Price-Based Joint Beamforming and Spectrum Management in Multi-Antenna Cognitive Radio Networks. **IEEE Journal on Selected Areas in Communications**, v. 30, n. 11, p. 2295–2305, Dec. 2012.

60 KIM, S. J.; GIANNAKIS, G. B. Optimal Resource Allocation for MIMO Ad Hoc Cognitive Radio Networks. **IEEE Transactions on Information Theory**, v. 57, n. 5, p. 3117–3131, May 2011.

61 WANG, F.; KRUNZ, M.; CUI, S. **Price-Based Spectrum Management in Cognitive Radio Networks**. In: PROC. Conference on Cognitive Radio Oriented Wireless Networks and Communications. [S.l.: s.n.], Aug. 2007. p. 70–78.

62 HUANG, J.; BERRY, R. A.; HONIG, M. L. Distributed interference compensation for wireless networks. **IEEE Journal on Selected Areas in Communications**, v. 24, n. 5, p. 1074–1084, May 2006.

63 MUHAMMAD, B.; MOHAMMED, A. **Uplink closed loop power control for LTE system**. In: PROC. International Conference on Emerging Technologies (ICET). [S.l.: s.n.], Oct. 2010. p. 88–93.

64 GRANT, M.; BOYD, S. **CVX: Matlab Software for Disciplined Convex Programming, version 2.1**. [S.l.: s.n.], Mar. 2014. `http://cvxr.com/cvx`.

65 _____. Graph implementations for nonsmooth convex programs. In: BLONDEL, V.; BOYD, S.; KIMURA, H. (Eds.). **Recent Advances in Learning and Control**. [S.l.]: Springer-Verlag Limited, 2008. (Lecture Notes in Control and Information Sciences). p. 95–110.

66 R.H TUTUNCU, K. T.; TODD, M. **Solving semidefinite-quadratic-linear programs using SDPT3**. [S.l.]: Mathematical Programming Ser. B, 2003. p. 189–217.

67 TOH, K.-C.; TODD, M. J.; TÜTÜNCÜ, R. H. On the Implementation and Usage of SDPT3 - A Matlab Software Package for Semidefinite-Quadratic-Linear Programming, Version 4.0. In: ANJOS Miguel F. and Lasserre, J. B. (Ed.). **Handbook on Semidefinite, Conic and Polynomial Optimization**. Boston, MA: Springer US, 2012. p. 715–754.

68 LUO, Z. q. et al. Semidefinite Relaxation of Quadratic Optimization Problems. **IEEE Signal Processing Magazine**, v. 27, n. 3, p. 20–34, May 2010.

69 3GPP. **R1-120948: Simulation assumptions for multi-cell scenarios for TDD eIMTA**. [S.l.: s.n.], Feb. 2012.

70 YANG, H.; MARZETTA, T. L. Performance of Conjugate and Zero-Forcing Beamforming in Large-Scale Antenna Systems. **IEEE Journal on Selected Areas in Communications**, v. 31, n. 2, p. 172–179, Feb. 2013.

71 TELATAR, I. E. Capacity of multi-antenna Gaussian channels. **European Transactions on Telecommunications**, v. 10, p. 585–595, 1999.

72 W BLISS, D.; W FORSYTHE, K.; M CHAN, A. MIMO wireless communication. v. 15, p. 30, Jan. 2005.

73 LARSSON, E. G. et al. Massive MIMO for next generation wireless systems. **IEEE Communications Magazine**, v. 52, n. 2, p. 186–195, Feb. 2014. ISSN 0163-6804.

74 TSE, D.; VISWANATH, P. **Fundamentals of Wireless Communication**. New York, NY, USA: Cambridge University Press, 2005. ISBN 0-5218-4527-0.

75 COSTAS, J. P. Coding with Linear Systems. **Proceedings of the IRE**, v. 40, n. 9, p. 1101–1103, Sept. 1952. ISSN 0096-8390. DOI: 10.1109/JRPROC.1952.273899.

76 YANG, J.; ROY, S. On joint transmitter and receiver optimization for multiple-input-multiple-output (MIMO) transmission systems. **IEEE Transactions on Communications**, v. 42, n. 12, p. 3221–3231, Dec. 1994. ISSN 0090-6778. DOI: 10.1109/26.339844.

77 SCAGLIONE, A.; GIANNAKIS, G. B.; BARBAROSSA, S. Redundant filterbank precoders and equalizers. Part I: Unification and optimal designs. **IEEE Transactions on Signal Processing**, v. 47, n. 7, p. 1988–2006, July 1999. ISSN 1053-587X. DOI: 10.1109/78.771047.

78 GOLDEN, G. D.; MAZO, J. E.; SALZ, J. Transmitter design for data transmission in the presence of a data-like interferer. **IEEE Transactions on Communications**, v. 43, n. 2/3/4, p. 837–850, Feb. 1995. ISSN 0090-6778. DOI: 10.1109/26.380116.

79 WANG, J. et al. A Novel multhpath precoding for spread-spectrum signals in frequency-selective fading channels. **IEICE Transactions on Comunications**, p. 1706–1709, Oct. 1999.

80 IRMER, R.; BARRETO, A. N.; FETTWEIS, G. **ATransmitter Precoding for Spread-Spectrum Signals in Frequency-Selective Fading Channels**. In: PROC. 3G Wireless. [S.l.: s.n.], May 2001. p. 939–944.

81 JOHAM, M. **Optimization of Linear and Nonlinear Transmit Signal Processing**. 2004. MA thesis – Technischen Universität München. ISBN 3-8322-2913-2.

82 MARZETTA, T. L. **How Much Training is Required for Multiuser MIMO?** In: 2006 Fortieth Asilomar Conference on Signals, Systems and Computers. [S.l.: s.n.], Oct. 2006. p. 359–363. DOI: 10.1109/ACSSC.2006.354768.

83 JAYASINGHE, P. et al. **Bi-directional signaling for dynamic TDD with decentralized beamforming**. In: 2015 IEEE International Conference on Communication Workshop. [S.l.: s.n.], June 2015. p. 185–190.

84 O. CAVALCANTE, E. d. et al. Distributed Beamforming in Dynamic TDD MIMO Networks with BS to BS Interference Constraints. **IEEE Wireless Communications Letters**, p. 1–1, 2018. Early access. ISSN 2162-2337. DOI: 10.1109/LWC.2018.2825330.

85 KOMULAINEN, P.; TÖLLI, A.; JUNTTI, M. Effective CSI Signaling and Decentralized Beam Coordination in TDD Multi-Cell MIMO Systems. **IEEE Transactions on Signal Processing**, v. 61, n. 9, p. 2204–2218, May 2013.

86 SPENCER, Q.; SWINDLEHURST, A.; HAARDT, M. Zero-forcing methods for downlink spatial multiplexing in multiuser MIMO channels. **IEEE Transactions on Signal Processing**, v. 52, n. 2, p. 46–471, Feb. 2004. ISSN 1053-587X. DOI: 10.1109/TSP.2003.821107.

87 SCHMIDT, D.; UTSCHICK, W. **Algorithms for improper single-stream MIMO interference networks**. In: PROC. Wireless Communication Systems. [S.l.: s.n.], Nov. 2011. p. 251–255.

88 AMARA, M.; LE RUYET, D.; PISCHELLA, M. **Recursive stream selection for sum-rate maximization on the interference channel**. In: PROC. Signal Processing Advances in Wireless Communications (SPAWC). [S.l.: s.n.], June 2012. p. 269–273.

89 AMARA, M.; PISCHELLA, M.; LE RUYET, D. **Enhanced stream selection for sum-rate maximization on the interference channel**. In: PROC. Wireless Communication Systems. [S.l.: s.n.], Aug. 2012. p. 151–155. DOI: 10.1109/ISWCS.2012.6328348.

90 AMARA, M.; PISCHELLA, M.; RUYET, D. L. **Distributed Beamformer Construction for Successive Stream Selection on the Interference Channel**. In: PROC. Wireless Communication Systems. [S.l.: s.n.], Aug. 2013. p. 1–5.

91 MOREIRA, D. C. et al. Interference alignment, concepts and algorithms for wireless systems. In: CAVALCANTI, F. R. P. (Ed.). **Resource Allocation and MIMO for 4G and Beyond**. [S.l.]: Springer, 2014. chap. 10, p. 439–474.

92 GHASEMI, A.; MOTAHARI, A. S.; KHANDANI, A. K. **Interference alignment for the K user MIMO interference channel**. In: PROC. International Symposium on Information Theory. [S.l.: s.n.], June 2010. p. 360–364.

93 GOU, T.; JAFAR, S. A. Degrees of Freedom of the K User $M \times N$ MIMO Interference Channel. **IEEE Transactions on Information Theory**, v. 56, n. 12, p. 6040–6057, Dec. 2010. ISSN 0018-9448. DOI: 10.1109/TIT.2010.2080830.

94 ZHENG, L.; TSE, D. N. C.; M, W. Packing Spheres in the Grassmann Manifold: A Geometric Approach to the Non-coherent Multi-Antenna Channel. **IEEE Trans. Inform. Theory**, v. 48, p. 359–383, Feb. 2000.

95 GOU, T.; JAFAR, S. A. Degrees of Freedom of the K User $M \times N$ MIMO Interference Channel. **IEEE Transactions on Information Theory**, v. 56, n. 12, p. 6040–6057, Dec. 2010.

96 YETIS, C. M. et al. **Feasibility Conditions for Interference Alignment**. In: PROC. IEEE Global Telecommunications Conference. [S.l.: s.n.], Nov. 2009. p. 1–6.

97 _____. On Feasibility of Interference Alignment in MIMO Interference Networks. **IEEE Transactions on Signal Processing**, v. 58, n. 9, p. 4771–4782, Sept. 2010.

98 RUAN, L.; LAU, V. K. N.; WIN, M. Z. The Feasibility Conditions for Interference Alignment in MIMO Networks. **IEEE Transactions on Signal Processing**, v. 61, n. 8, p. 2066–2077, Apr. 2013.

99 PETERS, S. W.; JR, R. W. H. Cooperative Algorithms for MIMO Interference Channels. **IEEE Transactions on Vehicular Technology**, v. 60, n. 1, p. 206–218, 2011.

100 CADAMBE, V. R.; JAFAR, S. A. **Interference Alignment and Spatial Degrees of Freedom for the K User Interference Channel**. In: PROC. International Conference on Communications. [S.l.: s.n.], May 2008. p. 971–975.

101 SUNG, H. et al. Linear precoder designs for K-user interference channels. **IEEE Transactions on Wireless Communications**, v. 9, n. 1, p. 291–301, Jan. 2010.

102 SCHMIDT, D. A. et al. **Minimum Mean Squared Error interference alignment**. In: PROC. Conference on Signals, Systems and Computers. [S.l.: s.n.], Nov. 2009. p. 1106–1110.

103 PAPAILIOPOULOS, D. S.; DIMAKIS, A. G. Interference Alignment as a Rank Constrained Rank Minimization. **IEEE Transactions on Signal Processing**, v. 60, n. 8, p. 4278–4288, Aug. 2012.

104 GOMADAM, K.; CADAMBE, V. R.; JAFAR, S. A. A Distributed Numerical Approach to Interference Alignment and Applications to Wireless Interference Networks. **IEEE Transactions on Information Theory**, v. 57, n. 6, p. 3309–3322, June 2011.

105 SCHMIDT, D. et al. **Minimum Mean Squared Error interference alignment**. In: PROC. Conference on Signals, Systems and Computers. [S.l.: s.n.], Nov. 2009. p. 1106–1110. DOI: 10.1109/ACSSC.2009.5470055.

106 YETIS, C. et al. **Feasibility Conditions for Interference Alignment**. In: PROC. IEEE Global Telecommunications Conference. [S.l.: s.n.], Dec. 2009. p. 1–6. DOI: 10.1109/GLOCOM.2009.5425326.

107 YETIS, C. M. et al. On Feasibility of Interference Alignment in MIMO Interference Networks. **IEEE Transactions on Signal Processing**, v. 58, n. 9, p. 4771–4782, Sept. 2010. ISSN 1053-587X. DOI: 10.1109/TSP.2010.2050480.

108 RUAN, L.; LAU, V.; RAO, X. Interference Alignment for Partially Connected MIMO Cellular Networks. **IEEE Transactions on Signal Processing**, v. 60, n. 7, p. 3692–3701, July 2012.

109 GUILLAUD, M.; GESBERT, D. **Interference alignment in the partially connected K-user MIMO interference channel**. In: PROC. European Signal Processing Conference. Barcelona: [s.n.], 2011. p. 1095–1099.

110 YERRAPRAGADA, A. K.; KELLEY, B. **An IoT self organizing network for 5G dense network interference alignment**. In: SYSTEM of Systems Engineering Conference (SoSE). [S.l.: s.n.], June 2017. p. 1–6.

111 IMAM, S.; EL-MAHDY, A. **Selective interference alignment in 5G networks**. In: SIGNAL Processing: Algorithms, Architectures, Arrangements, and Applications. [S.l.: s.n.], Sept. 2016. p. 147–151.

112 BOYD, S.; VANDENBERGHE, L. **Convex Optimization**. New York, NY, USA: Cambridge University Press, 2004. ISBN 0521833787.

APPENDIX A – CONVEXITY OF TRACE FUNCTION

A given function $f(x)$ is convex if $f((1-\lambda)x_1 + \lambda x_2) \leq (1-\lambda)f(x_1) + \lambda f(x_2)$ for all x_1,$x_2 \in \text{dom}(f)$ and $\lambda \in (0, 1)$ [112]. Notice that $\text{Tr}(\mathbf{W}_{m,k}) = \text{Tr}(\mathbf{w}_{m,k}\mathbf{w}_{m,k}^H)$ and $\text{Tr}(\mathbf{w}_{m,k}\mathbf{w}_{m,k}^H) = \sum_i |\{w_{m,k}\}_{ii}|^2$, where $\{w_{m,k}\}_{ii}$ is the element of i-th row and i-th column of $\mathbf{w}_{m,k}$. Let $\mathbf{W}_{m,k}$ and $\mathbf{W}_{m',k'}$ be two precoder matrices. Then:

$$\text{Tr}\left((1-\lambda)\mathbf{W}_{m,k} + \lambda\mathbf{W}_{m',k'}\right) \tag{A.1}$$

$$= \sum_i \left((1-\lambda)|\{w_{m,k}\}_{ii}| + \lambda|\{w_{m',k'}\}_{ii}|\right)^2 \tag{A.2}$$

$$\leq (1-\lambda)\sum_i |\{w_{m,k}\}_{ii}|^2 + \lambda\sum_i |\{w_{m',k'}\}_{ii}|^2 \tag{A.3}$$

$$= (1-\lambda)\,\text{Tr}(\mathbf{W}_{m,k}) + \lambda\,\text{Tr}(\mathbf{W}_{m',k'}). \quad \square \tag{A.4}$$

APPENDIX B – RANK ONE PROOF FOR LOW SINR

For low values of x, $\log_2(1+x) \approx x/(log(2))$. Therefore, problem (3.14) can be reformulated as:

$$\begin{aligned} \underset{\mathbf{W}_{m,k}}{\text{minimize}} \quad & \mu \mathcal{I}_{m,k} - (1-\mu)\text{Tr}(\tilde{\mathbf{H}}_{m,(m,k)}\mathbf{W}_{m,k}) \\ \text{subject to} \quad & \sum_{k} \text{Tr}[\mathbf{W}_{m,k}] \leq P_{\max}^{\text{DL}}, \\ & \mathbf{W}_{m,k} \succcurlyeq 0. \end{aligned} \tag{B.1}$$

where $\tilde{\mathbf{H}}_{m,(m,k)} = \mathbf{h}_{m,(m,k)}\mathbf{h}_{m,(m,k)}^{H}/(\log(2) \times I_{m,k})$.

By setting $\Theta_{m,k} \triangleq \sum_{d\in\mathcal{D}} \sum_{j\in\mathcal{K}} \pi_{d,j}\mathbf{H}_{m,(d,j)} + \sum_{u\in\mathcal{U}} \sum_{l\in\mathcal{K}} \pi_{u,l}\mathbf{T}_{m,u} - \pi_{m,k}\mathbf{H}_{m,(m,k)}$, (B.1) can be rewritten as:

$$\begin{aligned} \underset{\mathbf{W}_{m,k}}{\text{minimize}} \quad & \mu\text{Tr}(\Theta_{m,k}\mathbf{W}_{m,k}) - (1-\mu)\text{Tr}(\tilde{\mathbf{H}}_{m,(m,k)}\mathbf{W}_{m,k}) \\ \text{subject to} \quad & \sum_{k} \text{Tr}[\mathbf{W}_{m,k}] \leq P_{\max}^{\text{DL}}, \\ & \mathbf{W}_{m,k} \succcurlyeq 0. \end{aligned} \tag{B.2}$$

The rank-relaxed problem (B.2) is a quadratically constrained quadratic program (QCQP) optimized over one user at one BS at a time, having only one constraint. Therefore, for low SINR values, although (3.14) is a relaxation of (3.12), solving the relaxed problem of (3.14) is equivalent to solving the rank-constrained problem (3.12), which always leads to rank($\mathbf{W}_{m,k}$) = 1 [68]. □

APPENDIX C – CONVERGENCE PROOF OF SEQUENTIAL IMPLEMENTATION

For the sequential implementation, only one user updates its precoders while the others keep their precoders fixed. The objective of our optimization problem is to maximize the follow cost function, $U_{m,k}$, for one user in each downlink cell,

$$U_{m,k} = (1-\mu)C_{m,k}^{\mathrm{DL}}(\mathbf{W}_{m,k}) - \mu \mathcal{I}_{m,k}. \tag{C.1}$$

Now, let $\mathbf{W}_{m,k}^{*} = p_{m,k}\mathbf{w}_{m,k}^{*}\mathbf{w}_{m,k}^{*H}$, where $\mathbf{w}_{m,k}^{*}$ is the updated beam-vector for user (m,k) while the other beam-vectors are fixed. Hence,

$$\sum_{j=1}^{K}\sum_{d=1}^{|\mathcal{D}|} U_{d,j}^{(t+1)}(\mathbf{W}_{d,j}) + \sum_{l=1}^{K}\sum_{u=1}^{|\mathcal{U}|} C_{u,l}^{\mathrm{UL}(t+1)}(\mathbf{W}_{d,j}) \tag{C.2}$$

$$= U_{m,k}^{(t+1)}(\mathbf{W}_{m,k}^{*}) + \sum_{\substack{j=1\\ j\neq k}}^{K}\sum_{\substack{d=1\\ d\neq m}}^{|\mathcal{D}|} U_{d,j}^{(t+1)}(\mathbf{W}_{d,j})$$

$$+ \sum_{l=1}^{K}\sum_{u=1}^{|\mathcal{U}|} C_{u,l}^{\mathrm{UL}(t+1)}(\mathbf{W}_{d,j}), \tag{C.3}$$

where, without loss of generalization we consider only the rate of the UL UEs, $C_{u,l}^{\mathrm{UL}(t)}(\mathbf{W}_{d,j})$, to characterize the utility for the uplink, since there is not any updating at the UL UEs. At this point, note that the utility function, for the DL, and the capacity function, for the UL are both convex with respect to the total interference:

$$\frac{\partial^2 U_{i,j}(\mathbf{W}_{i,j})}{\partial I_{i,j}^2} = \frac{\partial^2 C_{i,j}^{\mathrm{UL}}(\mathbf{W}_{i,j})}{\partial I_{i,j}^2}$$

$$= \frac{B}{\log 2}\left[\left(\frac{1}{I_{i,j}}\right)^2 - \left(\frac{1}{I_{i,j}+s_{i,j}}\right)^2\right] \geq 0, \tag{C.4}$$

Hence, we have:

$$U_{m,k}^{(t+1)}(\mathbf{W}_{m,k}^{*}) + \sum_{\substack{j=1\\ j\neq k}}^{K}\sum_{\substack{d=1\\ d\neq m}}^{|\mathcal{D}|} U_{d,j}^{(t+1)}(\mathbf{W}_{d,j}) + \sum_{l=1}^{K}\sum_{u=1}^{|\mathcal{U}|} C_{u,l}^{\mathrm{UL}(t+1)}(\mathbf{W}_{d,j}) \tag{C.5}$$

$$\leq U_{m,k}^{(t+1)}(\mathbf{W}_{m,k}^{*}) + \sum_{\substack{j=1\\ j\neq k}}^{K}\sum_{\substack{d=1\\ d\neq m}}^{|\mathcal{D}|}\left(U_{d,j}^{(t)}(\mathbf{W}_{d,j}) + \frac{\partial U_{d,j}^{(t)}}{\partial I_{d,j}}(I_{d,j}^{(t+1)} - I_{d,j}^{(t)})\right) +$$

$$+ \sum_{l=1}^{K}\sum_{u=1}^{|\mathcal{U}|}\left(C_{u,l}^{\mathrm{UL}(t)}(\mathbf{W}_{d,j}) + \frac{\partial C_{u,l}^{\mathrm{UL}(t)}(\mathbf{W}_{d,j})}{\partial I_{u,l}}(I_{u,l}^{(t+1)} - I_{u,l}^{(t)})\right) \tag{C.6}$$

$$= U_{m,k}^{(t+1)}(\mathbf{W}_{m,k}^{*}) + \sum_{\substack{j=1 \\ j\neq k}}^{K} \sum_{\substack{d=1 \\ d\neq m}}^{|\mathcal{D}|} U_{d,j}^{(t)}(\mathbf{W}_{d,j}) + \sum_{l=1}^{K} \sum_{u=1}^{|\mathcal{U}|} C_{u,l}^{\mathrm{UL}(t)}(\mathbf{W}_{d,j}) -$$

$$- \sum_{\substack{j=1 \\ j\neq k}}^{K} \sum_{\substack{d=1 \\ d\neq m}}^{|\mathcal{D}|} \pi_{d,j}(I_{d,j}^{(t+1)} - I_{d,j}^{(t)}) - \sum_{l=1}^{K} \sum_{u=1}^{|\mathcal{U}|} \pi_{u,l}(I_{u,l}^{(t+1)} - I_{u,l}^{(t)}) \tag{C.7}$$

$$= U_{m,k}^{(t+1)}(\mathbf{W}_{m,k}^{*}) + \sum_{\substack{j=1 \\ j\neq k}}^{K} \sum_{\substack{d=1 \\ d\neq m}}^{|\mathcal{D}|} U_{d,j}^{(t)}(\mathbf{W}_{d,j}) + \sum_{l=1}^{K} \sum_{u=1}^{|\mathcal{U}|} C_{u,l}^{\mathrm{UL}(t)}(\mathbf{W}_{d,j}) -$$

$$- \mathbf{w}_{m,k}^{*}\Delta_{m,k}^{\mathrm{DL}}\mathbf{w}_{m,k}^{*H} + \mathbf{w}_{m,k}\Delta_{m,k}^{\mathrm{DL}}\mathbf{w}_{m,k}^{H} - \mathbf{w}_{m,k}^{*}\Delta_{m,k}^{\mathrm{UL}}\mathbf{w}_{m,k}^{*H} + \mathbf{w}_{m,k}\Delta_{m,k}^{\mathrm{UL}}\mathbf{w}_{m,k}^{H} \tag{C.8}$$

$$\leq U_{m,k}^{(t+1)}(\mathbf{W}_{m,k}^{*}) + \sum_{\substack{j=1 \\ j\neq k}}^{K} \sum_{\substack{d=1 \\ d\neq m}}^{|\mathcal{D}|} U_{d,j}^{(t)}(\mathbf{W}_{d,j}) + \sum_{l=1}^{K} \sum_{u=1}^{|\mathcal{U}|} C_{u,l}^{\mathrm{UL}(t)}(\mathbf{W}_{d,j}) -$$

$$- \mathbf{w}_{m,k}\Delta_{m,k}^{\mathrm{DL}}\mathbf{w}_{m,k}^{H} + \mathbf{w}_{m,k}\Delta_{m,k}^{\mathrm{DL}}\mathbf{w}_{m,k}^{H} - \mathbf{w}_{m,k}\Delta_{m,k}^{\mathrm{UL}}\mathbf{w}_{m,k}^{H} + \mathbf{w}_{m,k}\Delta_{m,k}^{\mathrm{UL}}\mathbf{w}_{m,k}^{H} \tag{C.9}$$

$$= \sum_{j=1}^{K} \sum_{d=1}^{|\mathcal{D}|} U_{d,j}^{(t+1)}(\mathbf{W}_{d,j}) + \sum_{l=1}^{K} \sum_{u=1}^{|\mathcal{U}|} C_{u,l}^{\mathrm{UL}(t+1)}(\mathbf{W}_{d,j}), \tag{C.10}$$

Where (C.9) holds because $U_{m,k}^{(t+1)}(\mathbf{W}_{m,k}^{*}) \geq U_{m,k}^{(t)}(\mathbf{W}_{m,k})$. As the sum rate is bounded from above, the sequential approach must converge. □